VOLUME 83 NUMBER 4

THE ASTROPHYSICAL JOURNAL

AN INTERNATIONAL REVIEW OF SPECTROSCOPY AND ASTRONOMICAL PHYSICS

Founded in 1895 by GEORGE E. HALE *and* JAMES E. KEELER

Edited by

HENRY G. GALE
Ryerson Physical Laboratory of the University of Chicago

FREDERICK H. SEARES
Mount Wilson Observatory of the Carnegie Institution of Washington

OTTO STRUVE
Yerkes Observatory of the University of Chicago

MAY 1936

THE UNIVERSITY OF CHICAGO PRESS
CHICAGO, ILLINOIS, U.S.A.

May 1936 Vol. 83, No. 4

THE ASTROPHYSICAL JOURNAL

AN INTERNATIONAL REVIEW OF SPECTROSCOPY AND ASTRONOMICAL PHYSICS

The Astrophysical Journal is published by the University of Chicago at the University of Chicago Press, 5750 Ellis Avenue, Chicago, Illinois, during each month except February and August. ¶The subscription price is $6.00 a year; the price of single copies is 75 cents. Orders for service of less than a half-year will be charged at the single-copy rate. ¶Postage is prepaid by the publishers on all orders from the United States, Mexico, Cuba, Porto Rico, Panama Canal Zone, Republic of Panama, Dominican Republic, Canary Islands, El Salvador, Argentina, Bolivia, Brazil, Colombia, Chile, Costa Rica, Ecuador, Guatemala, Honduras, Nicaragua, Peru, Hayti, Uruguay, Paraguay, Hawaiian Islands, Philippine Islands, Guam, Samoan Islands, Balearic Islands, Spain, and Venezuela. ¶Postage is charged extra as follows: for Canada and Newfoundland, 30 cents on annual subscriptions (total $6.30); on single copies, 3 cents (total 78 cents); for all other countries in the Postal Union, 80 cents on annual subscriptions (total $6.80), on single copies, 8 cents (total 83 cents). ¶Patrons are requested to make all remittances payable to The University of Chicago Press, in postal or express money orders or bank drafts.

The following are authorized agents:

For the British Empire, except North America, India, and Australasia: The Cambridge University Press, Fetter Lane, London, E.C. 4. Prices of yearly subscriptions and of single copies may be had on application.

For Japan: The Maruzen Company, Ltd., Tokyo.

For China: The Commercial Press, Ltd., 211 Honan Road, Shanghai. Yearly subscriptions, $6.00; single copies, 75 cents, or their equivalents in Chinese money. Postage extra, on yearly subscriptions 80 cents, on single copies 8 cents.

Claims for missing numbers should be made within the month following the regular month of publication. The publishers expect to supply missing numbers free only when losses have been sustained in transit, and when the reserve stock will permit.

Business correspondence should be addressed to The University of Chicago Press, Chicago, Illinois.

Communications for the editors and manuscripts should be addressed to: Otto Struve, Editor of THE ASTROPHYSICAL JOURNAL, Yerkes Observatory, Williams Bay, Wisconsin.

The cable address is "Observatory, Williamsbay, Wisconsin."

The articles in this journal are indexed in the *International Index to Periodicals*, New York, N.Y.

Applications for permission to quote from this journal should be addressed to The University of Chicago Press, and will be freely granted.

Entered as second-class matter, January 17, 1895, at the Post-Office, Chicago, Ill., under the act of March 3, 1879.

Acceptance for mailing at special rate of postage provided for in Section 1103, Act of October 3, 1917, authorized on July 15, 1918.

PRINTED IN THE U.S.A.

THE ASTROPHYSICAL JOURNAL

AN INTERNATIONAL REVIEW OF SPECTROSCOPY AND ASTRONOMICAL PHYSICS

VOLUME 83 — MAY 1936 — NUMBER 4

KINEMATICS AND WORLD-STRUCTURE. III

H. P. ROBERTSON

ABSTRACT

The structure of a *statistical system* of particles satisfying the cosmological postulate is examined from the standpoint of the kinematics developed in the two previous parts of this paper. It is found to depend on a single arbitrary function χ of two variables, in addition to the constant k and the function ξ of one variable, which specify the kinematical background of the idealized space-time. The distribution function χ is interpreted as a significant *constant of the motion;* and the complete determination of the entire system is discussed on imposing (*a*), the general relativistic theory of gravitation; (*b*), the extension of the Newtonian theory discussed in Part II; and (*c*), the kinematical-statistical theory proposed by E. A. Milne. The conclusions, if not actually favorable to the relativistic theory, at least nullify certain formal objections which have been raised against it.

INTRODUCTION

We conclude our general kinematical theory[1] with an investigation of the situation arising upon augmenting the original hydrodynamical system of fundamental particles by a statistical system which may contain at each space-time event particles of all possible velocities, and which is so constituted that the cosmological postulate still holds for the privileged observers associated with the fundamental particles. This analysis of the structure of such a system is activated by the twofold purpose of evaluating the possibilities of erecting a kinematical-statistical theory of gravitation along the lines pro-

[1] H. P. Robertson, "Kinematics and World-Structure," *Ap. J.*, **82**, 284–301, 1935; *ibid.*, **83**, 187–201, 1936; hereinafter referred to as "Part I" and "Part II," respectively. The numeration of sections and equations is again carried on from the previous work; references to secs. 1–3 and to eqs. (0.1)–(3.3) are to those of Part I, and to secs. 4–6 and eqs. (4.1)–(6.12) are to those of Part II.

posed by E. A. Milne,[2] and of laying the foundations for the treatment of statistical systems within the frame of any gravitational theory, including that of Einstein, imposed from without.

7. STATISTICAL SYSTEMS

We begin, therefore, with a re-examination and a completion, in a form suitable for our general kinematics, of the statistical analysis initiated by Milne for the case in which the kinematical background (2.1) is defined by $k=-1$, $\xi(\tau)=\tau$. Since the cosmological postulate is still to be in force, the conditions of Part I of the present investigation assure us that the natural space-time geometry is again defined by the invariant metric (2.1) for some choice of k and $\xi(\tau)$, and those of Part II that the equations of motion of that particle of the statistical system having the direction vector $\zeta^\mu = d\eta^\mu/ds$ at the event $E(\eta^\mu)$ are again given by (4.4) for some choice of the acceleration function $\Gamma(\tau, \omega)$; it is then the task of any complete theory of gravitation to permit the determination of these functions. For the present purpose it is clearly preferable to employ cosmic time τ as independent variable, thus avoiding a multiplicity of proper times s; and hence the equations of motion are to be taken in the form (4.5).

The number dN of particles at time τ within the volume element defined by the displacements $d\eta^a$ about the point η^a, and having velocities whose components $v^a = d\eta^a/d\tau$ are within the range dv^a about v^a, must be of the form

$$dN = F(\tau, \eta^a, v^a)d\eta^1 d\eta^2 d\eta^3 dv^1 dv^2 dv^3 , \tag{7.1}$$

and our first task is to determine the extent to which the functional dependence of the distribution function F is restricted by the uniformity postulate. To accomplish this we first express the products of co-ordinate and of velocity differentials appearing in (7.1) in terms of the invariant measures[3]

$$d\Sigma \equiv \zeta dV \equiv \zeta R^3 h^{\frac{1}{2}} d\eta^1 d\eta^2 d\eta^3, \quad d\Omega \equiv \zeta^4 \xi^3 h^{\frac{1}{2}} dv^1 dv^2 dv^3 \tag{7.2}$$

[2] *Relativity, Gravitation and World-Structure*, Oxford, 1935; in particular, Part III.

[3] Cf. H. P. Robertson, "On E. A. Milne's Theory of World-Structure," *Zs. f. Ap.*, **7**, 153–66, 1933. We have again retained the fundamental velocity c (which is unity in the units adopted in the present investigation) in order to facilitate interpretation, and have reintroduced the quantity $R(\tau)=c\xi(\tau)$ having the physical dimensions of a length.

of the projection orthogonal to v^μ of the volume element dV in the space $\tau=$const., and of the "solid angle" swept out in space-time by the velocity vector v^μ, respectively. Now, in order that the uniformity postulate be fulfilled, the density of particles in phase space, whose volume element may be taken as $d\Sigma d\Omega$, must be a formally invariant scalar function of the event $\mathrm{E}(\eta^\mu)$ and the direction ζ^μ through it. But, as established in section 4 of Part II, the only independent scalars of this kind under the group G_6 of transformations between the preferred observers are the cosmic time τ of E and the direction cosine $\zeta=\zeta^0$ of the path C of the particle; hence (7.1) must be of the form

$$dN=\frac{\psi(\tau,\zeta)}{R^3(\tau)}\,d\Sigma d\Omega\,, \tag{7.3}$$

where ψ is an arbitrary dimensionless function of its arguments. The original distribution function F is, accordingly,

$$F(\tau,\eta^a,v^a)=\zeta^5\xi^3(\tau)h(\eta^a)\psi(\tau,\zeta)\,. \tag{7.4}$$

We shall, for the time being, consider τ and ζ as the independent arguments of both ψ and Γ, rather than τ and ω, for, although the latter pair lead to somewhat simpler expressions, the former is more easily interpreted and allows more immediate comparison with the results obtained by Milne.

We must now find the condition on the distribution function which assures the permanence of the particles constituting the statistical system. That particle described at time τ by position η^a and velocity v^a will be described at time $\tau+d\tau$ by

$$\eta_1^a=\eta^a+v^a d\tau\,,\quad v_1^a=v^a+g^a(\eta^\mu,v^a)d\tau\,, \tag{7.5}$$

where g^a is the time rate of change $dv^a/d\tau$ of v^a, expressed in terms of position and velocity by (4.5) on transposing the terms involving Christoffel symbols to the right-hand side. If we now let $d\eta_1^a$, dv_1^a be the co-ordinate and velocity ranges at time $\tau+d\tau$ of those particles which are at time τ within the ranges $d\eta^a$, dv^a, then, in order that the particles constitute a permanent set of objects, we must have the equality

$$F(\tau+d\tau,\eta_1^a,v_1^a)d\eta_1^1\,\ldots\,dv_1^3=F(\tau,\eta^a,v^a)d\eta^1\,\ldots\,dv^3 \tag{7.6}$$

between the numbers of such particles at the two times. In order to reduce this relation to a differential condition on F, we have merely to expand the integral part of the left-hand side with the aid of Taylor's theorem and to evaluate the differential product with the aid of the Jacobian[4]

$$\frac{\partial(\eta_1^1 \ldots\ldots v_1^3)}{\partial(\eta^1 \ldots\ldots v^3)} = 1 + \frac{\partial}{\partial v^\alpha}\, g^\alpha(\eta^\mu, v^\alpha)\cdot d\tau + \cdots\cdots . \tag{7.7}$$

The equation (7.6) is then readily found to be equivalent to the differential equation

$$\frac{d}{d\tau}\, F(\tau, \eta^\alpha, v^\alpha) + \frac{\partial g^\alpha}{\partial v^\alpha}\cdot F(\tau, \eta^\alpha, v^\alpha) = 0 , \tag{7.8}$$

where $d/d\tau$ represents total differentiation along the path C of that particle characterized by η^α, v^α at time τ. We have now to evaluate $\partial g^\alpha/\partial v^\alpha$ from (4.5), express F in terms of its value (7.4), and carry out the total differentiation with the aid of (4.5) and its consequence (5.3); after a long and tedious, but straightforward, manipulation, (7.8) reduces in this way to a partial differential equation involving $\psi(\tau, \zeta)$ and $\Gamma(\tau, \zeta)$, which can be written in the significant form

$$\frac{\partial}{\partial\tau}\left[\zeta(\zeta^2-1)^{\frac{1}{2}}\psi\right] = \frac{\partial}{\partial\zeta}\left[(\zeta^2-1)^{\frac{3}{2}}\left(\Gamma+\frac{\xi'}{\xi}\right)\psi\right] , \tag{7.9}$$

τ and ζ being considered as independent variables. But this is precisely the condition that

$$(\zeta^2-1)^{\frac{3}{2}}\left(\Gamma+\frac{\xi'}{\xi}\right)\psi d\tau + \zeta(\zeta^2-1)^{\frac{1}{2}}\psi d\zeta \tag{7.10}$$

be the exact differential of some function, say $\chi(\tau, \zeta)/4\pi$, of τ and ζ. Hence both ψ and Γ can be derived from this single function in accordance with the equations

$$4\pi\psi = \frac{1}{\zeta(\zeta^2-1)^{\frac{1}{2}}}\,\frac{\partial\chi}{\partial\zeta} , \quad 4\pi\left(\Gamma+\frac{\xi'}{\xi}\right) = \frac{1}{(\zeta^2-1)^{\frac{3}{2}}\psi}\,\frac{\partial\chi}{\partial\tau} . \tag{7.11}$$

[4] Obtained as in Milne, *op. cit.*, p. 353.

Our statistical problem is thus reduced to an examination of the properties of this dimensionless function $\chi(\tau, \zeta)$.

We next note that $\chi(\tau, \zeta)$ is constant along the trajectory of each particle of the system, for, on replacing ζ by its value (5.2) in terms of τ and ω, the total differential (7.10) becomes

$$\omega^2\xi^{-3}\psi[d\omega+\omega\Gamma d\tau]=\frac{d\chi}{4\pi}\,; \tag{7.12}$$

and along a trajectory this vanishes by virtue of the equation of motion (5.3). But this means that $\chi(\tau, \zeta)$ may be regarded as a function of the initial values ζ_0 (or ω_0) assumed by the direction cosine ζ (or the quantity ω) at some given epoch τ_0, which we take as fixed once and for all; we find it convenient to adopt the second of these more obvious possibilities. The transformation to this new variable ω_0 is given by (5.4), which defines ω in terms of τ and ω_0 as that solution of the differential equation (5.3) which assumes the values ω_0 at the given epoch τ_0. Upon evaluating $d\omega$ in terms of $d\tau$ and $d\omega_0$ and noting that by (5.3) the coefficient of the former is $-\omega\Gamma$, the total differential (7.12) becomes

$$\omega^2\xi^{-3}\,\frac{\partial\omega}{\partial\omega_0}\,\psi d\omega_0=\frac{d\chi}{4\pi}\,. \tag{7.13}$$

Hence χ may be considered as a function $\chi(\omega_0)$ of ω_0 alone, as predicted above; and ψ, considered as a function of τ and ω_0 instead of τ and ζ, is given by

$$4\pi\psi(\tau, \omega_0)=\frac{\xi^3(\tau)}{\omega^2(\tau, \omega_0)}\,\chi'(\omega_0)\Big/\frac{\partial}{\partial\omega_0}\,\omega(\tau, \omega_0)\,, \tag{7.14}$$

where the prime indicates differentiation with respect to the argument ω_0. We could retain the epoch τ_0 as a second independent variable, in which case we would find an expression for Γ analogous to that given by the second equation of (7.11); but the equation thus obtained is tautological in virtue of (5.3); furthermore, the procedure outlined in the present paragraph will be found of greatest value in those applications in which the form of the acceleration

function is known from the beginning, as in (*a*) and (*b*) of section 8 below.

The function $\chi(\tau, \zeta)$ can now be given an illuminating interpretation in terms of the density $n(\tau, \zeta)$ in the three-space $\tau=$const. of particles passing through a spatial element at $E(\tau, \eta^a)$ and having a direction cosine with the τ-axis lying between 1 and ζ. This particle-density is defined as the coefficient of the volume element dV in the expression obtained on integrating (7.1) or (7.3) over all velocities v^a for which the corresponding direction cosine, defined by (4.6), does not exceed the given ζ. On choosing normal co-ordinates η^a, in which $h_{\alpha\beta}=\delta_{\alpha\beta}$ at E, and transforming to spherical polar co-ordinates in the velocity space, the triple integral defining n reduces to a simple integral which may readily be thrown into the form

$$n(\tau, \zeta)=R^{-3}(\tau)\int_{1}^{\zeta}4\pi\zeta(\zeta^2-1)^{\frac{1}{2}}\psi(\tau, \zeta)d\zeta \tag{7.15}$$

on employing the direction cosine (4.6) as the integration variable.

Now, by (7.11) the integral in the expression (7.15) for n is, if it exists, merely the difference $\chi(\tau, \zeta)-\chi(\tau, 1)$ of the function χ evaluated for a particle of direction cosine ζ and for a particle $\zeta=1$ sharing the motion of the fundamental observer at the event in question. But, since χ is constant along the world-line of each particle, we may conclude, upon applying this fact to that particle characterized for all time by $\zeta=1$, that $\chi(\tau, 1)$ is actually independent of τ; and since, further, χ is so far determinate only to within an additive constant, we may now normalize it by imposing the condition

$$\chi(\tau, 1)=0\,. \tag{7.16}$$

The expression (7.15) then assumes the significant form

$$n(\tau, \zeta)=\frac{\chi(\tau, \zeta)}{R^3(\tau)}=\frac{\chi(\omega_0)}{R^3(\tau)}\,. \tag{7.17}$$

Hence, $\chi(\tau, \zeta)$ itself is the density at time τ in the representative space (0.2) of those particles having at this time velocities v ranging from zero to that value associated with the direction cosine ζ; and its

constancy, when expressed as a function of ω_0, is the trivial assertion that those particles which had initially values of ω ranging from zero to ω_0 will always have initial values in this same range! If, further, the total number of particles passing through a given event is finite, their total density is given by[5]

$$n(\tau)=\frac{D}{R^3(\tau)}\,,\ \text{where}\ D=\lim_{\omega_0\to\infty}\chi(\omega_0)\,. \qquad (7.18)$$

This result is in complete agreement with the considerations of section 6, Part II, leading to the formula (6.1) for the density of fundamental particles. We may even, if we like, consider the fundamental particles as themselves members of the statistical system which are characterized by $\omega_0=0$,[6] provided we express our results in terms of Stieltjes' integrals with a distribution function $\chi(\omega_0)$ which has a step of magnitude d at $\omega_0=0$, and interpret D above as referring to the combined system.

We have gone as far with this as pure kinematics will take us, for the completion of the problem requires the introduction of considerations foreign to the general and kinematical character of the analysis. We have so far established the existence of the quantities k, $\xi(\tau)$ and $\chi(\tau, \zeta)$ from the cosmological postulate and the assumption that we are dealing with a system of particles which preserve their identity. That from these we can obtain the acceleration function

[5] Cf. *ibid.*, n. 3, eq. (2.11). The numerical factor in this equation is erroneously given as 8π instead of 4π. Also, we should there have been able to conclude the constancy of D, in any case in which it exists, from elementary considerations, even though we had not obtained explicitly the condition of permanence. Professor Milne's assertion that the integral here involved diverges (p. 671 of his "Remarks on World-Structure," *M.N.*, **93**, 668–80, 1933; p. 183 of his "Note on H. P. Robertson's Paper on World-Structure," *Zs. f. Ap.*, **7**, 180–87, 1933) applies to that special case to which he has committed himself, but not necessarily to the more general systems with which we were there, and are here, primarily concerned.

[6] Without thereby "claim[ing] to have established the full equivalence of the statistical and hydrodynamical systems," as alleged by Professor Milne (article in *M.N.*, **93**, 671) in his criticism of this procedure in the paper referred to in n. 3 above. It should have been clear from the context that our passage containing the phrase "pass immediately from the statistical to the hydrodynamic case" (p. 161) was to be interpreted as asserting that the latter could be considered as that special case of the former in which all particles have "a unique direction of motion at P."

$\Gamma(\tau, \zeta)$ by (7.11) is hardly surprising, for by (7.17) a knowledge of ξ and χ implies a knowledge of the number of particles in an arbitrary velocity range *at all times* τ—and clearly the kinematical behavior of the entire system is completely specified by this latter. Alternatively, the treatment given in terms of the initial values ω_0 implies a knowledge of ξ and $\Gamma(\tau, \omega)$ in addition to the initial distribution $\chi(\omega_0)$, for it requires that ω be a known function of τ and ω_0. Now, a dynamical description in the traditional sense should, on the other hand, enable us to predict the state of the system at any time τ in terms of its state at the given epoch τ_0, subject, of course, to the limitations of our quasi-classical standpoint and to a reasonably circumscribed interpretation of the phrase "state at a given time." It therefore remains for us to show how our general kinematics can be augmented into a complete dynamical theory by the imposition of further physical laws—in particular, by the imposition of an adequate gravitational theory.

8. STATISTICAL SYSTEMS AND GRAVITATION

We conclude our investigations with a brief account of the manner in which the aims discussed at the close of the last section are to be achieved on (*a*), the general relativistic theory of gravitation; on (*b*), the extension sketched in section 6, Part II, of the Newtonian theory; and on (*c*), the kinematical-statistical theory proposed by Milne.

a) *Einstein's theory of gravitation.*—In order to illustrate the treatment of statistical systems within the frame of the general theory of relativity, we derive in some detail the matter-energy tensor for the most general system of non-colliding particles satisfying the cosmological postulate. We first note that each particle moves in a geodesic, whence we again have the result (6.3); and, since for all time $\omega = \omega_0$, we may drop the distinction between the two. The proper mass m of each particle is conserved, and in order simply to insure the validity of the uniformity postulate we require that it be at most a function $m(\omega)$ of ω; this latitude allows us, in particular, to consider the fundamental particles as members $\omega = 0$ of the statistical system with a mass $m(0)$ which may differ from that of the other members of the system.

The matter-energy tensor for such a system must be of the form[7]

$$T^{\mu\nu}=\left(\rho+\frac{p}{c^2}\right)\delta_0^\mu\delta_0^\nu-\left(\frac{p}{c^2}\right)g^{\mu\nu}\,, \tag{8.1}$$

where ρ and p are two functions of τ alone. Although this result could be established with the aid of the uniformity postulate alone, we do not trouble to do so here, as we obtain incidentally a direct proof in calculating the descriptive quantities ρ and p from the statistical distribution. We first note that the contribution of $T^{\mu\nu}$ at η^μ which is due to those particles whose world-directions lie within the solid angle $d\Omega$ about the direction ζ^μ is

$$\rho_{0v}\frac{d\eta^\mu}{ds}\frac{d\eta^\nu}{ds}=\frac{m(\omega)\psi(\tau,\,\omega)}{R^3(\tau)}\,d\Omega\cdot\zeta^2v^\mu v^\nu\,, \tag{8.2}$$

where $v^0=1$ and ρ_{0v}, the proper mass-density of these particles, is the coefficient of $d\Sigma$ in the expression obtained upon multiplying their number (7.3) by their mass $m(\omega)$. Upon replacing $d\Omega$ by its value (7.2) and integrating over all timelike directions v^μ, we find

$$T^{\mu\nu}=c^{-3}\int\!\!\int\!\!\int\zeta^6m(\omega)\psi(\tau,\,\omega)v^\mu v^\nu h^{\frac{1}{2}}dv^1dv^2dv^3\,, \tag{8.3}$$

which must now be evaluated in order to determine the quantities ρ, p, and incidentally to establish the form (8.1) for all cases in which these integrals exist. Again introducing normal co-ordinates η^a in which $h_{\alpha\beta}=\delta_{\alpha\beta}$ at the event in question, it is seen immediately from considerations of symmetry that all non-diagonal components $T^{\mu\nu}(\mu\neq\nu)$ vanish, and that the three diagonal components $T^{\alpha\alpha}(\alpha=1,\,2,\,3$—not summed) are equal to each other—and are therefore equal to one-third the integral obtained upon replacing $(v^a)^2$ by the sum

$$\sum_a(v^a)^2=\frac{\omega^2}{\zeta^2\xi^4} \tag{8.4}$$

obtained from (5.1). The two triple integrals thus found for T^{00}, T^{aa} may now be reduced to simple integrals, as in the derivation of (7.15)

[7] As shown in secs. 2 and 3 of the author's report, "Relativistic Cosmology," *Rev. Mod. Phys.*, **5**, 62–90, 1933.

above, except that we shall here find it more convenient to employ ω as the variable of integration in place of ζ. Upon replacing $4\pi\psi$ by its value

$$4\pi\psi(\tau,\,\omega)=\frac{\xi^3(\tau)\chi'(\omega)}{\omega^2} \tag{8.5}$$

obtained from (7.14) upon setting $\omega=\omega_0$, all components $T^{\mu\nu}$ are found to be expressible in the form (8.1) at the origin of our normal co-ordinate system, where ρ and p have the values given by

$$\left.\begin{aligned} \rho(\tau)&=R^{-3}(\tau)\int_0^\infty\left[1+\frac{\omega^2}{\xi^2(\tau)}\right]^{\frac{1}{2}}m(\omega)d\chi(\omega)\ , \\ \frac{3p(\tau)}{c^2}&=R^{-3}(\tau)\xi^{-2}(\tau)\int_0^\infty \omega^2\left[1+\frac{\omega^2}{\xi^2(\tau)}\right]^{-\frac{1}{2}}m(\omega)d\chi(\omega)\ . \end{aligned}\right\} \tag{8.6}$$

Finally, on returning to general co-ordinates η^a, it is seen that (8.3) is of precisely the form (8.1), where ρ and p are the functions of τ defined by (8.6). In case we wish to allow for the possibility of a finite density of particles having a given ω, such as the hydrodynamical system $\omega=0$, these results are still valid, provided the integrals involved are considered as Stieltjes' integrals—although their derivation must, of course, be supplemented by an examination of the situation at those points ω at which χ has a discontinuity.[8] The conservation equation[7]

$$\frac{d\rho}{d\tau}+\frac{3R'}{R}\left(\rho+\frac{p}{c^2}\right)=0\ , \tag{8.7}$$

[8] These results include, as the case in which $\chi(\omega)$ is a step function, those obtained by previous investigators in their consideration of systems consisting of one or more homogeneous groups of particles such that all members of one group have the same speed v: cf. G. Lemaître, "On the Random Motion of Material Particles in the Expanding Universe. Explanation of a Paradox," *B.A.N.*, **200**, 273–74, 1930; O. Heckmann, "Über die Metrik des sich ausdehnenden Universums," *Gött. Nachr.*, **1931**, 126–30. Apparently, Professor Milne is unaware of these investigations, or of the ease with which they can be extended to the general case discussed above, when he asserts: "The features of our statistical kinematical model . . . . are beyond the present resources of 'general' [*sic!*] relativity" (*Relativity, Gravitation and World-Structure*, p. 341, or more cautiously, in the discussion on p. 172). We must freely admit, however, that, although the relativistic procedure is straightforward *in principle*, the actual solution of the field equations for a general distribution function $\chi(\omega)$ does involve *mathematical* difficulties of a high order.

which these quantities must, and do, satisfy, is here merely a consequence of the condition of permanence.

We have made no attempt to take account of the contribution to $T^{\mu\nu}$ arising from a homogeneous and isotropic distribution of radiant energy, which may for some purposes be considered as an ensemble of corpuscles for which $\omega=\infty$. It is of passing interest to note, however, that this may be formally included in (8.1), (8.6) by adding to the distribution function $\chi(\omega)$ a singular part at $\omega=\infty$, which is the limit of a set of functions $\chi^*(\omega)$ having the property

$$\int_0^\infty \omega m(\omega) d\chi^*(\omega)=\frac{\beta}{c^3}, \tag{8.8}$$

where $m(\omega)$ is suitably chosen and β is a finite constant. For, if we now allow $\chi^*(\omega)\to 0$ for all $\omega\neq\infty$, subject always to the condition (8.8), the contributions to ρ and p resulting from χ^* are in the limit

$$\rho c^2=3p=\frac{\beta}{R^4}. \tag{8.9}$$

All of this digression is, of course, the baldest sort of mathematical nonsense, but the results (8.9) do correctly describe the matter-energy tensor arising from such a distribution of radiant energy—as can fortunately be shown by a more justifiable analysis.[7]

The field equations resulting from the matter-energy tensor (8.1), (8.6) define $\xi(\tau)$ implicitly in terms of the distribution $\chi(\omega)$ and the two constants k and λ. The function ψ with which we started our statistical analysis is expressed in terms of ξ and χ by the equation (8.5); the form of its dependence on ξ implies that the density in phase space is also a constant of the motion. The complete dynamical description of the system is thus reduced, in principle, to the empirical determination of the three quantities k, λ, $\chi(\omega)$, and of the value of ξ at some given epoch τ_0.

b) Extension of the Newtonian theory.—Here we must first determine the scalar potential $V(\tau)$ in terms of the known $\xi(\tau)$ and the given distribution function $\chi(\omega_0)$. On any extension of the type considered in section 6 of Part II, this is to be accomplished in terms of a scalar density $\rho(\tau)$, not to be confused with the phenomenological

quantity $\rho(\tau)$ appearing in (*a*) above as equal to the time-time component of a tensor. We propose that this mass density is here to be taken as the coefficient of dV in the expression obtained on multiplying (7.3), the number dN of particles in a given co-ordinate and velocity range, by their mass $m(\omega_0)$, and integrating over all velocities up to that of light. The resulting triple integral may again be reduced to a simple integral with the aid of the devices employed before; and, on introducing the value (7.11) or (7.14) of ψ, this integral becomes

$$\rho(\tau)=\frac{M}{R^3(\tau)}\,, \quad M=\int_0^\infty m(\omega_0)d\chi(\omega_0)\,. \tag{8.10}$$

The potential $V(\tau)$ which we seek is then determined from $\rho(\tau)$ by solving the equation of the gravitational field; thus, by way of illustration, we find as in section 6 that for a Lanczos–de Sitter world (6.5) the field equation (6.7) for the distribution (8.10) leads to the potential (6.9), in which dm is to be replaced by M.

The acceleration function $\Gamma(\tau)$ is then obtained from $V(\tau)$ as in (6.11), and the solution $\omega(\tau, \omega_0)$ of (5.3) is again given by (6.12). This completes the solution of the dynamical problem, for all of the foregoing has been obtained from the known $\xi(\tau)$ and the given initial distribution $\chi(\omega_0)$; the entire system is defined explicitly at any time τ by the distribution function

$$4\pi\psi(\tau, \omega_0)=\frac{\xi^3(\tau)\omega_0}{\omega^3(\tau, \omega_0)}\,\chi'(\omega_0) \tag{8.11}$$

obtained from (7.14) with the aid of (6.12).

c) *Milne's kinematical-statistical theory.*—Finally, we indicate the manner in which the theory proposed by Milne fits into the general kinematics developed in this investigation. As shown in Part I, the restrictions which he imposes at the outset on the kinematical background lead him to the unique solution $k=-1$, $\xi(\tau)=\tau$. He then demands that the kinematics be built up without the use of any natural constant, such as b, equation (6.9), having the physical dimensions of time; but, since in the case to which he has restricted himself no dimensionless function of τ can be constructed from $\xi(\tau)$

and τ alone, he is forced to conclude that the acceleration and distribution functions assume the extremely restricted forms

$$\Gamma(\tau, \zeta) = \frac{G(\zeta)}{\tau}, \; \psi(\tau, \zeta) = \psi(\zeta), \tag{8.12}$$

where G and ψ, are, so far, arbitrary functions of the dimensionless scalar ζ.

We examine the implications of these restrictions, from the standpoint of the formal theory developed in the previous section. A glance at equation (7.11) shows that our function χ must here assume the form

$$\chi(\tau, \zeta) = \mathrm{X}(\zeta) - 4\pi C \log \tau, \tag{8.13}$$

where X is a dimensionless function of ζ alone and C is some dimensionless constant;[9] (7.11) then determines G in terms of ψ, in complete agreement with Milne's results. The number $\bar{n}(\tau, \zeta)$ of particles having velocities *in excess* of that corresponding to the direction cosine ζ is, by the analysis leading to (7.17) above, readily found to be

$$\bar{n}(\tau, \zeta) = (c\tau)^{-3}[\mathrm{X}(\infty) - \mathrm{X}(\zeta)], \tag{8.14}$$

and is assumed to be finite for all $\zeta > 1$.[10] The integral $\chi = \text{const.}$ of the equations of motion is here

$$\mathrm{X}(\zeta) - \mathrm{X}(\zeta_0) = 4\pi C \log \frac{\tau}{\tau_0}. \tag{8.15}$$

Now, this equation contradicts the assumed behavior of X; however, Milne's treatment implies that it is to hold only until $\zeta = \infty$, and

[9] It may rightfully be objected that this equation is dimensionally impossible, for $\log \tau$ can enter only in the form $\log (\tau/b)$, where b is some pertinent constant having the physical dimensions of time; and in Milne's theory there exists no such constant. It is clear, however, that the analysis only requires that the difference of two values of χ be defined, and this may always be written in a dimensionally correct form without the introduction of such a constant b. We therefore employ (8.13) as a shorthand notation, with the understanding that only the differences of χ values are physically interpretable.

[10] Milne, *Relativity, Gravitation and World-Structure*, p. 190.

hence by (8.15) there exists a finite time τ_l at which the particle acquires the velocity of light.[10] Similarly, as $\tau \to 0$ we must have $X(\zeta) \to -\infty$, and from this it follows that ζ must $\to 1$ if $\bar{n}(\tau, \zeta)$ is to be finite for all $\zeta > 1$; hence by (8.14) the total number $\bar{n}(\tau, 1)$ of particles passing through each event must be infinite.[11] In following the career of the particle subsequent to time τ_l, Milne finds himself "driven to suppose that the velocity only momentarily reaches c, and that it then decreases again," and shows that this behavior can be fitted into his kinematics only at the expense of considering the acceleration as a two-valued function of the history of the particle.[12]

One could in this way derive Milne's further results, but we consider the foregoing as sufficient illustration of the paradoxical properties of his system and of the rôle which it plays in the general scheme. We confine ourselves to the remark that its necessity could in any event only be maintained provided a complete theory of gravitation could be built up along the same lines. And of this we have not the least hope, for in the last analysis the simplicity and power of the general kinematics developed here for the cosmological problem is directly attributable to the extreme uniformity thereby implied—in any less restrictive situation we should expect such a wealth of undetermined functions that it would seem impossible to develop a completely kinematical-statistical gravitational theory without going far beyond the methods and hypotheses thus far proposed.

CONCLUSION

In the three parts of this investigation we have followed out the general consequences of the uniformity postulate, first formulated by us within the frame of the general theory of relativity[13] and subsequently restated by Milne as the "cosmological principle" on which his kinematical theory is based. On freeing the postulate of the

[11] *Ibid.*, p. 188.

[12] *Ibid.*, chap. xiii; quotation from p. 235.

[13] H. P. Robertson, "On the Foundations of Relativistic Cosmology," *Proc. Nat. Acad.* **11**, 822–29, 1929. Professor Milne's characterization (article *Zs. f. Ap.*, **7**, p. 182) of our formulation as a "*local* experience postulate" and of his as a "*world-wide* experience postulate" is quite irrelevant; in either case the local experiences, *including observations*, of the privileged observers are the raw data on which the theory is built.

limitations implied in both of these previous applications, we have been led to a general kinematical theory sufficient for the description of the motion of fundamental observers, statistical systems of particles, and photons on any gravitational theory which does not differ too radically from those thus far proposed. We have, in particular, examined its relationship to the general relativistic theory of gravitation, to a general class of extensions of the Newtonian theory, and to the kinematical-statistical theory proposed by Milne; we have found it adequate for each but have given reasons for believing that the latter cannot be considered as complete, even in the extremely idealized cosmological problem under consideration. And, although we must hold that, at least in so far as the present problem is concerned, the Newtonian theory could be adapted to fit its requirements, we would nevertheless hesitate to claim serious consideration for such an attack. *In fine*, we are inclined to believe that our investigations may in some measure strengthen, on purely formal grounds, the claims of the general theory of relativity; in any event, we maintain that it cannot be rejected on such grounds, and are the more content to rest the case with the empirical.

PRINCETON UNIVERSITY
December 1935

NOTES ON THE SPECTRA OF SEVERAL LONG-PERIOD VARIABLE STARS AT VARIOUS PHASES OF THEIR LIGHT-CURVES*

PAUL W. MERRILL

ABSTRACT

Low-dispersion spectrograms of a number of long-period variables of classes Me and Se, taken during the fainter phases, are briefly described. The chief general results are: (1) the continuous spectrum of Me variables is remarkably strong between λ 4226 and H; (2) the intensities of the dark H and K lines differ widely in different variables; (3) large changes in total light may occur without marked changes in the absorption spectrum; (4) the bright hydrogen lines, as well as λλ 4202, 4308, 4571, behave in the manner previously outlined; (5) certain long-period variables do not have observable "companion" spectra at minimum light; (6) interesting peculiarities were found in the spectrum of χ Cygni near minimum.

The spectra of many hundred long-period variables appear on photographs taken in the course of the objective-prism surveys of the Harvard College Observatory, while more than two hundred stars have been observed with slit spectrographs at various observatories. Most of the spectrograms were taken near maximum light, and the appearance of the spectra of variables of classes M, S, and N at this phase is therefore familiar. Moreover, the general behavior of the spectra throughout the phases just before and just after maximum (during the interval corresponding to, say, the upper half of the light-curve) is fairly well known, although our information is derived largely from observations of ten or fifteen stars and is less complete for classes N and Se than for class Me.

In Me variables the bright hydrogen lines, which are absent at minimum, reappear during the pre-maximum period. The high intensity of the $H\delta$ line compared to $H\gamma$ is characteristic. During the post-maximum period the bright lines λλ 4202, 4308, 4571 (and λ 3852 in the ultra-violet) are outstanding and their intensities change in a systematic manner.[1]

Our knowledge of spectral details near the minimum phase is very meager. Even the brighter variables are so faint in the violet region

* *Contributions from the Mount Wilson Observatory, Carnegie Institution of Washington*, No. 539.

[1] *Mt. W. Contr.*, No. 399; *Ap. J.*, **71**, 285, 1930.

where the most interesting features are found that the task of obtaining spectrograms is heavy, and, even with large telescopes, low dispersion must be employed. The discovery of anomalous "companion" spectra in *o* Ceti and R Aquarii, together with the presence of bright lines of ionized iron in several other variables, has, however, raised the question whether high-excitation phenomena are not characteristic of Me and Se variables near minimum.

TABLE I

JOURNAL OF OBSERVATIONS

Star	Desig.	Ref.*	J.D. of Obs.—2420000; Mag.; Quality†
T Cas	001755	2	7969,10.6,4; 8003,9.6,4; 8028,9.3,4; 8063,8.7,5
R And	001838	1	8063,8.7,4; 8082,9.6,5
U Ori	054920a	2	8063,11.5,3; 8082,11.1,3
R LMi	093934	.....	7943,8.7,5
R Leo	094211	2	7943,8.0,4
R Ser	154615	2	7943,13.0,2; 7969,13.4,2; 8002,12.8,2; 8028,11.7,2; 8063,10.3,3
U Her	162119	.....	8028,9.6,5; 8063,10.2,3
R Aql	190108	.....	7943,9.8,1; 7969,10.7,4; 8002,11.5,3; 8028,11.5,3; 8063,10.7,4
R Cyg	193449	1,2	7944,8.3,3; 8002,10.0,4; 8028,10.9,3; 8063,12.4,3; 8082,12.5,1
χ Cyg	194632	2	7943,8.9,5; 7969,10.0,4; 8002,11.2,4; 8028,12.6,3; 8063,13.0,3; 8082,13.1,2
R Aqr	233815	3	8002,10.5,3; 8003,10.5,3; 8028,9.1,4
R Cas	235350	2	7944(11.9),1; 7969,11.8,2; 8002,11.0,2; 8028,10.4,4; 8063,9.1,4

* 1, *Mt. W. Contr.*, No. 325; *Ap. J.*, **65**, 23, 1927.
2. *Mt. W. Contr.*, No. 399; *Ap. J.*, **71**, 285, 1930.
3. *Mt. W. Contr.*, No. 513; *Ap. J.*, **81**, 312, 1935.

† 1. Very poor
2. Poor
3. Fair
4. Good
5. Excellent

It is obvious, therefore, that further spectroscopic observations of the minimum phase are highly desirable. If feasible, the dispersion employed should be as great as 50 or 60 A/mm, but as this scale would entail long exposures, preliminary observations of several variables with much smaller dispersion have been deemed expedient.

Accordingly, one or more spectrograms of each of the variables listed in Table I were made during 1935 with a small two-prism spectrograph having a Rayton camera lens of 32-mm focal length yielding a dispersion at $H\gamma$ of about 500 A/mm. This instrument has been employed by M. L. Humason for observations of faint neb-

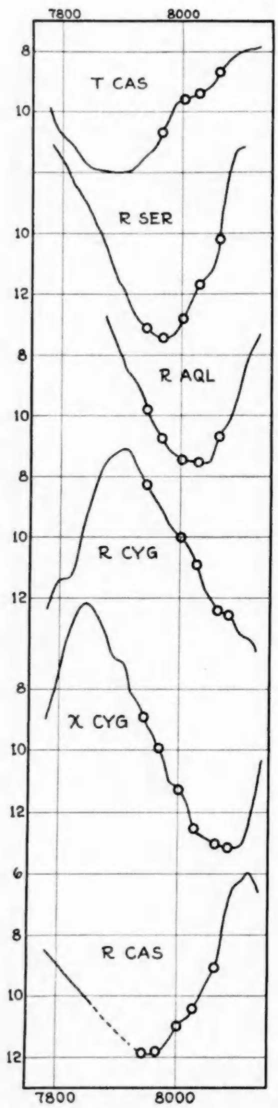

FIG. 1.—Light-curves of long-period variables. Ordinates: visual mag.; abscissae: J.D. *minus* 2,420,000. The dates of spectroscopic observations are indicated by circles.

ulae, and is similar to the one already described by him.[2] In the present investigation it was used by the writer on seven nights at the Cassegrain focus of the 100-inch telescope, and on one night at the 60-inch telescope. The emulsion employed was Eastman 33, and most of the spectra were widened.

T Cas, M8e, *period 447 days, mag. 6.7–12.5* (Fig. 1).—The titanium bands as well as the strong calcium lines λ 4226, H, and K changed but little as the star brightened 2 mag. The last three plates show the gradual pre-maximum development of bright $H\delta$ and $H\zeta$.

R And, Se, *period 407 days, mag. 5.6–14.7* (Plate XII*a*).—The two observations are approximately one-third of the way from maximum to minimum. The distribution of intensity in the continuous spectrum is quite different from that in Me spectra, the portion from $H\beta$ to λ 4226 being very much stronger relative to the shorter wave-lengths. Compare the photographs in Plate XII. Of the characteristic S-type bands due to zirconium oxide, the one at λ 4470 (degraded toward the red) is especially prominent. Titanium bands are probably present in low intensity. *Ca* 4226 is of moderate intensity, while H and K are rather weak. In addition to the hydrogen series, the lines $\lambda\lambda$ 3852, 3905, 4202, 4308 are bright and show a considerable increase in intensity in the nineteen-day interval between the two plates. This observation is of interest

[2] *Mt. W. Contr.*, No. 400; *Ap. J.*, **71**, 351, 1930.

PLATE XII

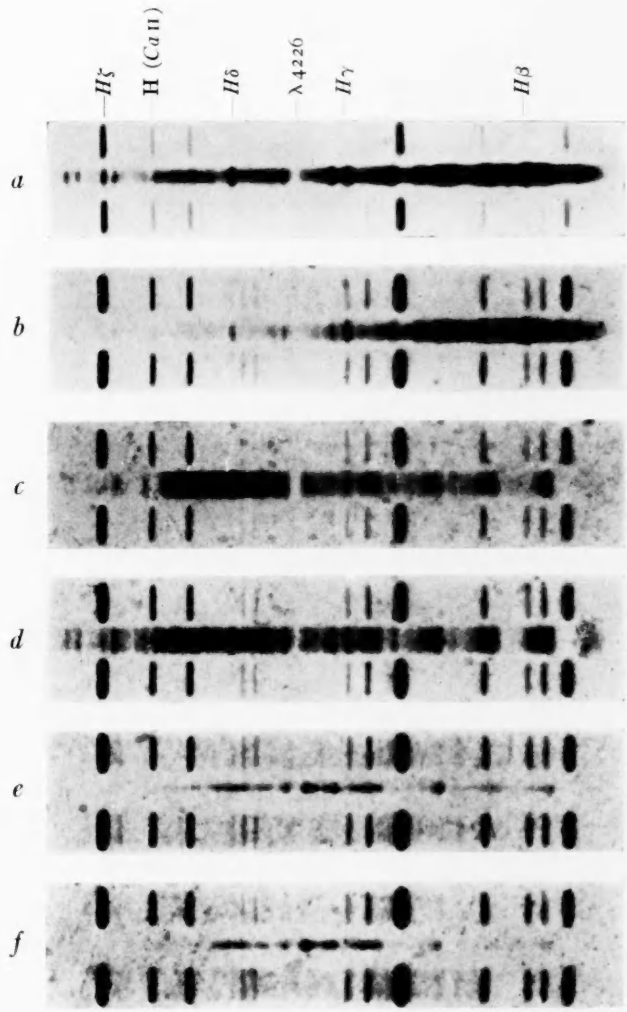

LOW-DISPERSION SPECTROGRAMS OF LONG-PERIOD VARIABLES

Star	Type	Date 1935	J.D. *minus* 2420000
a) R And	Se	Oct. 6	8082
b) R Cyg	Se	July 18	8002
c) R Leo	M8e	May 20	7943
d) χ Cyg	M6pe	May 20	7943
e) χ Cyg	M6pe	Sept. 17	8063
f) χ Cyg	M6pe	Oct. 6	8082

The comparison spectrum is of helium.

because it adds λ 3852 (identification unknown) and λ 3905 *Si* I to the list of post-maximum bright lines which are common to Me and Se variables.[3]

U Ori, M8e, *period 377 days, mag. 5.4–12.2.*—The first plate was probably about thirty days after minimum. No change is noticed on the second plate nineteen days later. *Ca* 4226, H, and K are strong. No bright lines are seen with certainty, although λ 4571 may be present in low intensity.

R LMi, M8e, *period 378 days, mag. 6.3–13.0.*—The single plate is about two-thirds of the way from minimum to maximum. The continuous spectrum is of nearly uniform intensity from λ 4226 to H, and slightly stronger than at longer wave-lengths. *Ca* 4226, H, and K are very strong. Pre-maximum $H\gamma$ and $H\delta$ are present.

R Leo, M8e, *period 315 days, mag. 5.0–10.5* (Plate XII*c*).—The single observation is about halfway up the ascending branch of the light-curve. The continuous spectrum is stronger between λ 4226 and H than at other wave-lengths, with a flat maximum near λ 4050. *Ca* 4226, H, and K are very strong. Pre-maximum $H\delta$ is bright.

R Ser, M7e, *period 353 days, mag. 5.6–13.8* (Fig. 1).—The continuous spectrum has a flat maximum near λ 4040. *Ca* 4226, H, and K are strong. The first three observations show the decline in intensity of the post-maximum bright lines λλ 4202, 4308, 4571. On the third plate only λ 4571 is visible, and on the fourth plate no bright lines are seen. The last plate, about halfway up the ascending branch, shows the pre-maximum $H\delta$.

U Her, M7e, *period 402 days, mag. 6.7–13.0.*—The two observations are about halfway from maximum to minimum light, but the intensities of the bright lines appear to correspond to a somewhat earlier phase. It is possible that this fact has some connection with the rapid rise of the light-curve to maximum. The bright lines $H\gamma$, $H\delta$, $H\zeta$, and $H\eta$ are considerably less intense on the second plate than on the first, while λ 4202 is stronger. The continuous spectrum has a flat maximum near λ 4100. The calcium lines are comparatively weak, especially on the second plate.

R Aql, M7e, *period 302 days, mag. 5.5–11.8* (Fig. 1).—The con-

[3] *Ibid.*, Table VIII.

tinuous spectrum has nearly uniform intensity from λ 4200 to λ 4000. *Ca* 4226 is well marked, but H and K are not very strong. The post-maximum bright lines, not outstanding on any of the spectrograms, do not (with the possible exception of λ 4571) appear on the last plate.

The next to last plate shows superposed on the M-type spectrum a wide continuous spectrum of low intensity, apparently without lines or bands. Its source was probably an electric lamp in the dome.

R Cyg, Se, *period 428 days, mag. 5.6–14.4* (Fig. 1, Plate XII*b*).—The contrast with Me stars in the distribution of energy in the continuous spectrum is brought out in a striking fashion by comparing Plate XII*b* and *c*. The spectrum resembles that of R And, Plate XII*a*, but appears to be relatively less intense from λ 4226 toward the ultra-violet. The lack of energy in the short wave-lengths might arise from a lower effective temperature, but this explanation apparently is not borne out by other features of the spectrum. As the light of the star decreased from mag. 8.3 to 12.4, the zirconium bands increased slightly in intensity, but the titanium bands failed to appear. *Ca* 4226 is strong; the region of H and K is not well shown. The fact that the chief features of the absorption spectrum remained almost unchanged while the total light decreased by about 98 per cent should not be neglected in considering theories of long-period variables.

A rapid decrease in the intensity of the bright hydrogen lines is accompanied by the development of the post-maximum lines λλ 4202, 4308. The line λ 4571 is probably present in low intensity on the later plates.

χ Cyg, M6pe, *period 413 days, mag. 4.2–14.0* (Fig. 1, Plate XII*d*, *e*, *f*).—On most of the spectrograms the general appearance of the spectrum resembles that of a typical Me star, but on the last two plates, taken near minimum light, the intensity of the continuous spectrum in the neighborhood of λ 4380 is relatively high and there is a conspicuous band-head near λ 4415 (see Pl. XII*e*, *f*). The effect might be caused by an emission band extending from λ 4415 toward the violet, but a more probable explanation is that the continuous spectrum is cut off at λ 4415 by an absorption band degraded toward

the red. This feature, which can be recognized on plates of higher dispersion taken in a previous investigation,[1] merits further study. Its wave-length is less by several angstroms than that of the normal titanium band-head near 4422 A. *Ca* 4226 is of moderate intensity, while H and K are exceptionally weak.

On the first three plates the bright hydrogen lines underwent a marked decrease in intensity while the post-maximum lines $\lambda\lambda$ 4202, 4308, 4571 became more and more conspicuous. The line λ 3852 is well marked. On the next plate little change appears except that the hydrogen lines are scarcely visible. On the following plate, $\lambda\lambda$ 4202, 4308, 4571 are still conspicuous; but on the very last plate, taken after an interval of only nineteen days, they are very much weaker. The strongest feature on the last plate is an emission line near λ 4245. On the preceding plate its intensity was comparable with that of λ 4202 and λ 4308. It may be the forbidden iron line λ 4243.97, since this line has previously been observed in this variable as well as in R Leonis and U Orionis,[1] but the absence of the related [*Fe* II] lines $\lambda\lambda$ 4287, 4359 throws some doubt on this identification. It may be remarked, however, that λ 4244 is the leading line in its multiplet, the quartet combination $a^4F - a^4G$, while the other lines arise from a transition between sextet terms.

R Aqr, M7e+Pec, *period 387 days.*—The observations, on the ascending branch of the light-curve, indicate a blend of the spectrum of the companion with that of the Me star. On the first plate the companion spectrum predominates; on the other, the Me spectrum. As the apparent (combined) magnitudes on the two dates of observation were 10.5 and 9.1, respectively, the magnitude of the companion must have been about 10.0. The spectrum includes bright lines of *H*, [*S* II], [*O* III], [*Fe* II], [*Ne* III], and possible [*O* II].

R Cas, M7e, *period 426 days, mag. 4.8–13.6* (Fig. 1).—The first two plates near minimum light are poor, but the post-maximum bright lines λ 4308 and λ 4571 are probably present. On the remaining three plates, taken during increasing light, no bright lines are seen except a trace of pre-maximum $H\delta$ on the last plate. On the last two plates *Ca* 4226 is very intense; H and K are also fairly strong.

CONCLUSIONS

1. The apparent distribution of energy in the continuous spectrum of Me variables differs strikingly from that of Se variables and of the black-body spectrum, the intensity between λ 4226 and H being unduly high. The effect is probably caused in large part by the heavy absorption of titanium oxide at longer wave-lengths.

2. The intensities of the calcium absorption line λ 4226, and especially of the ionized lines H and K, differ widely in different variables.

3. Large changes in total light may occur without marked changes in the absorption spectrum.

4. The behavior of various bright lines conforms, at least in the general pattern, to that outlined in *Mt. Wilson Contr.* No. 399.[1]

5. The behavior of the chief bright lines other than those of hydrogen is much alike in Me and Se spectra.

6. Not all long-period variables have observable "companion" spectra near minimum light.

7. Peculiarities in the spectrum of χ Cygni near minimum call for further observation.

I am indebted to Mr. Leon Campbell, of the Harvard Observatory, for the light-curves shown in Figure 1.

CARNEGIE INSTITUTION OF WASHINGTON
MOUNT WILSON OBSERVATORY
January 1936

ABSORPTION-LINE INTENSITIES IN B-TYPE STARS*

E. G. WILLIAMS

ABSTRACT

Tables of equivalent widths are given for all measurable lines on photometer tracings of 114 spectra of 84 B- and O-type stars. In addition, line depths are tabulated for *H* and *He*. The interval investigated is λ 4922 to λ 3820. Balmer lines below λ 3820 have been measured when their wings do not overlap.

Systematic total intensity differences between spectra obtained on four different scales are appreciable only for the weakest lines recorded with the camera of smallest dispersion (65 A/mm). Investigation of the instrumental effect on line depth shows that with the dispersion of 39 A/mm at $H\gamma$ the true line depth for hydrogen in no case exceeds the observed by more than 15 per cent. In most stars the instrumental filling is probably much less.

The probable error increases with decreasing total absorption; for the hydrogen lines $H\gamma$ to $H\zeta$ it is 5.7 per cent. The average percentage deviation from 67 published hydrogen intensities is 19 per cent, but for nine stars, each measured by three other observers, the deviations from their means are only 7.3 arithmetic and 1.7 algebraic.

The contours for both hydrogen and helium lines are exponential in form, although in n stars the lines are blunt at the center.

The total intensities of the Balmer lines $H\gamma$ to $H\theta$, expressed in equivalent angstroms, coincide within the limits of observational error. For unblended lines farther down the series, the intensity drops rapidly. Published results for $H\alpha$ are collected. $H\beta$, and probably $H\alpha$, are stronger than succeeding lines in the hottest stars; while in those with strong *H* lines (dwarfs) of later subtypes and in those of class A, $H\alpha$ has decidedly low intensities.

These results are compared with recent theoretical work on Stark effect by Pannekoek and Verwey. The relative intensities, $H\alpha$ to $H\delta$, agree well with prediction. Quantitative intensity agreement exists for the normal A stars, but calculated line widths in early B types and in A giants are too great. The theoretical contours, though closely exponential in form, have nearly black centers; and the explanation of the observed high central intensities remains the outstanding problem.

The many problems connected with the spectra of B-type stars have hitherto been attacked almost entirely by visual inspection. Although eye estimates of line intensities have given far-reaching results it is becoming increasingly necessary to make available the more precise measures of spectrophotometry. The present paper, after dealing with the observational methods and the accuracy of results, tabulates fully measurements of absorption-line intensities made on calibrated plates of 84 O- and B-type stars. The analysis of this material in terms of stellar temperature and luminosity will be presented in *Mount Wilson Contribution* No. 541.

* *Contributions from the Mount Wilson Observatory, Carnegie Institution of Washington*, No. 540.

I. OBSERVATIONAL DETAILS

The plates on which the results here presented are based were obtained at the Mount Wilson Observatory and are chiefly those which have already been used for a study of the interstellar calcium lines.[1] This material has been supplemented by a selection of spectra of late B-type stars and by a few uncalibrated plates of certain other stars of peculiar interest, which were reduced with the aid of the iron-arc comparison spectrum.

The measures aim at being complete over the wave-length range λ 4922 to λ 3820 with, in some cases, a further extension into the ultra-violet. Throughout this region nearly all the more prominent lines have been examined, unless awkwardly blended with other lines. The list is not exhaustive of the lines visible on the plates, as the weaker lines are more readily detectable under a micrometer than on the photometer record.

As is fully described in Paper I, the plates were calibrated with a series of ten continuous spectra taken through a step-slit. It was found convenient to combine measures made on the standardizing spectra at five different wave-lengths in order to form a mean reduction-curve, relating microphotometer tracing reading to $\log_{10}$(Intensity) for each plate. A typical mean curve for the Imperial Eclipse emulsion used throughout is shown in Figure 1. Measures for the green, violet, and ultra-violet regions are represented by circles, crosses, and dots, respectively. This particular curve was chosen to contrast the extremes of wave-length; measures made in the blue are found to be equally accordant. Such wave-length differences as may exist in the shape of the characteristic curve are negligible for studies of the kind made here.

The reduction of the tracings to an intensity basis was quickly made with the aid of a logarithmic scale. The figures on the scale gave the natural numbers 10 to 100, corresponding to the log(Intensity) range 1 to 2, in the abscissae of the reduction-curve. This scale was adjusted horizontally so that the mark for intensity 100 was under the ordinate of the curve corresponding to the hypothetical

[1] *Mt. W. Contr.*, No. 487; *Ap. J.*, **79**, 280, 1934. This paper, subsequently referred to as "Paper I," illustrates some of the spectra and gives further details of the technique employed.

PLATE XIII

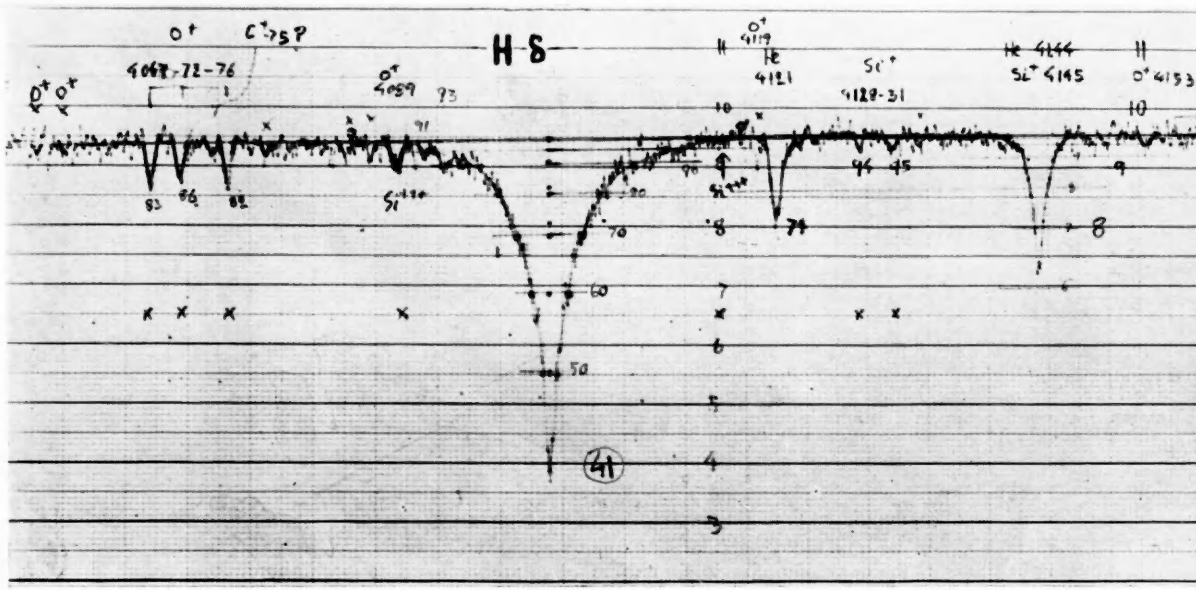

MICROPHOTOMETER TRACING OF THE $H\delta$ REGION IN γ PEGASI (15-IN. CAMERA)

[The line marked $Si+$ 4145 seems to be an error and should probably read $S+$.—EDITOR]

continuous background over the absorption lines to be measured; the ordinates corresponding to intensities 95, 90, 80, ... per cent, down to the line center, were then read from the curve above the graduations on the adjustable scale and were marked on the tracing (Pl. XIII). In each case, only the *total* width of the lines at these ordinates was recorded.

Cameras of three focal lengths were used on the "violet" spectrograph—focal lengths, 15 inches (dispersion, 27 A/mm at $H\gamma$; 33 plates), 10 inches (39 A/mm; 66 plates), and 6 inches (65 A/mm; 6

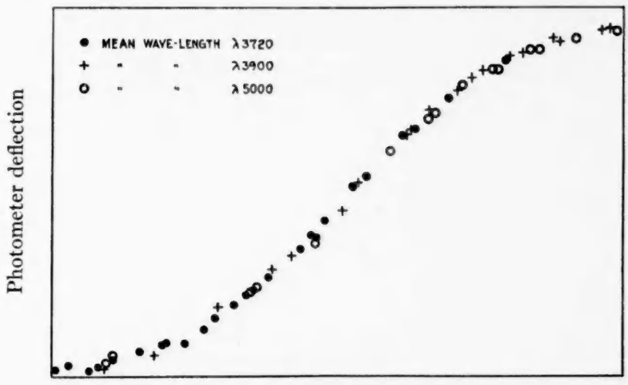

FIG. 1.—Composite tracing reduction-curve

plates). Before combining results collected with several dispersions, it is important to determine any systematic differences which may exist between absorption lines as measured on different scales. To this end two plates were measured, on each of which had been photographed three spectra of the same star taken with the 15-, 10-, and 6-inch cameras, respectively, and with the same slit-width in each case. The use of the same photometric calibration for the three spectra on each plate minimized errors introduced in reduction.

The stars selected were α Cygni, A2ss, and ι Herculis, B3. A calibrated plate (No. 314) taken with the coudé spectrograph, scale 10 A/mm at $H\gamma$, was also available for ι Herculis. The spectra of both these stars present absorption lines covering a wide intensity range; those in α Cygni are all very narrow, while those in ι Herculis

have broad wings; but the cores of the lines are sharp in both cases.

The comparison is shown graphically in Figure 2, where the total absorptions and percentage line depths for each camera are plotted against the mean for the other cameras. A logarithmic scale is used

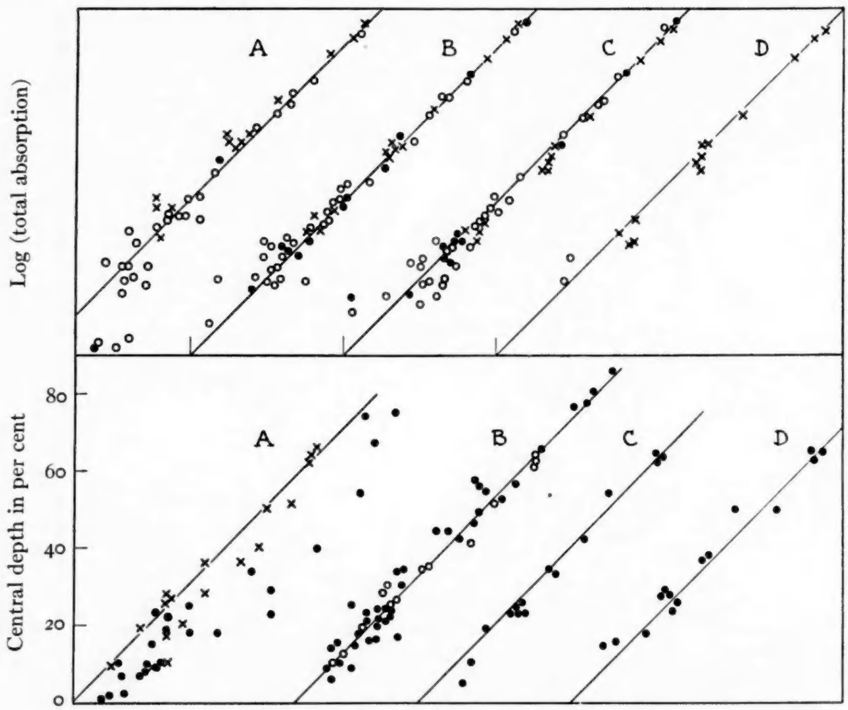

FIG. 2.—Comparison of equivalent widths and depths of lines on different scales: (*A*) 6-inch camera; (*B*) 10-inch camera; (*C*) 15-inch camera; (*D*) coudé spectrograph. Upper half of figure: dots, one observation; circles, mean of two; crosses, mean of three. Lower half: (*A*) crosses from ι Herculis, dots from α Cygni; (*B*), circles, mean of 15-inch and coudé; dots, 15-inch only; (*C*) mean of 10-inch and coudé; (*D*) mean of 10-inch and 15-inch.

for the total absorptions. The 6-inch depths were omitted in taking means.

Except for the weakest lines observed with the 6-inch camera, the total absorption measurements are agreeably free from systematic error and offer no support for Shajn's result[2] that with a smaller dis-

[2] *Bull. Poulkowa*, **13**, No. 4, 1934.

persion a greater equivalent width is found. The percentage deviations from the means for the four cameras are:

	6-inch	10-inch	15-inch	Coudé
Hydrogen lines	6	5	7	4
Helium lines	19	10	16	10
Weaker lines	35	21	22	15

II. APPARENT AND TRUE LINE DEPTH[3]

Assume that the true shape of absorption lines is of the form

$$1-r_\lambda=D_T e^{-a(\lambda-\lambda_c)^2}\,, \tag{1}$$

where r_λ = residual light intensity at wave-length λ, expressed in terms of the intensity in the adjacent continuous spectrum; λ_c = wave-length of line center; D_T = central depth, also in terms of the adjacent continuous spectrum; and a = a constant which has different values in different lines.

Assume also that the instrumental contour for monochromatic light of wave-length λ' is given by

$$I_\lambda=I_{\lambda'}e^{-k(\lambda-\lambda')^2}\,. \tag{2}$$

Let D_0 = observed central depth; A = equivalent width of the line *in millimeters on the plate.* A remains unchanged by instrumental redistribution of light.

The application of this scatter-curve to our assumed line yields the following equations:

$$D_0=\frac{A}{V}\sqrt{\frac{ak}{a+k}}\,, \tag{3}$$

$$D_T=\frac{A}{V}\sqrt{a}\,, \tag{4}$$

$$\frac{\left(\dfrac{D_0}{A}\right)^2}{\dfrac{k}{V^2}}+\left(\frac{D_0}{D_T}\right)^2=1\,, \tag{5}$$

[3] I am indebted to Mr. G. A. Carrick for a helpful discussion of the method of this section.

where

$$V=\int_{-\infty}^{+\infty}e^{-x^2}dx=1.77\ .$$

Equation (5) is that of an ellipse with semi-axes $\sqrt{k/V^2}$ and 1. Once k is known, the equation or the curve gives D_0/D_T, and hence D_T for any line of form (1) with measured D_0 and A.

If we put $D_T=1$ in (5), we obtain

$$D_0^2=\frac{A^2}{A^2+\frac{V^2}{k}}\ . \tag{6}$$

It is most probable that the interstellar calcium lines present a series of lines of different intensities all of which are saturated, i.e.,

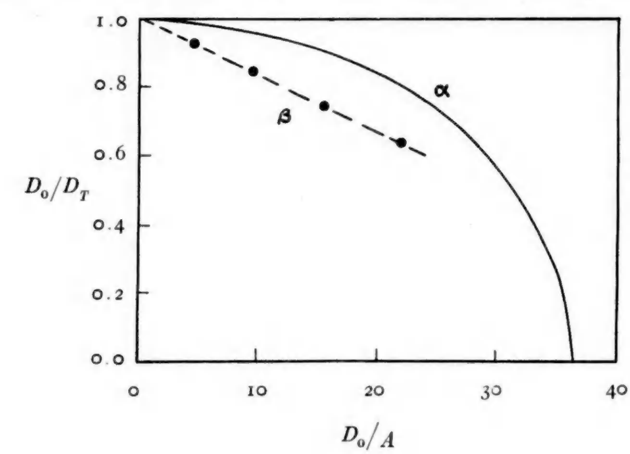

FIG. 3

for which $D_T=1$.[4] Figure 3 in Paper I shows the observed relation between D_0 and A. The curve there shown is excellently represented by (6), if we put $k=4200$.

In Figure 3 of the present paper the full line α represents equation (5) with this value of k. Actually, equation (1) gives lines which are much blunter at the center than any observed lines, while the instru-

[4] Eddington, *M.N.*, **95**, 2, 1934.

mental contour is not an error-curve. The broken curve (β, Fig. 3) is defined by points computed for the rather extreme case of an exponential absorption line,

$$1-r_\lambda = D_T e^{-b(\lambda-\lambda_c)} ,$$

and an instrumental contour similar in shape to one accurately determined by Redman[5] but adjusted to the scale of the scatter-curve for the 10-inch camera (D, Fig. 2, Paper I), which is closely similar to Redman's curve except where $I_\lambda < 0.3\ I_{\lambda'}$. To the degree of accuracy required, it is legitimate to assume constancy for k throughout the region of critical definition on the plate. The following values of D_0/D_T, which may be taken as giving the maximum size of the corrections for some representative absorption lines, have been found from curve β and refer to the 10-inch plates.

	For $H\delta$		For λ 4026 He	
	D_0	D_0/D_T	D_0	D_0/D_T
Typical O star	41	91.5	29	0.86
Typical B2 giant	48	85	40	.76
Typical B3 dwarf	61	95	50	0.83

III. ACCURACY OF RESULTS

Some idea of the accuracy attainable from spectra of the best quality is afforded by the results of section I. Unfortunately, the average precision is below this level, owing to overexposure or underexposure of the plate, to increased graininess effects for some of the fainter stars whose spectra were not fully broadened, and to the fact that the definition deteriorates somewhat for wave-lengths greater than λ 4400. The preceding comparison of cameras was confined to lines on the violet side of this wave-length.

Two or more spectra were obtained for each of 23 stars. As will be seen from Table I, the probable errors depend very much on intensity, and it is convenient to divide the absorption lines into three groups and to describe for each further points connected with their measurement.

[5] *Ibid.*, p. 742, 1935.

Hydrogen lines.—These lines are so strong that in the majority of cases the tracings give reliable results for the contours. For every hydrogen line the observed contour was plotted with a logarithmic scale for percentage of absorption. In the case of the best plates, all points except those very close to the line center fall nearly on a straight line, showing that the depth in the line contour diminishes exponentially with distance from the center; but for many of the underexposed or overexposed spectra the measured width for 1, and

TABLE I

PERCENTAGE PROBABLE ERRORS

	HYDROGEN		HELIUM	
	$H\gamma$ to $H\zeta$	Other Lines	Diffuse Triplets	Sharp Triplets
P.E. in total absorption	5.7	7.1	7.9	16.3
No. of lines	(146)	(66)	(92)	(63)
P.E. in depth	3.3	4.2	5.3	13.4
No. of lines	(130)	(57)	(75)	(64)
Mean total absorption	380		92	30
Mean plate weight	2.2		2.2	2.2

sometimes 5, per cent absorption falls well below the exponential value. In such cases, however, when the mean exponential contour was transferred back to the tracing with the aid of the logarithmic plot, the discrepancy was found to be within the uncertainty of grain irregularity. Consequently, in computing the area of the line, the "exponential" width at 1 per cent absorption dependent on the much more reliably measurable central parts of the line was used in every case,[6] together with the total line-widths as measured on the tracings for $r=0.95$, 0.9, 0.8, 0.7, etc.

Helium lines.—Contours of exponential shape were also found for helium lines by Elvey.[7] Our measures agree with his finding in the case of the stronger lines, for which alone the observations are sufficiently precise. The total intensities of the later, shallow members

[6] This procedure was also adopted for helium lines when their depth exceeded 20 per cent.

[7] *Ap. J.*, **70**, 141, 1929.

of the diffuse singlets are much less reliable than their depths, which here approximate the true values.

Other lines.—Almost all the other lines in B-type stars are relatively so weak that the observed contour bears very little relation to the true one. When the lines are sharp, apparent depths are easily enough measurable if they exceed 5 per cent; but in some stars the contour becomes so vague that the estimates of total absorption may be in error by a factor of 2 or 3 or more. Except for a few strong lines, the shapes have been drawn as triangles on the tracing and their areas found from the central depths and the extreme widths.

IV. TABULATION OF MEASURES

The remarks in this paragraph apply equally to all the tables which follow. Intensities printed in ordinary figures refer to the equivalent widths expressed in units of 0.01 A of total absorption. The observed line depths, expressed as percentages of complete absorption, are printed in italics. The 6-inch camera depths have been empirically reduced to the scale of the rest. The similarity of line shapes renders it unnecessary to tabulate more than these two parameters. A colon following figures indicates low weight. When a space is left blank, for some reason no observation was made. A dash means that the line was invisible on the photometer tracing; and a question mark, that it was only doubtfully present; while "d" indicates a defect on the plate at the wave-length of the line. The letters "b" and "f" following the HD number represent the brighter and fainter components of a binary.

Table II gives the data from each plate for the hydrogen lines. Asterisks appended to the plate numbers in the second column indicate spectra taken with the 15-inch camera; similarly, a dagger marks 6-inch camera plates, while numbers in italics refer to spectra in the c-series, taken by other observers with another spectrograph, which have been calibrated for present use by means of the iron-arc comparison spectrum.[8] All the rest of the plates were taken with the 10-inch camera.

In general the measures continue to the last line in the Balmer series in which the wings appear to be free from overlap with their

[8] Hogg, *Harvard Circ.*, No. 377, 1929.

TABLE II

Total Absorptions and Central Depths of Hydrogen Lines

HD No.	Pl. Wt.	$H\beta$	$H\gamma$	$H\delta$	$H\epsilon$	$H\zeta$	$H\eta$	$H\theta$	$H\iota$	Mean
886	140* 2	545 55	386 59	460 63	513 59	584 59	559 60	495 55		
886	261* 3	437 47	485 54	461 59	503 58	474 54	530 58	541 56	442 50	483 58
3360	261* 2	397 33	437 43	490 55:	425 57:	448 55:				450 50:
4180	293 3	325 em	473 em	434 45	532 46	456 47	469 48	482 50		474 46
5394	301 3	o em	130: 9	226: 16	140: 11	178: 11	224 10			
5394	302 2	o em	92 7	150: 13	128 12	u				157 12
5394	318 3	o em	226 13	9	113 12	189 13	197 12			
11415	302 2	590 51	560 59	590 62	620 64	661 57				608 61
13854	412 3	200: 27	234 41	163 42	176 44	185 44	u			190 43
14134	417 3	195 28	179 45	158 45	181 43	136 46	u			164 45
21291	128* 2	211 44	226 63	265 80	200 68	215 66	229 67	181 53	195 52	
21291	262 2	164 25	240 54	240 63	208 61	190 61	220 57	196 48	139 45	223 65
21389	241 2	185 24	139 50	160 62	164 63	174 56	156 46	124 38	106 37	159 57
22928	319 3	550 49	530 55	613 57	650 60	623 61				604 58
23480	160* 2	477 em	637 45	579 45	550 47	579 49	u			591 47
24398	141* 2	241 44	184 55	204 49	186 48	222 47	302 50	45		
24398	259* 2	224 41	225 50	182 47	175 47	216 50	213 48	235 50	195: 39	206 49
24398	285 3	161 33	249 49	268 51	203 48	193 46	233 41	288 42	37	
24534	286 2	42 3	117 9	161 16	168 16	154 12	102 13	112 12		
24534	397 2	72 5	103 7	193 14	185 20	u				154 13
24760f	336	2130 67	1700 70	u						1925 69
24912	285 3	235 28	188 28	215 33	212 29	188 26	173 24	167 22		201 29
26125	928	980 57	931 59	u						
26125	1309	1090 61	851 66	848 67	u					877 62
28446b	303 1	276 28	295 28	289 32		268 31	284 32			
28446b	329† 1		259 27	215 28	249 30	245 30	318 30			269 30
28446f	303 1	568 50	470 52	376 52	379 50	u				
28446f	329† 1		315 55	310 56	369 56	382 55	u			372 54
30614	294 3	116 20	128 36		124 37	125 34	126 32	97 29	95 25	125 36
32343	415 2	532 45:	532 54:	720 63:	722 55	628 55	565 54	49		651 55
32630	141* 2	761 55	740 62	757 61	709 63	u				
32630	152* 2	804 54	830 65	788 67	862 62	830 64	61			785 63

34085[1]	—* 1		192 *46*	188 *51*	171 *49*	142 *52*	199 *52*	210 *52*	205 *54*	180 *49*
35497	318 3	590 *53*	738 *69*	775 *71*	767 *70*	868 *70*				787 *70*
36371	152* 1	188 *30*	179 *47*	197 *53*	200 *50*	190 *48*	168 *44*	201 *45*	*45*	179 *51*
36371	258* 2	203 *32*	176 *50*	177 *52*	148: *52*	180 *56*	220 *48:*	218 *52*	186: *48*	
36861	303 3	284 *40*	202 *41*	203 *43*	171 *38*	202 *36*	231 *39*	201 *40*	u	213 *42*
36861	304 2	310 *44*	294 *47*	241 *44*	187: *41:*	240: *44*	u			
36862	304 1	334 *43*	443 *53*	372 *47*	362 *45*	316 *45*	u			373 *48*
37128	258* 2	150 *27*	188 *43*	155 *40*	160 *36*	150 *43*	152 *42*	135 *36*	164: *34*	163 *41*
37202	263* 2	190 em	217: *24*	282: *24*	490 *30*	340 *26*				
37202	302 3	171 em	365 *34*	300 *33*	459 *32*	385 *25*				395 *29*
37202	326* 3		461 *31*	373 *30*	495 *26*	440 *26*				
38771	315* 2	203 *30*	165 *33*	156 *38*	167 *38*	171 *38*	180 *37*	204 *38*	132 *33*	165 *37*
39698	303 2	571 *47*	510 *48*	426 *50*	585 *63*	629 *57*		o		541 *55*
40111	128* 2	297 *38*	253 *44*	238 *43*	251 *42*	219 *38*		o		241 *42*
41117	79* 2	70 *23*	93 *37*	78 *38*	86 *45*	102 *40*	103 *43*	93 *41*	105 *41*	94 *39*
41117	263* 3	88 *21*	86 *28*	93 *39*	100 *44*	105 *44*	129 *41*	127 *43*	112 *38*	
41534	*703*	553 *51*	604 *57*	532 *57:*	u					571 *55*
44743	315* 2	329 *42*	293: *48*	288: *46*	270 *46*	306 *49*	328 *45*	297 *44*	260 *42*	289 *47*
47839	129* 2	330 *43*	240 *41*	213 *43*	243 *39*	280 *41*	*39*			260 *41*
47839	307* 3	307 *43*	342 *43*	258 *42*	242 *41*	275 *38*	251 *37*	*33*		
58050	330† 2		536 *43*	540 *43*	570 *44*	477 *44*				531 *44*
59088	300† 2		188 *23*	187 *32*	169 *38*	156 *38*	u			175 *33*
74280	338 3	549 *49*	581 *57*	542 *59*	598 *59*	610 *58*	*58*			583 *58*
87737	162* 2	481 *51*	457 *60*	440 *64*	495 *64*	499 *66*		o		473 *63*
87901	291* 3	700 *48*	875 *55*	731 *58*	900 *60*	759 *60*	797 *61*			811 *58*
87901	338 3	800 *49*	831 *57*	820 *58*	810 *58*	765 *58*				
89688	308 2	463 *41*	513 *50*	454 *51*	539 *53*	475 *53*				495 *52*
91316	297 3	204 *32*	187 *43*	178 *42*	141 *41*	196 *44*	205 *39*	198 *38*	180 *36*	176 *43*
93521	305 2	289 *31*	290 *29*	272 *31*	329 *29*	231 *26*	250 *23*	*25*		281 *29*
100600b	180 2	627 *41*	662 *52*	742 *54*	630 *49*	556 *50*	578 *49*			648 *51*
100600f	180 2	750 *54*	815 *52*	722 *50*	635 *51*	635 *52*	628 *50*			702 *51*
109387	162* 2	739 *40*	628 *51*	545 *53*	620 *53*	605 *53*				600 *53*
120315	305 3	785 *48*	746 *53*	780 *56*	842 *57*	708 *56*				769 *56*
147394	146* 2	808 *55*	888 *70*	731 *70*	795: *70:*	858: *70:*				805 *70*
148184	348 2	253: *22*	214 *15*	325 *23*	270 *23*	288 *20*				272 *21*
148479	382 1			620 *54*	660 *52*	671 *56*	u			716 *56*
148479	386 2	563 *41*	683 *54*	763 *54*	798 *59*	752 *59*	800 *57*			
149438	396 3	387 *39*	326 *48*	374 *50*	360 *49*	316 *48*	375 *44*			345 *49*
149757	159* 2	335 *28*	290 *26*	240 *25*	215 *22*	204 *23*	250 *24*			253 *24*
149757	348 2	194 *17*	281 *24*	303 *27*	275 *25*	213 *21*	232 *23*			
149881	393 3	288 *38*	223 *45*	250 *43*	285 *44*	216 *39*	*40*	*42*		243 *43*
160762	332* 3	650 *54*	532 *62*	552 *64*	588 *64*	622 *64*		o		582 *64*
160762	332 3	653 *52*	550 *61*	569 *62*	650 *65*	589 *65*		o		

TABLE II—*Continued*

HD No.	Pl.	Wt.	$H\beta$	$H\gamma$	$H\delta$	$H\epsilon$	$H\zeta$	$H\eta$	$H\theta$	$H\iota$	Mean
162732	255	2	762 *41*	820 *60*	947 *67*	915 *70*	810 *66*				873 *66*
164353	187	2	325 *50*	249 *52*	249 *51*	260 *53*	262 *49*	232 *45*			255 *51*
167971	396	1	82 *13*	231 *28*	161 *27*	u					196 *28*
169454	387	2	145 em	176 em	175	111	u				154
187811	188*	2	880 *42*	608 *50*	550 *49*	570 *48*	484 *48*				553 *49*
190603	384	3	108	132	95 *38*	103 *39*	97 *33*	102 *37*	u		107 *37*
191201	417	3	358 *39*	244 *46*	262 *43*	237 *41*	265 *42*	256 *36:*	244 *31:*	u	252 *43*
192422	383	2	193 *26*	150 *38*	171 *38*	175 *40*	163 *40*	222 *40*	u		165 *39*
193322	411	3	308 *36*	321 *40*	263 *39*	278 *37*	310 *42*	u			293 *40*
194279	410	2	122 *27*	123 *46*	125 *48*	93 *47*	113 *42*	138 *38*	u		114 *46*
194839	387	1	156 em	205 *44*	167 *37*	235 *53*	u				202 *45*
195592	394	2	*13*	*31*	119	104 *32*	122 *34*	u			115 *33*
197345[1]	289*	3	222 *48*	266 *71*	258 *74*	*76*	250 *78*			271 *81*	
197345[1]	388*	3	272 *46*	265 *73*	259 *78*		321 *76*				278 *76*
197345[1]	388	3	320 *57*	284 *76*	293 *80*		294 *77*				
197345[1]					274		296 *76*	359 *76*	384 *78*	341 *78*	
198478	77*	2	134 *25*	134 *49*	146 *53*	125: *49:*	138 *48*	143 *46*	u		131 *48*
198478	289*	3	144 *29*	125 *45*	116 *45*	129: *48:*	139 *49*	148 *46*	148 *44*	135 *44*	
200120	340	2	355 *28*	611 *30*	649 *35*	450 *34*	424 *33*	466 *33*			534 *33*
204172	383	2	198 *27*	186 *41*	217 *41*	174 *39*	209 *35*	215 *37*	*31*		197 *39*
205021	188*	1	424 *48*	377 *51*	330 *49*	370 *50*	353 *49*	346 *49*			
205021	260	2	335 *47*	395 *55*	337 *54*	320 *52*	315 *51*	332 *48*	370 *45*		380 *49*
205021	348	2	379 *28*	420 *43*	371 *51*	452 *46*	395 *46*	u			
205021	349	2	308 *28*	425 *47*	424 *46*	337 *44*	419 *48*	u			
206165	260	2	210 *43*	170 *44*	200 *48*	203 *51*	195 *46*	232 *44*	249 *50*	224 *41*	192 *47*
208185	419†	2		679 *61*	546 *61*	489 *57*	570 *57*				582 *59*
208392	397	2	425 *47*	486 *47*	410 *51*	411 *57:*	462 *59*	u			442 *53*
208947[2]	306	2	580 *43*	627 *54*	641 *56*	592 *57*	635 *60*				631 *54*
208947[2]	353	2	611 *50:*	620 *50*	613 *50*	657 *54*	663 *52*	*55*			
210809	418	2	178 *27*	185 *31*		199: *31:*	182 *30*	152 *31*	u		189 *31*
210839	349	3	194 *25*	168 *29*	179 *28*	203 *28*	149 *24*	147 *23*	149 *24*		175 *27*
212455	411	2	195 *37*	252 *55*	237 *56*	226 *56*	274 *60*	296 *55*	380: *60:*		247 *57*
212571	397	3		342 *16*	223 *21*	288 *25*	181 *20*	248 *21*			256 *21*
213420	306	2	484 *47*	362 *50*	409 *53*	414 *54*	469 *57*	456 *57*			414 *54*
214680	298†	2	360 *49*	285 *46*	275 *47*	263 *49*	265 *48*	u			270 *44*
214680	395	3	334 *41*	285 *51*	234 *51*	290 *48*	265 *46*	256 *42*	*41*		
+60°2522	*695*		63 *15*	84 *26*	138 *29:*	u					
+60°2522	*753*		160 *26*	154 *33*	u						137 *27*
+60°2522	*1308*		131 *25*	155 *27*	153 *23*	u					
224151	395	3	226 *29*	307: *36*	188 *32*	230 *32*	195 *34*	*37*	*34*		219 *34*

NOTES TO TABLE II

1. The figures in the last line for α Cygni and from $H\eta$ onward for β Orionis are Merrill and Wilson's values determined with the same instrument.
2. The line depths are from plate V306 taken when the similar spectra were coincident.

neighbors. When overlapping is present, difficulties in measurement and interpretation arise which are not considered here.[9] When underexposure, rather than overlap, is the reason for terminating the measures, the symbol "u" is inserted, while "o" indicates the first line with overlap when this is beyond the last line measured.

Table II*a* gives additional measures, less reliable than those in Table II, for those stars which show unblended lines farther down the series than $H\iota$. The last column of Table II gives the mean values of the total absorption and of the depth for $H\gamma$, $H\delta$, $H\epsilon$, and

TABLE II*a*

ADDITIONAL HYDROGEN LINES

HD No.	$H\kappa$	$H\lambda$	HD No.	$H\kappa$	$H\lambda$	$H\mu$
21291	157 *43*	150 *42*	38771	152 *33*		
21389	97 *32*	*26*	41117	110 *38*	105 *37*	113 *37*
24398	170: *35*:		91316	166 *37*		
30614	66 *23*	61 *18*	198478	119 *42*	128 *45*	
37128	113: *27*	87 *22*				

$H\zeta$, derived from the preceding figures by weighting each line according to its quality. It is believed that the inclusion of lines other than these four in deriving a working "mean hydrogen intensity" and "mean depth" would decrease, rather than increase, the dependability of the result.

The helium line measures, grouped according to series, are presented in Table III. For convenience, in this and succeeding tables we give only the weighted mean values from all plates of the star. Intensities for two lines of the ^1S-series will be found, for those stars in which they were measurable, in Tables IV and VII.

The remainder of the intensity measures should be self-explanatory. Those for stars showing comparatively few lines are grouped together in Table VII. Absence of a star from any table indicates that the lines were not noticeable. For each element the lines are arranged in order of wave-length. The selection includes most lines clearly visible on good tracings, although several which habitually blend, notably some strong O^+ lines in the immediate vicinity of $H\gamma$, have been neglected. Multiplet data taken from Miss Moore's

[9] Merrill and Wilson, *Mt. W. Contr.*, No. 494; *Ap. J.*, **80**, 19, 1934.

TABLE III

HELIUM LINES

HD No.	4471		4026*		3820		4922		4388		4144		4009		3927		3872		4713		4121		3867		3965	
γ Peg → 886	118	42	143	51	166	54	123	26	80	35	83	37	69	33	70	22	35	16	31	12	36	27	20	30	18	31
3360			112	44	130	49	123	14			68	31	59	29	54:	21	16:	9			49	19	23	26	29	29
4180	90	18	88	20	67	16	38	7	56	12	31	8	33:	7	23	7	10	4		2	15	6		1		
5394	48	7	55	10	70	13	10	3	37	9	102	9	36	7	46	8	38	6		2	25	6		2		
11415	87	28	114	38	114:	33	63	18	49	23	55	21	51	18	61	13	35:	6	23	14	25	15	25:	17	6:	7:
13854	97	39	81	36			97	22	60	26	40	22	32	19	34	11	16:	15:	55	20	49	21	13:	17:	21	20
14134	70	35	67	32			108	23	d		52	29	33	17	32	20	32:	15:	32	14	33	20	13:	17:	41	25
21291	38	19	36	24	23	19	35	10	32	12	16	9	15	16	20	16	13	7	—	—	14	12	7	9	14	17
21389	11	11	26	10	15	12	—	—	—	—	13	9		5		1	—	—	—	—		2:	—	—	12	11
22928	66	13	66	17	76	19	18	10	31	8	40	10	33	10	22	6			26	7	21	8			?	
23480	39	9	42:	10	25:	10	23	8	21	7	50	10		5:	22	6		3	—	—	19:	6	?			
24398	101	40	89	42	97	38	90	25	59	32	48	24	34	23	41	20	16	11	42	19	50	19	18	16	30	20
24534†	27	7	74	15	57	14	—	—	35	8	31	7	47	9	43	8		3	21	5	22	5				
24760f	25	8							—	—																
24912	75	13	85	18	47	9	32	8	13	6	14:	4	?		d		—	—	21:	6		4:	14:	3	—	—
26125		4							—	—																
28446b	123	16	88	17	85	15	89	15	40	8	44	9	22	6	19	5		1	28	6	38	9		3	?	
28446f	147	28	110	39			23	9	72	22	57	25	33	19	42	9		2	16	7	42	18	31	17	15	18
30614	111	34	88	33	65	24	74	15	30	14	33	12	32	15	10	4		2:	37	13	17	9	10:	4:	24	13
32343	76	24	132	41	105	32	54	15	56	18	63	21	68	18	30	8		1	35	10	18	12	4	5	?	
32630	171	35	187	38	94	29	103	15	120	33	71	19	75	20	34	9	27	11	105	14	34	19	26	14		
34085	55	28	35	23	36:	21	58	13	33	18	20	16	21	10	20	11	14	8			17	13	11	7	15	9
35497	51	17	80:	20	43	15	43	12	21:	8	49:	11	24:	8		2:		2:	14	9	15:	5:	38	9		
36371	94	36	79	41	62	36	60	15	55	27	42	22	39	25	22	19	26	15	34	15	28	18	19	15	30	25
36861	90	33	87	29	63	27	43	12	42	12	21	13	16	8	15	5		2	31	11	33	10		1	14	15
36862	154	37	131	41			63	16	d		65	15	35:	12	29:	10	4	4	27	14	32	18		3	10:	10:
37128	73	31	61	29	59	30	66	23	35	15	28	17	16:	8		2:	43:	3	23	11	26	11	10	8	18	12
37202	150	26	151	25	142	23	96	13	69	11	94	14	90	11	67	9	54	9	58	10	51	9	—	2	—	—
38771	108	29	75	29	81	34	112	22	57	18	48	18	23	12	34	10	11	7	38	13	36	14	9	7	20	13
39698	120	30	148	38			167	22	77	24	64	21	56	21	128:	18	58:	15	38	10	27	11	26	13	14:	16
40111	150	35	97	31	149	26	96	23	83	28	72	22	35	13	60	15		5	40	13	49	15	27:	12	23:	13
41117	59	30	61	37	42	40	89	29	44	24	44	21	36	21	22	18	23	15	37	16	21	15	17	14	31	22
41534	158	47					126	21	118	33	101	33							42	23	43	15				
44743	86	30	88	39	92	41	116	23	64	26	48	30	44	20	37	16	12	10	17	7	33	26	20	18	19	18
47839	77	28	94	29	59	22	31	11	22	10	22:	5	64:	3	18:	4	7:	2	31	12	11:	6	—	—	10	6
58050	154	46	140	46	133	38			107	31	111	27	66:	18	55:	13	18:	7			74	13	9:	8		
59088	98	27	105	37					d		—	—	19	7					—	—	—	—			d	
74280	102	21	106	32	92	25	79	17	71	19	64	17	59	14	35	10		4	28:	8	30	10	8	7	25:	12
87737	84	15	76	22	47	19	74	20	65	16	26:	9	27:	8	28	7	23	8	—	—		3	7	9		
87901	36	10	40	9	25	6	37	9	37	6	39	5	6	3	—	—	—	—	—	—	?					

89688	132 27	160: 28	124 30	122 21	71 18	76 18	78 24	49 14	28: 12	24: 4	40 12	7: 4	
91316	102 31	94 36	68 32	84 17	58 24	43 23	31 18	35 17	18 12	31 13	56 20	19 14	27 19
93521	156 18	138 14	85 11	91 14	47 6	70 8	54 8	18 4	2	79 12	9	— —	
100600b	131 25	125 28	105 24	83 16	72 18	111 22	55 12	25 7	16: 4	18 4	30: 12:	7 5	
100600f	78 19	51 15	79 14	8 3	47 13	37 11	14 6	2	— —	15 5	30 12	?	
109389	59 12	78 15	56 16	46 10	36 11	36 10	29 8	2	39: 3	7 5	10 5	2	?
120315	128 24	162 30	111 25	74 14	82 16	64 15	86 13	76 8	3	53 10	19 6	4	
147394	105 34	116 31	76: 33	41 13:	85 23	d	29 11	14 5	1	— —	25 16	15 12	
148184	106 20	136 28	128 28	?	47 13	74 17	51 14	29 8	21: 8	0	42 12	16 5	2:
148479	136: 26	171 26	132 29	166 21	69 22	100 23	88 15	67 10	3:	42: 12	50 12	22: 7	— —
149438	118 36	118 47	105 41	84 16	63 33	58 27	35 21	16: 8	11: 5	37 16	42 27	15 20	21 24
149757	110 14	85 11	90 13	69 14	41 6	17 4	35 4	27 3	2	53 9	25 5	10 4	— —
149881	106 33	98 31	92 26	108 24	65: 21	45 19	34 14	52: 18:	2	25 9	45 17	2	15 11
160762	134 42	138 53	132 49	106 21	91 34	79 34	69 27	51 19	25 11	36 16	24 25	22 29	18 27
162732	24: 11	47: 24	11:	bl	13 10	6 8:	6 10:	— —	— —	— —	— —	— —	
164353	86 37	51 36	31 33	68 21	44 24	42 22	32 20	30 20	24 16	44 17	26 14	14 17	19 20
167971	53 16	46 7		25 10	10 5	— —	23 5			10 4	— —		?
169454	84 29	61 34		53 14	53 29	39 15	18 11			13 9	36 18		11: 17:
187811	118 22	136 23	80 23	68 10	90 16	72 14	75 14	29 7			23 8		
190603	86: 32	59 31	63 30	92 24	61 29	32 20	27 17	27 11	17: 10	21 10	32 11	13: 9	28 20
191201	103 35	93 35	77 35	69 16	51 22	42 19	34: 11	24 7	4	22 12	33 14	9:	6 7
192422	94 28	74 30	90 29	85 18	51 20	44 17	31: 13	35: 11	11: 5:	28 10	39 20	4: 4:	25 18
193322	57: 23	88 25	72 22	57: 9	22: 11	15 11	2	13 7	— —	11 7	19 11	?	10 11
194279	117 35	95 43	68 32	79 22	99 40	33 20	38 24	20 16	58 18	15 7	37 25	23 15	34 22
194839	93 33	86 26		114 24	60 34	31 22	43 20	17: 7		25 12	27 15		19 16:
195592	122 37	83 37		90 18	48 18	52: 15	21 11	9: 5		37 4	25 10		23 9
197345	9: 9	6 10:											
198478	83 37	67 40	55 37	85 25	52 26	35 21	24 21	42 21	30 18	36 17	20 13	22 18	34 27
200120‡	87 10	97 16	110 17	93 11	56 7	75: 16	26: 5	51 6	13: 3	13 3			
204172	107 34	96 35	79 27	34 15	49 19	d	21 13	13: 5	10: 7	18: 12	50 17	26: 10	32 18
205021	138 36	119 42	118 38	103 19	74 30	68 28	51 22	45 14	23 8	42 13	51 22	19 15	22 13
206165	108 40	80: 40	94 43	87 34	57 30	42 24	48 21	50 19	32 17	60 17	43 22	21 18	42 23
208185	230 47	182 58	186 47		107 53	95 49	92 42	47: 15		14 13	40 40		24 28
208392	164 33	140 42		68 18	84 28	57 23	64 22	51 12		15 4	52 20		27 20
208947§	160 40	177 44	140 36	91 22	103 29	96 25	74 21	47 14	26 11	40 12	49 23	29 16	15 14
210809	125 31	94 27	84 26	57 14	41 18	22 9	24 8	15: 8	6	29 11	16 9	14 11	11: 13
210839	41 9	72 15	61: 14	?	6 4	2	— —	— —	— —	25 5	d	8 5	?
212455	94 41	70 34	120 47	76 21	45 26	50 31	26 21	32 20	9	39 21	16 13	8 9	21 22
212571	72 13	100 15	66 20	89: 14	47: 9:	42 10	16 10	4	3:	3:	37 9	1	— —
213420	125 33	141 40	119 37	90 24	82 28	75 25	79 24	74 22	27 13	56 15	56 20	22 11	23 20
214680	79 37	103 45	65 37	62 19	51 25	23 17	21 10	20 7	6 6	40 11	22 11	2 3	17 18
224151	69 18	79 21	73: 20	79 14	57 14	35 10	29 7	33 9	17: 6	36 11	43 12	12 8	4

NOTES TO TABLE III

* Line λ 4026.2 blends with λ 4025.64 He^+ in O-type stars.

† Value for λ 4009 is from V286. The line is asymmetric and over twice as intense on V397.

‡ A defect is suspected in λ 4144.

§ The line depths are from plate V306 taken when the similar spectra were coincident.

TABLE IV

HD No.	He		C+		N+											Mg+	Si+		Si++		
	4438	4169	4267	3920	4631	4614	4607	4601	4447	4242	4237	4044	4041	3995	3956	4481	4131	4128	4575	4568	4553
886	10	14	32	15	16	9	3	1	7	4	–	4	6	11	4	28	3	3	8	8	9
3360	16	8	16	14						–	–	11	7	15	7	25	–	–			
11415	9	6	25	18	3	–	–	–	–	–	–	–	–	3	–	38	8	10	–	?	?
13854	11	16	16	4	40	11	9	9	15	12	11	6	8	32	2	21	–	–	20	62	55
14134	18	–	18	?	47	15	30	30	15	16	15	9	8	33	2	35	–	–	20	37	53
24398	13	6	31	15	16	4	6	5	16	–	–	6	5	23	5	24	–	–	30	48	58
24912	–	–	–		–	–	–	–	–	–	–	–	–	3	–	8	–	–	–	–	–
28446b	–	–	1	3	–	–	–	–	–	–	–	–	–	?	–	7	–	–	–	–	–
28446f[1]	7	10	8	7	–	–	–	–	4	7	6	8	–	–	–	14	–	–	12	21	17
30614[2]	–	–	7	3	–	–	–	–	–	–	–	–	–	–	–	28	–	–	–	9	20
36371	18	17	25	12	2	–	–	–	?	–	–	3	9	15	3	61	25	19	7	14	16
36861	–	3	–	–	23	–	–	–	–	–	–	–	–	–	–	20	–	–	–	6	4
36862	2	–	19	?	–	–	–	–	–	–	–	–	–	5	–	10	2	1	–	4	18
37128	–	–	–	–	–	–	–	–	?	–	–	–	–	2	–	14	–	–	9	26	37
38771	–	–	2	2	8	2	6	11	12	–	–	4	6	11	?	28	–	–	5	36	47
39698	–	13	26	5	–	–	–	–	–	–	–	5	–	–	–	16	–	–	9	15	20
40111	14	?	–	–	–	–	–	–	?	–	–	–	–	9	–	4	–	8	14	40	55
41117	8	7	3	4	53	20	29	31	6	?	?	16	14	48	13	19	–	4	34	47	63
44743	–	–	21	9	13	–	–	1	5	6	5	–	–	12	1	9	?	?	32	59	58
47839	–	–	–	–	–	–	–	–	–	–	–	–	–	–	–	8	–	–	–	–	–
91316	11	9	22	7	30	3	5	9	19	10	6	12	11	28	6	23	?	–	20	37	48
149438[3]	–	6	8	3	–	–	–	–	6	10	8	4	8	14	1	5	–	–	4	12	24
149881	–	–	23	10	–	–	–	–	–	–	–	–	–	12	4	10	–	–	16	37	34
160762	12	10	27	14	3	1	–	2	2	–	–	–	–	5	1	39	9	6	3	5	12
164353[4]	6	?	30	10	6	–	–	–	–	–	–	1	1	6	6	36	20	25	5	6	10
169454	–	–	8	1	26	5	9	–	11	5	7	1	1	15	6	16	–	–	41	76	64
190603	16	9	14	4	47	20	30	30	16	14	9	3	4	41	14	32	4	1	d	48	83
191201	–	–	7	2	10	–	–	–	–	–	–	–	–	10	–	–	–	–	7	18	20
192422	9	6	11	5	7	–	–	–	6	4	1	3	3	16	–	2	–	1	24	60	68
194279	20	–	13	3	59	27	18	19	24	12	–	11	9	56	31	45	–	–	18	48	52
194839	10	3	26	6	12	–	–	–	–	–	–	25	–	13	–	8	–	8	11	32	51
195592	–	–	–	–	?	–	–	–	–	–	–	–	–	?	–	–	–	–	10	17	46
198478	12	2	27	14	17	6	5	8	7	10	6	3	2	27	6	46	11	8	9	8	17
204172	–	–	13	1	7	–	–	–	–	–	–	8	6	4	–	18	–	?	–	27	57
205021	–	–	22	12	?	–	–	–	2	4	4	11	12	13	8	25	–	–	17	19	31
206165	–	–	25	20	19	–	–	–	–	9	3	6	3	25	4	43	7	10	20	26	42
208185	8	–	23	9	–	–	–	–	–	–	–	–	–	5	–	d	12	14	–	–	–
208392	–	–	14	3	–	–	–	11	9	13	10	5	5	–	–	10	–	–	–	16	25
208947	11	7	26	10	–	–	–	–	–	–	–	–	–	3	–	31	6	4	–	4	9
210809	–	–	7	–	–	–	–	–	–	–	–	–	–	–	–	1	–	–	–	–	–
210839	–	–	–	–	–	–	–	–	–	–	–	–	–	–	–	1	–	–	13	4	1
212455[5]	2	2	29	13	–	–	–	–	–	–	–	–	–	19	–	73	24	24	–	–	–
214680	–	3	–	–	–	–	–	–	–	–	–	–	–	–	–	10	–	–	–	–	–
224151	–	–	14	4	3	–	–	–	–	–	–	–	–	4	–	4	–	–	12	27	36

NOTES TO TABLE IV

1. N^+ probably not present.
2. λ 4481 Mg^+ is diffuse on both plates.
3. Although there is no sign of the first four N^+ lines on our tracing, Marshall gives λ 4631, intensity 3, and λ 4614, intensity 1. λ 4631, which appears very diffuse on his reproduction, blends with a Si^{+++} line.
4. Defect suspected at λ 3956 N^+.
5. There is a line at λ 4641, but no other O^+ lines are visible.

TABLE V

OXYGEN LINES

HD No.	4676	4662	4650	4641	4417	4415	4367	4326	4320	4317	4276	4190	4076	4072	4070	3983	3973	3954	3945
886	10	9	19	6	–	–	7	1	4	9	3	8	11	8	10	6	2	7	5
3360[1]											–	–	13	7	11	–	6	1	1
13854	24	14	93	60	28	36	30	12	20	20	10	10	23	19	26	7	17	12	5
14134	20	15	75	43	6	6	10	9	6	9	9	–	22	20	5	6	8	6	4
24398	15	11	70	46	25	33	26	10	18	21	8	7	29	27	45	10	17	15	7
28446b	7	9	42	16	5	7	9	2	–	–	–	4	12	23	8	2	–	2	2
28446f	5	5	46	13	15	16	9	3	13	19	9	15	7	12	10	7	8	10	9
30614	–	–	13	–	–	5	6	–	3	–	–	–	6	5	8	–	2	–	–
36371	4	4	10	4	–	–	–	–	2	2	–	–	?	3	–	2	1	1	2
36861	–	–	21	–	–	–	–	1	–	2	–	–	11	3	7	–	–	–	1
36862	–	–	29	14	?	?	–	–	–	–	–	7	22	4	9	5	5	4	3
37128	8	8	38	19	9	2	2	–	14	1	–	–	19	8	12	–	–	–	–
38771	25	17	49	36	19	19	38	6	21	53	–	–	15	13	14	6	14	8	5
39698[2]	–	11	–	14	–	–	–	–	–	–	–	–	–	–	–	4	–	5	6
40111	14	29	67	46	22	30	16	1	–	–	–	–	23	17	24	7	d	7	5
41117[3]	22	11	54	40	11	13	13	1	8	6	–	–	12	4	5	1	21	3	4
44743	20	41	70	31	4	9	10	14	23	23	–	d	31	18	24	11	15	11	7
91316	24	24	73	64	24	24	21	6	19	12	5	7	27	23	27	4	15	6	4
149438	–	–	46	19	3	3	9	11	10	11	11	9	18	13	24	5	9	7	9
149881	29	24	53	30	32	–	10	5	11	14	4	13	23	14	21	5	2	7	3
160762	–	–	5	–	–	–	–	–	–	–	–	1	5	1	2	2	–	2	1
164353	–	–	8	6	–	–	3	–	4	3	–	?	–	3	–	2	2	2	–
169454	47	64	100	83	34	26	45	15	28	32	14	6	32	35	40	11	34	10	3
190603	28	38	80	56	26	31	32	–	38	19	8	–	18	21	23	7	24	5	6
191201	9	7	40	10	19	25	18	16	16	15	15	4	12	11	12	6	1	1	–
192422	20	9	66	47	11	13	18	3	11	13	4	9	16	20	24	5	d	9	12
193322	–	–	?	–	–	–	–	–	–	–	5	–	–	1	2	–	1	–	–
194279	12	7	41	38	2	2	23	11	20	10	–	–	17	15	15	11	9	1	1
194839[4]	23	28	80	55	24	30	25	–	18	7	15	11	15	14	15	3	1	–	1
195592	3	5	51	34	–	3	12	–	2	2	–	–	2	6	4	–	?	2	4
198478	4	–	9	8	1	4	6	–	8	6	1	–	2	7	8	2	7	3	2
204172	13	24	53	29	29	6	2	4	2	11	16	6	16	15	19	10	9	6	1
205021	8	4	51	14	3	5	13	3	10	15	–	9	19	16	22	10	11	9	10
206165	9	23	57	19	6	22	–	5	13	11	–	9	21	13	15	5	10	8	4
208185[5]	–	–	31	17	–	–	?	–	–	?	–	?	–	?	–	–	–	?	?
208392	24	12	34	9	2	2	9	6	8	8	4	11	31	5	20	3	17	–	–
208947	–	–	14	–	–	–	–	–	–	–	–	–	6	3	–	–	–	3	–
212571[6]	–	–	20	26	–	–	–	–	–	–	–	–	?	14	7	–	–	?	–
214680	–	–	22	5	2	–	–	9	10	6	–	–	9	9	17	–	2	1	–
224151	10	13	54	33	8	10	16	3	19	9	2	9	21	15	14	11	4	10	2

NOTES TO TABLE V

1. Lines in the region λ 4400 to λ 4700 have not been measured.
2. O^{+} lines doubtfully present.
3. λ 3973 has abnormal intensity on both plates. Marshall gives intensity 3, and intensity 2 for λ 3954, but does not note the other two lines of the multiplet.
4. The division of the blend λ 4650 between C^{++} and O^{+} is very provisional.
5. O^{+} lines may be absent.
6. All these lines are very uncertain.

TABLE VI

High Excitation Lines

HD No.	He^+			C^{++}			N^{++}				O^{++}	Si^{+++}	
	4686	4542	4200	4650	4187	4069	4379	4200	4196	4097	3962	4116	4089
886	–	–	–	–	–	–	–	–	–	–	–	?	7*
3360	–	–	–	–	–	–	–	–	–	?	–	–	4*
5394[1]	8	4	?	32	?	7	–	–	–	–	–	17	33
13854	–	–	–	–	–	–	2	?	?	9	–	12	26
14134	–	–	–	–	–	–	?	–	–	?	–	8	5
24398	–	–	–	–	5	10	–	–	–	9	2	15	30
24534	38	–	–	–	–	–	–	–	–	–	–	–	–
24912	41	54	29	40	2	6	?	–	–	?	4	7	22
28446b	16	5	?	53	6	8	–	–	–	–	–	27	34
28446f	10:	6	?	44	18	–	–	–	–	4	–	23	36
30614	10	25	25	76	14	9	10	bl	4	58	7	51	82
36371	–		–	–	8	–	–	–	–	3	–	–	–
36861	92	58	53	40	5	9	–	bl	3	35	12	21	52
36862	47	15	15	29	2	8	–	bl	–	2	–	–	21
37128	20	–	–	102	15	5	14	–	–	30	–	46	57
38771	14	–	7	56	11	16	?	–	–	31	4	37	58
40111[2]	19	–	–	25	–	–	11	–	–	?	–	18	42
41117	–	–	–	–	–	–	–	–	–	7	–	3	7
44743	?	–	–	10	d	4	–	–	–	15	1	6	23
47839	74	58	55	22	2	5	–	–	–	35	8	6	22
59088	em	136	78	–	–	–	–	–	–	–	?	–	–
91316	4	–	–	?	?	–	11	–	–	13	?	20	33
93521[3]	52	33	39	–	–	–	–	–	–	–	–	bl	43
149438	38	7	5	19	6	3	13	bl	2	13	?	18	32
149757	59	28	23	–	–	–	–	–	–	?	–	6	5
149881	8	–	–	46	12	–	–	–	–	8	–	11	30
167971[4]	em	47	8	–	–	–	18	–	–	26	–	13	29
169454	–	11	–	33	4	–	4	–	–	12	–	13	25
190603	–	–	–	12	3	3	7	–	6	8	?	9	16
191201	61	14	16	67	11	16	19	bl	?	24	?	40	61
192422	27	–	?	59	2	–	6	bl	1	43	–	35	52
193322	67	38	21	–	–	8	–	–	–	23	?	19	30
194279	–	–	–	?	–	–	–	–	2	9	?	7	3
194839[5]	7:	–	–	53	9	?	–	–	–	31	–	47	58
195592[6]	–	28	14	69	3	–	8	bl	2	57	–	55	92
198478	–	–	–	–	–	–	–	–	–	5	–	–	3*
204172	12	–	–	67	11	21	6	?	–	20	15	46	75
205021	–	–	–	–	–	–	–	–	–	?	–	9	26*
208185[7]	–	–	–	–	–	–	–	–	–	–	–	21	25
208392	–	–	–	–	–	–	–	–	–	17	–	10	11
210809	3	44	16	45	15	18	12	bl	8	58	22	30	64
210839	em	79	55	–	1	1	6	bl	–	13	1	d	3
212571	–	–	–	?	–	9	–	–	–	?	–	?	–
214680[8]	98	48	40	29	3	13	2	bl	?	25	11	25	37
224151	–	–	–	33	?	–	–	–	–	–	5	13	25

NOTES TO TABLE VI

* The O^+ line λ 4089.28 is responsible.

1. All intensities very uncertain, owing to extreme diffuseness.
2. The only evidence for C^{++} is the asymmetry and intensity of the blend at λ 4650.
3. λ 4116 Si^{+++} blends with λ 4121 *He*.
4. The N^{++} pair, λλ 4641, 4634, appear in emission.
5. The proportion of C^{++} in the λ 4650 blend is very uncertain. The abnormal intensity for λ 4044 N^+ is possibly due to a defect.
6. The complete absence of λ 4686 He^+ is surprising.
7. A B3 star. The two Si^{+++} lines are possibly, but not probably, defects. The Si^{++} lines are not seen.
8. The line λ 4213 Si^{+++} is also measurable (intensity = 5), which suggests a low gradient.

table[10] are collected in Table VIII, together with mean relative intensities for stars in which the lines of the various atoms are strong. The excitation potential, fourth column, is that of the lower level

TABLE VII*

INTENSITIES FOR STARS WITH FEW ABSORPTION LINES

HD No.	*He*		C^+		N^+	O^+		Mg^+		Si^+		Ca^+	Fe^+
								4481					
	4438	4169	4267	3920	3995	4650	4070	W	D	4131	4128	3934	4233
4180	–	–	20	4	7	24	–	31	9	13	9	–	–
5394	–	–	–	11	2	57	33	–	–	–		–	em
21291	–	–	22	10	?	–	–	95	40	43	39	74†	31
21389	–	–	5	5	4	–	–	79	26	28	26	77†	35
22928	24	–	–	–	–	–	?	30	8	8	7	7	
23480	–	–	18	9	–	–	–	17	5	13	10	4	
24760f						–		35	8				?
26125			–			–		35	18	–	–		–
32343	25	14	–	–	16	–	–	–	–	15	–	–	–
32630	–	–	28	10	8	–	–	52	15	10	13	–	–
34085	–	–	19	8	–	–	–	52	31	36	38	62†	23
35497	–	–	10	–	–	–	–	39	19	21	30	35	8
37202	15	11	–	–	19	34	29	41	13	18	12	18	12:
41534	25	6	30			–	–	40	20	8	8		–
58050	–	–	29	14	–	–	–	25		6	6	–	–
74280	–	?	16	5	1	11	–	30	10	11	10	–	–
87737	–	–	–	–	–	–	–	33	18	12	12	34†	14
87901	–	–	–	–	–	–	–	38	9	18	18	20	–
89688	49	10	51	18	?	–	15	28	9	14	–	14	–
93521	–	–	–	–	16	86	18	18	5	–	–		–
100600b	–	–	24	?	7	–	–	20	6	14	14	i	–
100600f	–	–	15	3	–	–	?	48	14	50	45	i	–
109387	–	–	–	–	–	5	–	32	10	?	?	–	–
120315	–	–	5	3	–	–	–	27	9	–	–	–	–
147394	–	–	28	d	–	–	–	49	18	10	28	–	–
148184	–	–	4	?	5	37	40	–	–	–	–	i	em
148479	–	–	9	3	9	16	–	20	7	–	–	i	–
149757	–	–	9	–	?	106	47	?	–	–	–	–	–
162732	–	–	9	–	–	–	–	38	14	29	29	36†	46
187811	–	–	–	–	–	–	–	36	7	–	–	15	–
197345	–	–										144†	
200120	–	–	9	–	–	33	–	–	–	4	3	–	–
212571	–	–	–	–	?	20	21	3	1	–	–	–	–
213420	–	–	38	5	–	11	–	26	10	8	6	i	–

* The second column for Mg^+ gives the line depth. The symbol "i" in the column for Ca^+ indicates an interstellar line.

† Perhaps partly interstellar.

involved. Important cases of blending are mentioned in the footnotes.

Comparison with previous measures for hydrogen is made in

[10] *A Multiplet Table of Astrophysical Interest*, Princeton, 1933.

TABLE VIII

Multiplet Data

λλ	Int. Lab.	Int. Star	E.P.	Multiplet
		C^+ I.P. = 24.3		
3920.68	8	10	18.0	$3p\,^2P^o - 4s\,^2S$
4267.02	8	25	18.0	$3d\,^2D - 4f\,^2F^o$
67.27	10			
		C^{++} I.P. = 47.7		
4068.94	7	9	39.7	$4\,^3F^o - 5\,^3G$
70.43	8			
4187.05	10	8	39.8	$4\,^1F^o - 5\,^1G$
4650.16	9	45*	29.4	$3\,^3S - 3\,^3P^o$
51.35	8			
		N^+ I.P. = 29.5		
3955.85	6	5	18.4	$3s\,^3P^o - 3p\,^1P$
3995.00	10	18	18.4	$3s\,^1P^o - 3p\,^1P$
4041.33	5	4	....	....
43.54	3	4	....	....
4237.98	6	3	....	....
41.80	8	5	....	....
4447.04	10	7	20.3	$3p\,^1D - 3d\,^1P^o$
4601.49	8	8	18.4	$3s\,^3P^o - 3p\,^3P$
07.17	7	8		
13.88	6	6		
30.55	10	16		
		N^{++} I.P. = 47.4		
4097.31	10	30§	27.3	$3s\,^2S - 3p\,^2P^o$
4195.70	5	2	38.5	$4p\,^2P^o - 5s\,^2S$
4200.02	6	2‖		
4379.09	10	11	39.7	$4f\,^2F^o - 5g\,^2G$
		O^+ I.P. = 34.9		
3945.05	5	4	23.3	$z\,^2P - e\,^2P^o$
54.37	7	6		
73.27	10	10		
82.73	5	6		
4069.64	4	17	25.5	$e\,^4D^o - z\,^4F$
69.90	6			
72.16	8	15		
75.87	10	17		

TABLE VIII—*Continued*

λλ	Int. Lab.	Int. Star	E.P.	Multiplet
O^+ (*continued*)				
4189.79	10	5	28.2	$e^2F^o-z^2G$
4275.52	4	5	28.7	$z^4D-e^4F^o$
4317.16	8	12	22.9	$y^4P-e^4P^o$
19.65	8	12		
25.77	3	5		
66.91	7	15		
4414.89	10	13	23.3	$z^2P-e^2D^o$
16.97	8	12		
4641.83	9	32†	22.9	$y^4P-e^4D^o$
49.15	10	52*		
50.83	6			
61.65	9	15		
76.25	8	14		
O^{++} I.P. = 54.9				
3961.59	8	....	33.7	$3s^1P^o-3p^1S$
Mg^+ I.P. = 15.0				
4481.14, 81.34	100	....	8.8	$3^2D-4^2F^o$
Si^+ I.P. = 16.3				
4128.05	8	16	9.8	$3^2D-4^2F^o$
30.88	10	16		
Si^{++} I.P. = 33.3				
4552.61	9	38	18.9	$4s^3S-4p^3P^o$
67.83	7	30		
74.75	4	14		
Si^{+++} I.P. = 45.0				
4088.86	10	38‡	24.0	$4^2S-4^2P^o$
4116.10	8	22		

* These C^{++} and O^+ lines blend badly in B0, B1. In each case the proportion of the blend to be assigned to each atom had to be estimated from the intensities of other unblended C^{++} and O^+ lines. The measured intensity is the sum of the tabulated figures.

† From the behavior of other lines it was decided that λλ 4640.6, 4641.9 N^{++} contribute negligibly to this line in all cases.

‡ The influence of λ 4089.28, O^+, is noticeable in B1, B2.

§ Proximity to $H\delta$ renders this line difficult in diffuse-line stars.

‖ The line blends with He^+ in O-type stars.

Figure 4. The agreement is, on the whole, satisfactory. Günther,[11] using an objective prism, measured intensities in 28 stars common to the present list. The average difference between his mean intensity for the lines $H\gamma$ to $H\zeta$ and ours is 15 per cent. His values tend to be larger than ours for weak lines and smaller for strong lines.

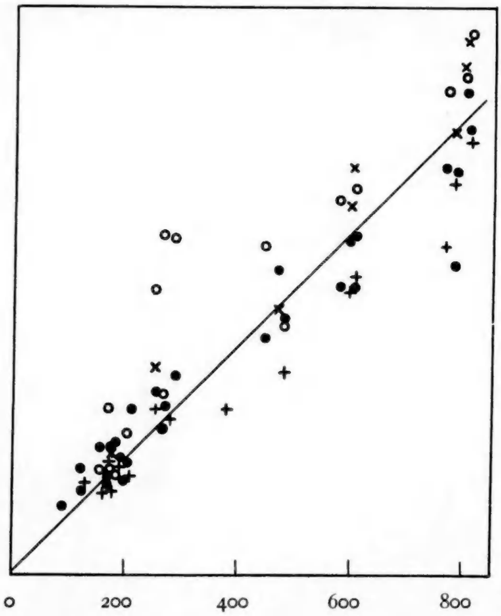

FIG. 4.—Hydrogen line intensities compared with other determinations. Oblique crosses, E. T. R. Williams; circles, Elvey; vertical crosses, E. G. Williams; dots, Günther.

Figure 4 also includes results from three other lists. These yield the following mean (numerical) percentage differences: Harvard[12] (8 stars, $H\gamma$, $H\delta$), 12; Yerkes[13] (16 stars, $H\gamma$), 34; Cambridge[14] (15 stars, $H\beta$, $H\gamma$, $H\delta$), 14. The Yerkes values for 10 Lacertae and 67 Ophiuchi exceed ours by a factor of more than 2. It is true that we have compared Elvey's measures for $H\gamma$ with our mean for four

[11] *Zs. f. Ap.*, **7**, 107, 1933.

[12] Miss E. T. R. Williams, *Harvard Circ.*, No. 348, 1929.

[13] C. T. Elvey, *Ap. J.*, **71**, 191, 1930.

[14] E. G. Williams, *Ann. Solar Physics Obs.* (Cambridge), **2**, 25, 1932.

lines; but when we come to compare relative line strengths, it will be seen that this procedure can account for only a very small part of the discrepancy.

Comparing our results with the unweighted means for 11 stars common to three other lists, we find an average percentage difference of 11.5 (arithmetic), or -5.9 (algebraic, Mt. W. *minus* mean); if the two very discordant Yerkes measures are omitted, these figures become 7.3 and -1.7, respectively. We conclude that our systematic errors are small.

V. BALMER-LINE INTENSITIES

In line with numerous previous investigations[9,15] and as has already been mentioned, we find that in the great majority of cases the intensity in a Balmer line is represented within the limits of error of measurement by the exponential formula

$$1-I_\lambda=(1-I\lambda_0)e^{-k(\lambda-\lambda_0)}\ ,$$

where I_λ is the intensity at wave-length λ, expressed in terms of the intensity in the hypothetical continuous spectrum, λ_0 the wave-length of the line center, and k a constant. Merrill and Wilson cite α Cygni and β Orionis as cases in which the exponential form of the wings continues almost to the line center. In the majority of stars, however, there is a certain bluntness at the center which seems to correlate with the appearance of other absorption lines, being most pronounced in stars graded as "nn."

In order to study the intensity variation in the Balmer lines with series number, the spectra have been divided into three groups, as follows:

a) Mean H intensity <300, type earlier than B1.0.

b) Mean H intensity <300, type later than B0.5.

c) Mean H intensity >300, types B0 to A.

For statistical treatment the intensity of each line in each star was expressed in terms of the mean for $H\gamma$ to $H\zeta$ in the same star. The resulting group-means for each line in the series appear in Table IX. The figures for each star have been weighted according to the number of spectra.

[15] Elvey, *Ap. J.*, **68**, 145, 1928; **71**, 191, 1930; Lindsay, *Harvard Circ.*, No. 368, 1931.

Under each Balmer line the first number is the percentage of total absorption; the second, in italics, the percentage depth expressed in the same manner; and the third, in parentheses, the number of lines observed. In deriving mean depths, lines which showed emission tendencies, either at the line center or in the wings, and also one or two others of low weight were omitted.

TABLE IX

RELATIVE INTENSITIES OF LINES IN THE BALMER SERIES

Group	$H\beta$	$H\gamma$	$H\delta$	$H\epsilon$	$H\zeta$	$H\eta$	$H\theta$	$H\iota$	$H\kappa$	$H\lambda$
a (early subtypes)	113.5 *87.5* (22)	104.4 *100.9* (24)	99.4 *102.9* (23)	99.4 *98.5* (24)	97.3 *96.2* (24)	101.0 *95.2* (16)	92.1 *87.5* (7)			
b (weak *H* lines)	101.8 *71.9*: (24)	103.1 *96.6* (25)	100.4 *101.6* (26)	97.1 *101.4* (24)	99.3 *99.9* (26)	111.0 *95.1* (20)	109.8 *92.5* (13)	96.1 *85.1* (11)	86.0 .... (6)	
c (strong *H* lines)	98.7 *83.7* (39)	100.8 *97.4* (42)	98.3 *100.2* (43)	101.1 *101.0* (43)	99.3 *101.0* (41)	98.8 *100.0* (13)	103.5: .... (4)			
All stars together	103.4 *82.3* (85)	102.4 *98.1* (91)	99.1 *101.2* (92)	100.4 *100.5* (91)	98.8 *99.4* (91)	104.5 *96.6* (49)	103.6 *91.5* (24)	93.7 *84.3* (15)	81.2 *75.9* (9)	75.8 *67.3* (5)

For completeness, we summarize below the somewhat meager published results for $H\alpha$. The figures, which are total intensities ex-

	B1–B2 (3 Stars) (Mean *H* Int. = 318)	B3–B8 (6 Stars) (Mean *H* Int. = 735)	A1–A3 (Weak *H* Lines) (3 Stars, Mean *H* Int. = 770)	A0–A5 (Normal *H* Lines) (14 Stars, Mean *H* Int. = 1460)
$H\alpha$...........	108.0	80.0	96.7	71.1
$H\beta$...........	97.4	94.5	97.4	91.7

pressed in terms of the mean for $H\gamma$ to $H\zeta$ in the same stars,[16] are based on Günther's[11] work with the addition of three measures made at Cambridge by the writer.[17]

Dealing first with the total absorptions, we find that in the B stars the mean equivalent widths in angstroms for each of the six lines $H\gamma$ to $H\theta$ coincide within the limits of their probable errors. For lines

[16] Except for the dwarf A stars, where the mean intensity is found from $H\gamma$, $H\delta$, and $H\epsilon$ only, as $H\zeta$ may blend in the wings.

[17] *M.N.*, **95**, 182, 1934.

farther down the series the intensity drops rapidly with increasing serial number. This result is based on those lines only in which there is no overlapping. In the case of $H\beta$ there is a marked rise of 13.5 per cent in total intensity for the hotter stars with weak hydrogen lines, and it is probable that the intensity for $H\alpha$ is also high. The other two groups, (*b*) and (*c*), do not show the effect: $H\beta$ is no stronger than the following lines, while for $H\alpha$ in the B dwarfs there is a pronounced drop. This low relative intensity for $H\alpha$ is very marked in normal (dwarf) A stars, though it is almost absent in the more luminous group of similar type.

The behavior of line depths in the series is somewhat similar to that of total intensities. In each group three or four lines are nearly equal; then follows a very regular drop in depth till the lines become mutually blended. A tendency is apparent for the deepest line to be farther down the series for dwarfs than for giants, and for cooler subtypes than for hotter. Further, in each group the depths begin to fall away from the flat maximum about two lines earlier in the series than do the total absorptions.

The effect of reduced purity at $H\beta$ is marked for the very sharp lines in B2 to B8 giants; the 28 per cent depth decrease may be wholly spurious even, as may also be a considerable part of the $12\frac{1}{2}$ per cent drop for the hottest group. In the dwarfs, however, the small relative depth for $H\beta$ is largely real, a finding supported by two reliable measures for $H\alpha$, giving a relative depth of only 65 per cent. The same figure was also found for ζ Persei, a B1 giant.

No interpretation of these results can be expected until a theory explaining the high central intensities has been produced. A promising start has been made by invoking fluorescent emission following the capture of free electrons. With this mechanism Woolley[18] finds satisfactory agreement in the case of $H\beta$ in the sun, and Strömgren[19] obtains large intensities in other strong solar lines. But the theory has not yet been extended to cover the lines in B-type stars. It may be necessary to take into account also free-free electronic transitions producing continuous spectra in the upper atmospheres. Finkelnburg[20] points out that such radiation will be particularly plentiful in turbulent atmospheres such as may be expected in hot stars.

[18] *M.N.*, **94**, 631, 1934. [19] *Zs. f. Ap.*, **10**, 237, 1935. [20] *Ap. J.*, **80**, 313, 1934.

Meanwhile it is gratifying to find three points of correspondence with the recent calculations of Pannekoek and Verwey[21] on Stark effect in the Balmer lines:

1. Their published curves are exponential in shape to as close a degree as are the observed contours.

2. Their total absorptions in a star at a temperature of 16,800° increase by only 2 per cent in passing from $H\beta$ to $H\delta$. In normal A-type stars they find a total absorption for $H\alpha$ which is 28 per cent less than that for $H\gamma$; this prediction agrees excellently with the data given above.

3. The figures in their Table II represent in a general way the variation in line width with both temperature T and surface gravity g. Qualitative accordance is good for the normal A-type star, but the theoretical half-width at $r=0.9$ in early B types ($\log g=3.6$) is twice the observed (this is for sharp-line stars). Similarly, the predicted luminosity effect in A stars is too small. For α Cygni the observed half-width at $r=0.9$ is 3.42 A. Even with a temperature as high as 12,000° the mass required by this half-width on their data is only seven times that of the sun, while with the more probable figure of 8400° it is less than unity.

I wish again to express my warm gratitude to Dr. Adams for the facilities given to me at Mount Wilson; also to Dr. Olin Wilson for making tracings of three stars for me after I had left the Observatory. My stay in Pasadena was rendered possible by the grant of a fellowship on the Commonwealth Fund.

Carnegie Institution of Washington
Mount Wilson Observatory;
Trinity College, Cambridge
November 1935

[21] *Proc. Amsterdam Acad.*, **38**, 479, 1935.

CLASSIFICATION OF THE B-TYPE STARS*

E. G. WILLIAMS

ABSTRACT

The Draper system of classification is reviewed. Classification methods based on line intensities and on line ratios are distinguished, and objections to the former are raised. The principles to be observed and the procedure to be followed in using line ratios based on measured intensities are discussed. Seven ratios, most of which involve numerous lines of several elements, are set up, which apparently give a good index of average characteristics. Usually three ratios are applicable in any one case and their accordance is good. The stars observed having been reclassified, intensity-type and intensity-luminosity variations are examined for each atom. The very smooth progression of type of maximum with ionization potential substantiates the ionization-temperature basis of the classification.

For stars belonging to the main sequence, hydrogen shows a steady, fivefold increase in total absorption in passing from the earliest types to class A. Very luminous stars retain roughly the same low hydrogen intensity in all subtypes, and in class O the two groups are indistinguishable. The real central intensities in sharp-line stars decrease regularly from 60 per cent at O8 to 20 per cent at A0.

An absolute-magnitude effect similar to that for hydrogen is found for all helium lines. This observation, together with the intensity variations with serial number in the two diffuse series, supports the view that the lines are subject to Stark effect. A twofold increase occurs between O8 and B1 in the singlet-triplet ratio for the diffuse series, but no luminosity effect on this ratio is detected. The evidence is not against a similar fading-out of the sharp singlets with respect to the sharp triplets as the temperature increases.

Ten diagrams are given connecting type and intensity for metallic atoms. N^+, Si^+, Mg^+ show a very pronounced luminosity effect, the lines being stronger in the brighter stars. C^+ alone shows no such influence. For N^+ and O^+ the gradient effect is examined by grouping stars and treating the line intensities statistically. There is a progressive increase in gradient with luminosity. No appreciable difference is found between stars with sharp and nebulous lines, nor between types earlier and later than the maximum for O^+.

A statistical discussion of the proper motions and radial velocities of 56 stars with measured interstellar K lines establishes the linear relation:

K = K-line intensity = 0.37 equivalent angstroms per kiloparsec. Thus the expression

$$M = m - 12.2 - 5 \log K$$

may be used to compute absolute magnitudes.

The material (78 stars) is next divided into six type- and luminosity-groups solely from spectral criteria (neglecting K-line intensity). Mean absolute magnitudes derived for these groups from parallactic motions and the galactic rotational term and also from K-line intensities justify the spectroscopic division into the luminosity groups. To the brightest groups is assigned uniformly an absolute magnitude of -5.5, and a difference of 3 mag. is established between these groups and the low-luminosity group in early subtypes, and of more than 4 mag. for this group at B5.

Table VIII gives collected results for each star, including absolute magnitudes from both spectrometric grouping and K intensity. Comparison of these assigned magnitudes with those obtained from published spectroscopic parallaxes shows a serious systematic divergence, the range in our values being 2 mag. greater.

* *Contributions from the Mount Wilson Observatory, Carnegie Institution of Washington*, No. 541.

Some peculiar spectra are commented on. Three Bne stars are found to have abnormally low total line intensity for their type. Of especial interest is the nucleus of the giant planetary NGC 1514, which has hydrogen lines as strong as those in a B8 dwarf, while both He^+ and Mg^+ are prominent.

Suggestions are made for the extension of the classification system adopted here to visual work on unstandardized spectra.

This paper attempts to find spectroscopic criteria of temperature and surface gravity. The spectral classification discussed is based on the observational material of the preceding paper, *Mount Wilson Contribution* No. 540.[1] When the behavior of the lines of the different atoms with respect to the revised type is examined, clear indications of absolute-magnitude effects are revealed which enable stars to be classed as "giants," "intermediates," or "dwarfs." In section III we attempt to establish these divisions on the basis of non-spectroscopic criteria, and to derive individual absolute magnitudes.

I. THE ASSIGNMENT OF SPECTRAL TYPE

The problem of the classification of the B-type stars has been discussed recently by numerous writers.[2] It is felt generally that there are unsatisfactory features in the present methods. The Henry Draper system,[3] which still forms the basis for almost all other classifications, is essentially one in which the absolute intensities of the absorption lines of an element, *and also* their intensities relative to those of other elements, are arranged in a continuous sequence.[4] The practical application of this system to the early-type stars is much as follows: Certain bright stars first photographed on large dispersion objective-prism plates have been defined as standards of Harvard subtype. Observers using slit spectrographs of moderate dispersion classify with reference to these standard stars largely by intensity ratios ("revised" types), whereas the great majority of faint stars have been classified in the *Henry Draper Catalogue* from objective-prism plates of such small dispersion that only the hydrogen and

[1] *Ap. J.*, **83**, 279, 1936.

[2] See R. H. Curtiss, *Handbuch d. Astrophys.*, **5**, Part I, 1, 1932; also, Edwards, *M.N.*, **87**, 364, 1927; Payne, Anger, Maulbetsch, and Wheelwright, *Harvard Circ.*, No. 365, 1931; Struve, *Ap. J.*, **78**, 73, 1933; Russell, Payne-Gaposchkin, and Menzel, *ibid.*, **81**, 107, 1935.

[3] *Harvard Ann.*, **91**, 1, 1918.

[4] For instance, we find in the Draper statement: "B3: . . . . *H* lines are 0.5 as intense as in *α* Canis Majoris. . . . . B5: . . . . Line 4481 is 0.7 as intense as 4471.5."

stronger helium lines are seen, with the result that types have been judged largely from the absolute intensities of these lines.

The system, when applied to the B stars, may be criticized on two main grounds. First, as has long been recognized, the one parameter, temperature, is insufficient to account for the details of these early-type spectra; the Draper statement takes no account of the widely different characters of absorption lines, which, though they may have the same total intensity, are deep and narrow in one star and shallow and broad in another of the same subtype. And, second, it is found that the various criteria of the method are, for a number of stars, mutually inconsistent.

In order to meet the difficulty about line character, it is customary to add symbols to the type describing their appearance. It should be noted, however, that these line grades refer primarily to the cores of the lines and ignore the wings, which, especially for hydrogen and helium lines, contribute the greater part of the intensity. Thus, for γ Pegasi and 55 Cygni, which are classified as B2ss and B2s by Pearce, the ratio of total absorption to depth for the hydrogen lines is 8.3 and 2.7, respectively. γ Pegasi is physically more closely related to stars with nebulous rotationally broadened lines than to a supergiant such as 55 Cygni.

It is important to realize that line-ratio methods must be clearly separated from absolute-intensity methods. Stars in which classification ratios are identical show wide variation in the total absorption of the lines involved.

Two methods based on absolute intensities only have been suggested, largely to meet the difficulty of conflicting criteria which appear even when ratios alone are used. The first of these, favored by the Harvard workers,[5] uses the strength of the hydrogen lines. The criterion has this to recommend it, that it gives at the same time a very fair measure of luminosity, because *H*-line intensity bears a much closer relation to absolute magnitude than it does to Draper type. It will, however, bring stars together which are widely separated on present standards. For example, 67 Ophiuchi, Harvard B5p, will fall with normal B1 stars. Struve,[6] on the other hand, concluded that a system based on the intensity of λ 4471 *He* would pro-

[5] Payne, Anger, Maulbetsch, and Wheelwright, *op. cit.*

[6] *Op. cit.*, p. 85.

vide for the arrangement of spectra in an unambiguous order with reference to which all peculiarities could be discussed. The present investigation shows that the helium lines also are subject to a luminosity effect; in addition, helium attains a maximum around type B3, which means that Struve's method must be restricted to the late-B types if any semblance of the present order is to be preserved. There appears to be no line suited to the definition of a type sequence without a radical upsetting of the accepted scheme.

In this connection it is worth noting that some recent work of Barbier, Chalonge, and Vassy[7] on the intensity of the continuous hydrogen absorption at the head of the Balmer series suggests that this may provide the desired type criterion. Since Stark broadening, which so greatly affects the Balmer lines, is here absent, the luminosity effects disappear. For the B stars the smooth progression of absorption at the series limit with spectral subtype is quite remarkable.[8] The list of these observers includes one object here rated as a giant, one dwarf, and seven normal stars.

The classification scheme tried for the present study is based wholly on intensity ratios. In forsaking a single criterion it is best to recognize, as Morgan[9] found in the case of type A, that the B stars are a very mixed lot, and therefore to try to devise ratios based on lines of as many elements as possible. The main desiderata are criteria which shall arrange the stars in an ionization-temperature sequence without being sensitive to luminosity or abnormalities. A system based on theoretical line ratios would be desirable, but at the moment appears impracticable. The resulting sequence naturally parallels closely the Draper system; but, since many more lines are here utilized, it should give a more precise index of average characteristics for both normal and abnormal objects.

The range of usefulness of a line for classification ratios is roughly that over which its intensity varies unidirectionally. As most of the lines here used show maxima in type B, it has been necessary to use as many as seven ratios. A smoothing of measuring errors in the case of ratios involving weak lines was effected by the following pro-

[7] *J. de Phys.*, Sér. VII, **6**, 137, 1935.

[8] Be stars and possible B-type white dwarfs will, however, need special treatment.

[9] *Pub. Yerkes Obs.*, **7**, 133, 1935.

cedure: For each atom the sum of the intensities of all observed lines in the given star was expressed in terms of its maximum in the spectral sequence. (The mean B8 intensity replaced the maximum for Mg^+, Si^+, Fe^+.) Next, these reduced intensities for the atoms whose lines increase in strength with decreasing temperature were added and divided by the similar sum for those atoms with lines of decreasing intensity. For example, in the ratio, conveniently designated by $Mg^+ \, Si^+ \, Fe^+/C^+ \, N^+ \, O^+ \, Si^{++}$, the summed intensity for atoms represented in the numerator increases eightfold from B1 to B8, while that for atoms in the denominator decreases steadily almost to zero. Actually in this case the ratio is essentially $Mg^+ \, Si^+/C^+$; the added ions merely give weight to the ends of the curve connecting ratio and type.

The complete list of ratios and their values for each subtype are given in Table I. The second line gives the ratio of the mean depth of the three ^3D lines of helium to the mean depth of the hydrogen lines $H\gamma$ to $H\zeta$. This ratio is more useful than that of the total absorptions because the latter ratio depends markedly on luminosity, so much so, in fact, that B7 giants fall with B3 dwarfs. Further, it is probable that the depth ratio corresponds more nearly to visual estimates, since the eye is more influenced by depth than by total absorption, much of which passes unrecognized in the wings. In the last ratio, which is really a combination of Plaskett's[10] two type-criteria for the *O* stars, the hydrogen figure is halved, to make it comparable with the mean diffuse triplet intensity for helium.

It is well known that the classes B4, B6, and B7 are not used in the *Henry Draper Catalogue*. In the Victoria classification also, the numbers of B3 and B5 stars are out of all proportion to those in adjacent subtypes, as the following figures[11] show: B0, 66; B1, 50; B2, 130; B3, 374; B4, 9; B5, 240; B6, 13. Such fluctuations are artificial and indicate merely that the criteria defining some subdivisions cover wider spectral ranges than do those defining others. The curves on

[10] *Pub. Dom. Ap. Obs.*, **1**, 325, 1922.

[11] From a count in *Pub. Dom. Ap. Obs.*, **5**, 99, 1930. Much more uniformity is, however, shown by the Mount Wilson revised types (Adams and Joy, *Mt. W. Contr.*, No. 262; *Ap. J.*, **57**, 294, 1923). Edwards' latest figures (private communication) also show a greatly improved smoothness, though the number of B3 stars remains excessive.

TABLE I

CLASSIFICATION RATIOS

Ratio	O7	O8.0	O9.0	B0.0	B1.0	B2.0	B3.0	B4.0	B5.0	B6.0	B7.0	B8.0
a) $\frac{He}{H}$ †	......	......	......	......	......	......	0.27*	0.21*	0.17*	0.13*	0.09*	0.07*
b) $\frac{He}{H}$ (depths)	......	......	......	......	......	0.82	0.74	0.60	0.47	0.36	0.27	0.16*
c) $\frac{Mg^{+}Si^{+}Fe^{+}}{C^{+}N^{+}O^{+}Si^{++}}$	......	......	......	......	0.0	0.2	0.5	1.1	1.9	4.0	7.5	12.5:
d) $\frac{N^{+}O^{+}Si^{++}Si^{+++}}{Mg^{+}\,Si^{+}}$	......	......	......	17:	8.1	2.9	0.7	0.1	0.0			
e) $\frac{C^{+}N^{+}O^{+}}{C^{++}N^{++}Si^{+++}}$	......	0.0	0.15	0.5	1.6	∞						
f) $\frac{C^{++}Si^{+++}}{O^{++}}$	0.5	1.3	2.8	5.1	8.5							
g) $\frac{He^{+}}{He_{2}^{H}}$ †	0.35	0.21	0.12	0.05	0.01							

* These figures are inapplicable to c stars.

† Equivalent widths in angstroms used for these ratios.

which Table I is based have been adjusted so that in dealing with a large typical section of stars the numbers assigned to each spectral subdivision should increase smoothly with advancing type. Victoria B2 corresponds to B2.0 in the present arrangement.

The adopted measured types are listed in the seventh column of Table VIII. In general the different ratios were accordant, but no attempt to classify more closely than to half a subtype was warranted. Cases of marked discordance between ratios are noted at the end of the table.

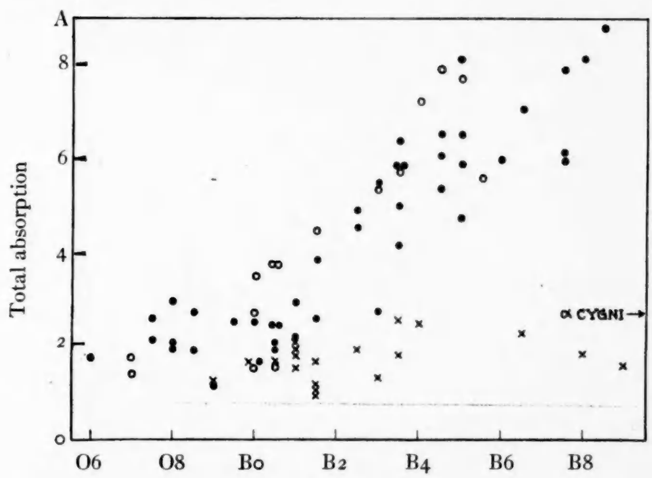

FIG. 1.—Variation of Balmer line intensity (equivalent width in angstroms) with spectral type. Crosses represent giants; dots, intermediate stars; and circles, dwarfs.

II. INTENSITY VARIATIONS WITH TYPE AND LUMINOSITY

Hydrogen.—The variation of total absorption for hydrogen is shown diagrammatically in Figure 1, where the mean intensity of the Balmer lines $H\gamma$ to $H\zeta$ for each star is plotted against the newly derived spectral class. Here, and in the following figures, the giants are indicated by crosses and the stars of abnormally low luminosity by circles, while intermediate or uncertain cases appear as dots.[12] It is of particular interest to note that for types later than B0 there is a well-marked separation of the very luminous stars from the normal B's,

[12] The assignment of stars to these luminosity groups is discussed farther on.

and that the normal stars have much stronger hydrogen lines. I can find no *measured* intensities occupying the wedge-shaped space between the two groups of B stars, though η Leonis, classed as A2 (Mount Wilson) but possessing reasonably strong helium lines, falls centrally in the gap with hydrogen intensity 473 units.

In class O the two groups merge completely; and two nuclei of planetaries, having absorption lines of hydrogen and absolute magnitudes in the neighborhood of +1, are not appreciably separated from typical O-type stars some hundred times more luminous.

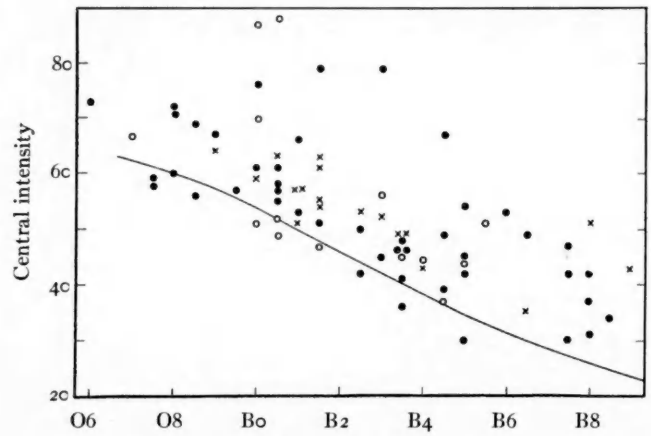

FIG. 2.—Relation between central residual intensity in the Balmer lines and spectral type. The curve represents the estimated mean relation for dwarf stars with perfectly sharp lines.

The giants of all subtypes retain roughly the same low hydrogen absorption. A curve published by Miss Payne[13] also illustrates this point.

Perhaps even more striking is the run of line depth with spectral type (Fig. 2). The high central intensity of the *H* lines in early B-type stars[14] is abundantly confirmed. With one possible exception no central intensities below 50 per cent are found for any star earlier than B0.5. This fact is not to be explained as a filling of the line center

[13] *The Stars of High Luminosity* (1930), p. 269.

[14] C. T. Elvey, *Ap. J.*, **71**, 191, 1930; E. G. Williams, *Ann. Solar Physics Obs., Cambridge*, **2**, 25, 1932.

through rapid axial rotation, as stars with perfectly sharp lines show the same high intensity. Stars in which the "dish-shaped" appearance of the weaker lines has been ascribed by Shajn and Struve[15] and Elvey[16] to such rotation all fall well above the curve drawn to represent the probable true depth in dwarfs. The tendency for the giants to have shallower lines is real; only a fraction of the difference can be accounted for by instrumental filling of their narrower lines.

Helium.—Lines of five different *He* series are included in our measures. Of these the diffuse triplets are always the strongest, and for

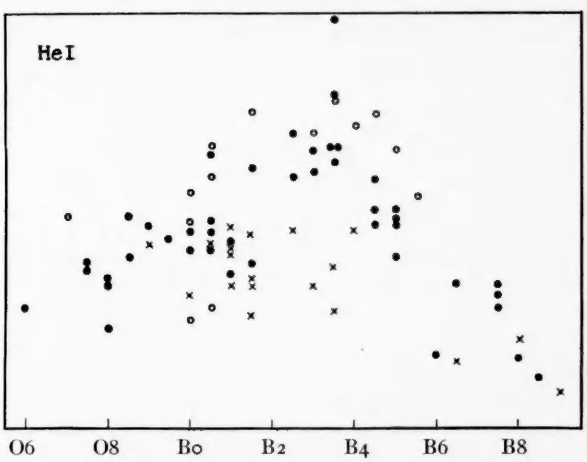

FIG. 3.—Variation with spectral type of total absorption in the diffuse triplet lines of helium. The two circles of low absorption at B0.0 and B0.5 represent the bright-line stars X Persei and γ Cassiopeiae.

each star the mean strength of the three lines λλ 4471, 4026, 3820 has been taken as the most suitable and dependable measure of helium intensity. This mean intensity is plotted against spectral type in Figure 3. The large amount of scatter in each subclass is remarkable. Maximum and minimum values in type B3 differ by a factor of more than 3. An absolute-magnitude effect similar in sign to that found for the *H* lines extends from the earliest types (within which the helium criterion is capable of distinguishing giants from dwarfs although hydrogen intensity is not) to type B5 at least, although the

[15] *M.N.*, **89**, 222, 1929. [16] *Op. cit.*, p. 221.

effect must reverse before class A, in which the c stars alone show helium. Miss Payne[17] and Struve,[18] on the other hand, both found a positive luminosity effect for helium.[19]

For the giants the flatness of the maximum is remarkable; it extends from O9 to B4, in marked contrast to all our other curves. There is some indication that the maximum shifts from B3.0 in the case of dwarfs to B2.0 for giants. Elvey[20] put the maximum at B2.5, but Miss Payne[21] finds a shift from B1.5 for normal stars to B5 for supergiants.[22]

It is convenient to study the behavior of the individual lines in each series with respect to the diffuse triplets. To do this, the total intensities and depths of each line have been expressed in terms of the mean diffuse-triplet intensity in the same star, and are denoted by w and d. For statistical treatment the material has been divided into the four intensity-type groups of Table II. The last column of this table gives the ratio of relative area to relative depth for the 20 stars with plates of greatest weight. This ratio is a measure of the relative line width. For λ 4922, λ 4713, and perhaps for λ 4471, the figures are too high through lack of instrumental purity.

In the case of the Balmer lines we found that Stark effect seemed capable of explaining the relative line intensities. For helium also the data are on the whole favorable to the idea that Stark effect influences the intensities. In supergiants where mol-electric fields are smallest, the helium lines weaken regularly as the series number increases. The present data for lines in the photographic region (Table II) are supplemented by published results[23] for the visual region in the c stars ζ Persei and β Orionis. These show that λ 5876 (D3), the leading line of the diffuse-triplet series, is its strongest member and that in ζ Persei the first line of the diffuse singlets at λ 6678 has relative intensity as high as 140. In the early-

[17] *Op. cit.*, p. 268, Table XV, XIII.

[18] *Op. cit.*, p. 82.

[19] Later objective-prism work at Harvard showed a negative effect earlier than the helium maximum and a positive effect in later types. See n. 5.

[20] *Ap. J.*, **70**, 141, 1929.

[21] *Op. cit.*, p. 280.

[22] From the ionization potential the maximum would be expected at B3.3.

[23] E. G. Williams, *M.N.*, **95**, 182, 1934.

type group with weak lines (giants) the intensity for the second singlet at λ 4922 is 107, which drops to 62 for the third at λ 4388.

But in the dwarf (high helium intensity) stars of type later than B2.0 we find maxima, pronounced at the third member in the case of

TABLE II

MEAN RELATIVE INTENSITIES FOR HELIUM LINES

(Expressed as Percentages of the Mean Intensity and Depth of the Diffuse Triplet Lines)

Lines	Types O6 to B1.5						Types B2.5 to B8						w/d*
	Intensity below Normal			Intensity above Normal			Intensity below Normal			Intensity above Normal			
	w	d	No. of Stars	w	d	No. of Stars	w	d	No. of Stars	w	d	No. of Stars	
$2^3P^o - m^3D$													
λ 4471	107.9	*95.2*	15	113.1	*101.7*	18	114.3	*100.6*	10	98.6	*90.8*	25	1.08
4026	100.3	*105.8*	15	98.2	*105.9*	18	103.6	*99.7*	10	109.0	*108.7*	26	0.97
3820	91.4	*97.9*	12	88.3	*91.6*	14	83.4	*95.8*	10	92.0	*101.3*	23	0.96
$2^1P^o - m^1D$													
λ 4922	106.3	*67.2*	15	67.9	*44.4*	18	94	*65*	9	71.6	*56.4*	24	1.46
4388	64.4	*72.9*	14	51.8	*62.0*	17	76	*68*	9	63.8	*68.7*	25	0.93
4144	46.1	*62.0*	15	40.9	*51.4*	17	70	*64*	9	58.8	*65.1*	24	0.82
4009	40.8	*47.3*	14	30.1	*40.0*	18	42	*53*	9	48.0	*53.8*	25	0.83
3927	36.4	*36.8*	14	26.8	*27.6*	18	45	*48*	9	37.5	*34.5*	24	1.00
3872	25.9	*28.8*	12	10.8:	*13.3*	16	30	*32*	9	23.5	*23.7*	21	0.73
$2^3P^o - m^3S$													
λ 4713	34.1	*36.7*	15	31.8	*35.9*	18	47	*38*	6	27.8	*33.0*	20	0.92
4121	44.4	*53.3*	15	33.4	*44.2*	18	37	*45*	7	27.4	*43.2*	24	0.77
3867	18.7	*33.3*	13	15.7	*26.9*	15	23	*39*	7	17.1	*34.4*	19	0.43
$2^1S - m^1P^o$													
λ 3965	29.0	*51.2*	13	18.4	*41.5*	16	39	59	7	14.4	*48.6*	9	0.46
$2^1P^o - m^1S$													
λ 4438	17.0	.....	8	6.2	.....	5	14	.....	4	14.4	.....	11	0.73
4169	8.3	.....	8	5.4	.....	5	9	.....	4	6.3	.....	11	0.38

* Twenty stars of weight 3.

the triplets, and suggested for the second line at λ 4922 in the singlets.[24] The decrease of both intensity and depth from λ 4922 to the

[24] This initial increase and final decrease with serial number was first noticed, for all series, by Struve (*Ap. J.*, **70**, 97, 1929).

last line observable is very regular, though the total line-width remains approximately constant. For the leading triplet line, D_3, two Cambridge measures for the dwarf stars η Ursae Majoris and α Leonis gave relative intensities as low as 50; also, the singlet λ 6678 was weaker than λ 4922.

The work of Ishida and Kamijima[25] has shown that the leading lines in helium series are relatively less affected by Stark effect than is $H\alpha$ with respect to other Balmer lines.[26] As Pannekoek and Verwey[27] predict that for hydrogen Stark effect produces a small initial intensity increase with series number, we may expect a rather greater enhancement from the first to the later series lines in helium. The above-noted differences between giants and dwarfs are therefore such as might be anticipated.

With Stark effect operating in the dwarfs, it is not surprising that the luminosity effect in the diffuse series is similar to that for hydrogen. For the two sharp series the enhancement in intrinsically fainter stars, though less in amount, is still present.[28] Hence, the intensity-type relation shows less scatter than Figure 1. The case for Stark enhancement of the two rather weak sharp singlet lines is, however, not clear, since in the laboratory λ 4169 is much more subject to electric fields than λ 4438, whereas our measures, though individually rather uncertain, plainly show the latter line to be stronger and more diffuse. An intensity ratio of 2+, similar for giants and dwarfs, is obtained when some allowance is made for a weak O^+ line at λ 4169.2. Actually, the last observed members of both sharp series are the two sharpest lines measured.

It will be noticed that in the diffuse singlets the depths decrease much more rapidly with series number for the dwarf than for the giant group. Thus for seven well-known c stars the mean depth ratio 3872/4414 is 0.63, while for five undoubted dwarf, or "normal,"

[25] *Sci. Papers Inst. Phys. and Chem. Research*, **9**, 117, 1928.

[26] This suggests that these leading lines are to be preferred as indices of helium abundance.

[27] *Proc. Amsterdam Acad.*, **38**, 479, 1935.

[28] The sharp singlets are about 15 per cent stronger in dwarfs. The figures for the principal singlet at λ 3965 are misleading. The line blends with $H\epsilon$ and the intensity tends to be underestimated, more so in dwarfs than in giants.

stars of similar type it is only 0.33. But in both these selections the total widths of the lines in angstroms decrease only slightly toward the ultra-violet.

The extra diffuseness of λ 3927 shown by the high value of w/d is somewhat puzzling. This diffuseness, common to all groups, was noticed on numerous tracings at the time of measuring.

A very noteworthy feature in helium, first noticed by Struve,[29] is the change with spectral type of the intensity ratio for singlet and triplet lines of the diffuse series. Elvey's[20] photometric measures showed up well the low relative intensity of the singlets in O-type stars, and the phenomenon has been further commented on by Marshall[30] and by Struve,[31] who has recently modified his earlier suggestion that the gradient effect was involved to an explanation in terms of departures from thermodynamic equilibrium.

The character of the variation is well shown by Figure 4, in which the ratio (mean intensity of 4388, 4144)/(mean diffuse triplet intensity) is plotted against spectral type. From O8 to B1 there is a twofold increase in the ratio, while for λ Cephei, O6, the singlets are relatively only one-eighth as strong as in B3 stars. Struve further suggested that the phenomenon might depend on the line intensity. This is not the determining factor, however, as the type relation is independent of luminosity. The abnormally high ratio for HD 14134, gB1, appears to be genuine. There is some evidence that the singlet-triplet ratio behaves in a similar manner for the sharp series, as the singlets could be detected in only one O-type star.

Lines of other elements.—As already mentioned, the individual intensities of the weaker lines are subject to considerable uncertainty. Nevertheless, the integrated intensities in cases where several lines of an atom have been measured are generally reliable and bear an almost linear relation to the intensities of the strongest lines of the atom. In order to weight lines in different parts of the spectrum according to the dispersion, these integrated intensities, which have been used already for classification purposes, were expressed in "tracing units" without correction to equivalent width in ang-

[29] *Nature*, **122**, 994, 1928.

[30] *Pub. Obs. U. Michigan*, **5**, 137, 1934.

[31] *Ap. J.*, **74**, 248, 1931; **82**, 252, 1935

stroms. The diagrams, Figures 5 and 6, show these intensities plotted for each atom against measured spectral class. The ordinates are arbitrary and on different scales for each atom. As in the figures for hydrogen and helium, crosses and circles represent giants and dwarfs, respectively. In drawing mean curves, points representing a few stars such as γ Cassiopeiae, Bonne, and π Aquarii, B1nne, were ignored, since, owing to the extreme diffuseness of the lines, the measured intensities are undoubtedly too small.

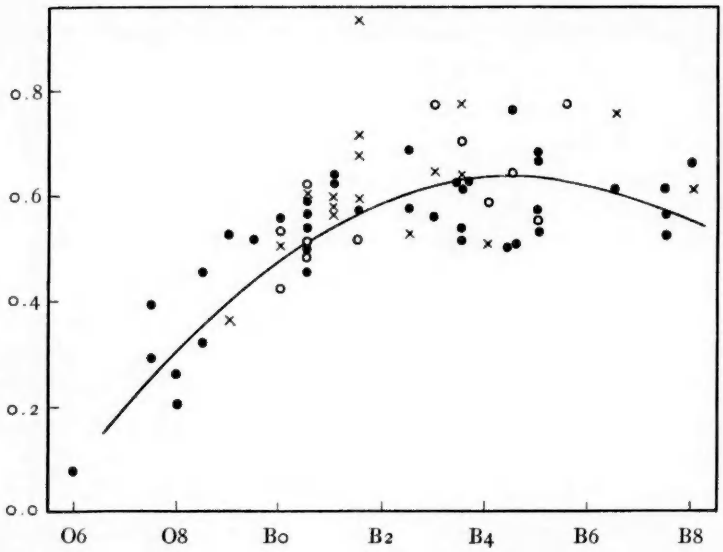

FIG. 4.—Variation of ratio of diffuse singlet to diffuse triplet lines of helium with spectral type.

Perhaps the most noteworthy feature of these diagrams is the sharpness of the maxima for C^{++}, N^{+}, N^{++}, and O^{+}, as compared with Miss Payne's[32] curves. This may result largely from the greater precision in classification. The mean curves for O^{+} and Si^{++} coincide almost exactly in shape and position. There is a very smooth progression of the spectral type of maximum for the curves as here drawn with the ionization potential of the corresponding atom; Figure 7 shows that except for C^{++} the expected maximum never differs from the observed by more than 0.2 of a subtype. This result from abso-

[32] *M.N.*, **92**, 368, 1932.

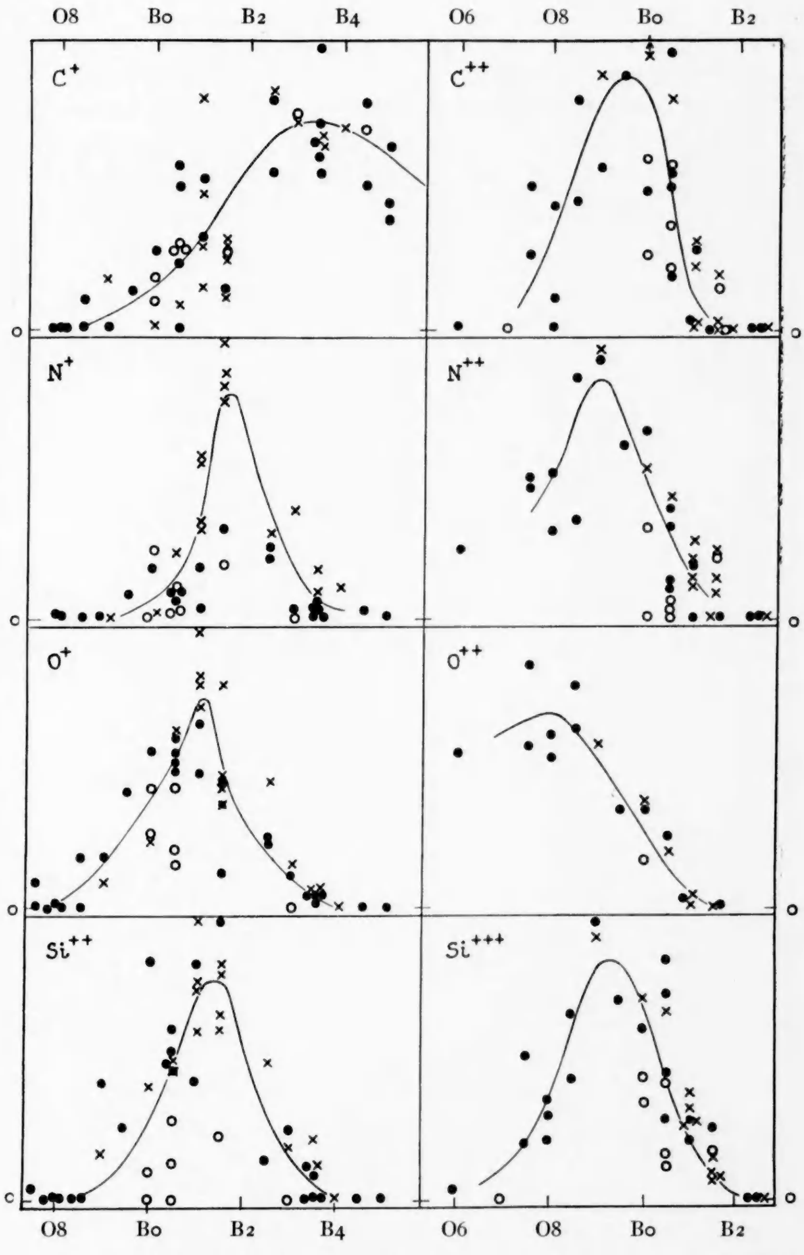

FIG. 5.—Variation of line intensity with spectral type. The scale of ordinates is arbitrary and differs for each atom.

lute line intensities demonstrates that the classification we have set up, based entirely on ratios, is indeed a temperature classification. As was noted by Struve,[33] lines of high excitation potential reach a

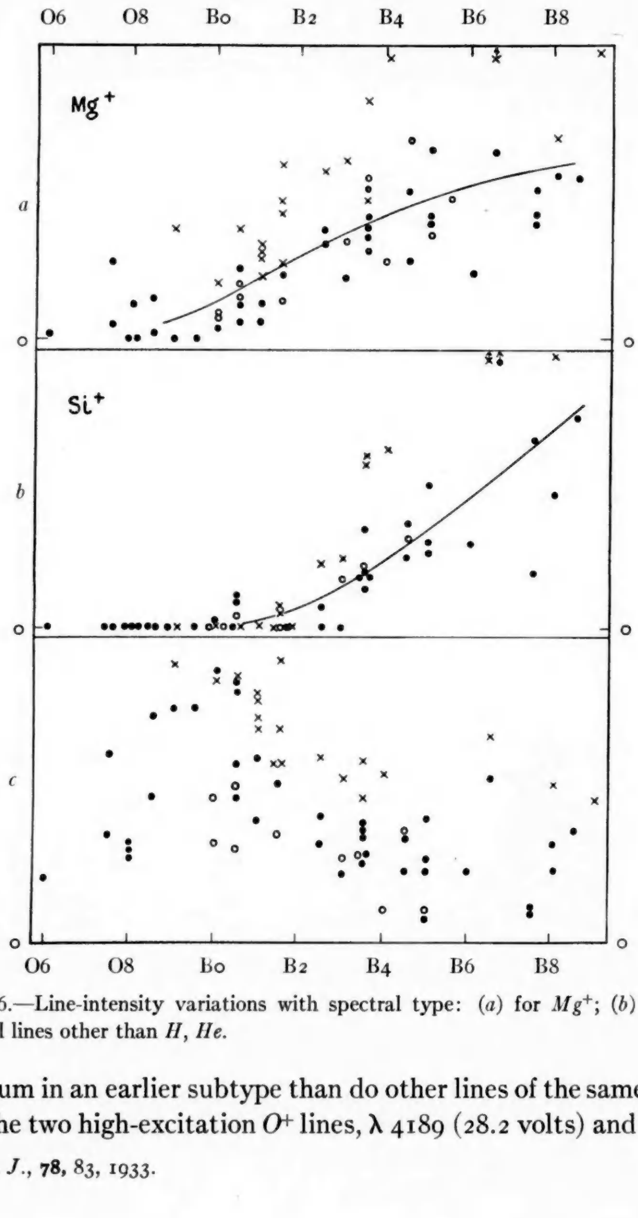

FIG. 6.—Line-intensity variations with spectral type: (*a*) for Mg^+; (*b*) for Si^+; (*c*) for all lines other than *H*, *He*.

maximum in an earlier subtype than do other lines of the same atom. Thus the two high-excitation O^+ lines, λ 4189 (28.2 volts) and λ 4275

[33] *Ap. J.*, **78**, 83, 1933.

(28.7 volts), attain greatest strength in type B0.5, whereas the normal maximum is at B1.0.

These curves must, however, be treated as representing statistical means, for in almost all the diagrams there is much scatter; and, though this might be reduced somewhat by adjustments to the assigned type, the greater part of it is undoubtedly real. The distribution of crosses and circles in nearly all the figures shows clearly that absolute-magnitude differences account for some, though not all, of this scatter; the stronger lines belong to the brighter stars. The effect is most pronounced for N^+, Si^+, Mg^+, while for C^+ it is totally absent.[34]

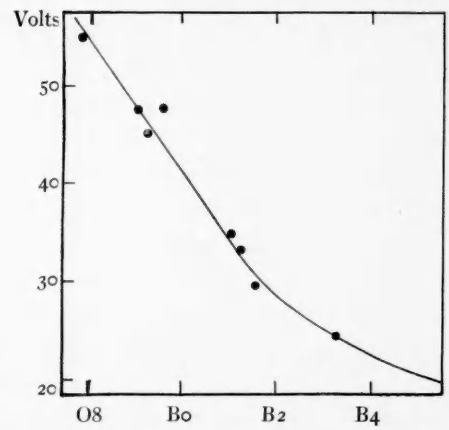

FIG. 7.—Relation between spectral type of maximum and ionization potential of corresponding atom.

The generality of this enhancement of line strength for giants is well illustrated by Figure 6c, which represents the summed intensities for all atoms other than H and He, the intensity for each atom being expressed in terms of its maximum. This diagram, in conjunction with those for H and He, gives us a powerful means of grading stars according to their intrinsic brightness; and the assignment of each star to one of the three categories—giant, intermediate, or dwarf, (Table VIII, col. 8)—has been made almost entirely by reference to its position in these three diagrams;[35] only in a few boundary cases has K-line intensity or total proper motion been invoked to determine the group.

Line character.—The measured spectral type in the seventh column of Table VIII is followed by the usual letters indicating line

[34] Morgan (*Ap. J.*, **77**, 291, 1933) and Struve (*ibid.*, **78**, 82, 1933) both found a null effect for Mg^+ in early subtypes.

[35] The occurrence of the effects was, of course, first found from consideration of other luminosity data. See a preliminary survey of Struve's luminosity groups in *Pub. A.S.P.*, **46**, 292, 1934.

grade. These letters have been assigned, not by visual inspection, but from the measures. For each spectrum a diagram was constructed showing the relation between measured width and depth for all lines other than those of *H* and *He*. Great variations from star to star were at once apparent, though in almost every case points from different plates of the same star agreed well with one another. The mean curves were graded according to slope, and the letters affixed to each grade were arranged to correspond in the mean to Pearce's grades. The several discordances between the two series of grades are not surprising, as ours take no account of the cores of *H* and *He* lines.

Following Edwards,[36] the grade intermediate between n and s is designated ns. Group nn covers a wider range of slope than any other. The width-depth relation for the interstellar K line is about one grade sharper than ss.

Gradient effects.—In numerous stellar spectra,[37] as well as for the sun,[38] it has been found that the relative intensities of absorption lines in multiplets depart from those predicted theoretically. The data for lines in type B are somewhat scanty, though Struve[39] has found in the case of O^+ that for giants all the stronger lines are greatly enhanced, while the weakest are visible only in the dwarfs. The effect was also noticed, though to a much less degree, for the Si^{++} lines.[40]

The present material is not well suited to a study of such gradient effects, since the weakest lines are completely lost, so that the maximum number of measured lines in any one multiplet is only four. For O^+ and N^+, however, we have totals of 19 and 11 measured lines, respectively; and the mean relative intensities of the strong and the weak lines, when grouped together irrespective of their multiplet membership, might reasonably be expected to show variation from star to star.

[36] *Op. cit.*

[37] For a full list of references see Struve and Elvey, *Ap. J.*, **79**, 409, 1934.

[38] Minnaert and van Assenbergh, *Zs. f. Phys.*, **53**, 248, 1929; Woolley, *Ap. J.*, **72**, 256, 1930; Allen, *Mem. Commonwealth Solar Obs. Canberra*, **1**, No. 5, 1935.

[39] *Ap. J.*, **78**, 73, 1933. See also the next reference, p. 412.

[40] Struve and Elvey, *op. cit.*, p. 413.

As a preliminary, the O^+ lines were divided into three groups (strong, 2 lines, mean intensity 42 units; medium, 11 lines, mean intensity 12; weak, 6 lines, mean intensity 5), and the N^+ lines into two groups (moderate, 2 lines, mean intensity 17; weak, 9 lines, mean intensity 5). For each star the ratios between the mean line intensities in each group were found for both O^+ and N^+. Spectra with but few weak lines were omitted. If the gradients persist unchanged throughout the measured intensity range for O^+, a high ratio between the strong and medium groups should repeat itself as between the medium and weak sets of lines. Actually, no correlation whatever was detected between the ratios, strong to medium and medium to weak, for the O^+ lines; nor, indeed, between either strong to medium or medium to weak, for the O^+ lines, and medium to weak for the N^+ lines.

This negative result is somewhat surprising. When, however, the stars are grouped and the line intensities treated statistically, effects are found which suggest a partial explanation.

For the purposes of Table III, where mean total absorptions are given for each of the O^+ and N^+ lines, the unit of equivalent width has been changed from 0.01 A to $10^{-6}\,\lambda$. Measured in this unit, the intensity of a line due to radiation damping only is proportional to the square root of the number of absorbing atoms at any wavelength.[41]

The second, third, and fourth columns divide the stars into luminosity groups; the next two, according to line sharpness; and the final three, for oxygen only, into types earlier than, at, and later than, the maximum. The individual lines behave in a consistent manner, but the effects are best seen by still further summarizing the results. This is done in Table IV, where means for lines in each intensity group are expressed relative to the middle group.

This table brings out clearly a progressive increase in gradient between the medium[42] and weak groups of O^+ as we pass from dwarfs through intermediate stars to giants. The weak lines are, relatively, over twice as strong in dwarfs as in giants. The same effect exists

[41] Dunham, *Pub. A.A.S.*, 7, 215, 1933.

[42] We note that several lines in our "medium" group are normally rated as strong lines.

TABLE III

MEAN TOTAL ABSORPTIONS EXPRESSED IN MICRO-WAVE-LENGTHS

λ	Giants	Intermediates	Dwarfs	Sharp Lines	Others	O9.0–B0.5	B1.0	B1.5–B3.0
	Oxygen Lines							
4650	125	112	85	128	97	103	165	101
4641	85	65	31	81	52	56	114	56
4676	40	29	16	37	27	24	50	33
4662	38	30	11	41	26	25	60	31
4417	33	29	12	31	26	31	47	14
4415	39	25	13	37	22	26	52	21
4367	45	29	17	38	29	29	57	29
4320	39	23	14	38	18	20	49	30
4317	38	23	18	33	25	24	45	24
4076	46	39	44	47	39	36	67	42
4072	40	34	28	40	31	31	56	30
4070	46	40	35	47	38	36	72	34
3973	35	18	20	31	21	17	43	31
4326	13	10	10	14	9	8	23	9
4276	10	12	11	14	8	12	15	7
4190	7	14	22	13	13	13	17	10
3983	14	16	11	15	14	11	23	14
3954	15	15	12	17	13	11	27	12
3945	9	11	12	11	9	10	12	10
No. of stars	13	12	5	16	13	14	6	9
	Nitrogen Lines							
4631	71	15	......	57	8			
3996	77	26	12	64	21			
4614	22	2	......	17	1			
4607	29	1	......	21	1			
4602	30	1	6	21	5			
4447	29	5	11	23	7			
4242	19	4	18	18	5			
4237	13	2	14	12	4			
4044	17	14	11	19	8			
4041	16	7	8	13	8			
3955	21	4	1	16	3			
No. of stars	11	10	4	15	10			

between giants and dwarfs for the N^+ lines, though here the intermediate group of stars behaves curiously. The ratio for this group is, however, hardly comparable with that for the giants, as *all* N^+ lines are some four times stronger in the giant group. For none of the four dwarf stars is the normally strong N^+ line λ 4631 measurable. This line is relatively much weaker in stars with weak nitrogen lines.

The two O^+ lines forming the strong group behave anomalously, as they are relatively strongest in the stars of intermediate luminosity. One of them, λ 4649.2, often blends with λ 4650.8, also O^+; but, even so, both components belong properly to the strong group. The other line, λ 4641, though also strongest in intermediate stars, is much weakened in dwarfs, as would be expected.

TABLE IV

SUMMARIZED MEAN RELATIVE INTENSITIES

	Oxygen Lines	Nitrogen Lines
	Strong : Medium : Weak	Medium : Weak
Giants	257 : 100 : 28	100 : 28
Intermediates	297 : 100 : 45	100 : 16
Dwarfs	274 : 100 : 67	100 : 140
Sharp-line stars	271 : 100 : 37	100 : 29
Others	267 : 100 : 40	100 : 29
Type earlier than B1.0	285 : 100 : 40	
Type B1.0	256 : 100 : 35	
Type later than B1.0	265 : 100 : 36	

That the effect is genuinely one of luminosity and not of line character is shown by the similarity of the figures for the stars graded ss and s, on the one hand, and those graded ns and n, on the other. We conclude also from this table that the gradient does not depend systematically on spectral type.

III. ABSOLUTE MAGNITUDES

In the foregoing discussion the stars have been divided into groups of high, normal, and low luminosity. We shall now attempt to justify this division and to find absolute magnitudes for the individual stars.

The most reliable index of distance known at present for isolated early-type stars is almost certainly the intensity of the interstellar K line. In order to derive absolute magnitudes the first requirement is, therefore, the mean relation between K-line intensity and distance. We say "mean relation" advisedly, because it appears very probable that the relation varies in different parts of galactic space.[43]

For statistical discussion 56 stars with measured interstellar lines are available. This total includes two measured by Beals[44] in addition to those from Paper I. The material has been divided into three intensity groups with approximately equal numbers in each. Mean distances of the groups can be found both from proper-motion data and from the galactic rotational term present in the radial velocities. The proper motions will give more reliable results for the nearer stars and the rotational term for the distant ones.

Through the great courtesy of Dr. J. S. Plaskett and Dr. Pearce[45] the υ- and τ-components derived from the proper motions supplied to them by Dr. R. E. Wilson have been forwarded to me for most of my stars in advance of publication. In a few additional cases I have computed the components from the data of the *Boss Catalogue*.

The distances in parsecs derived from these proper motions for three K-intensity groups are given in Table V. Mean parallaxes from υ components were computed by the formula

$$\bar{\pi} = 4.74 \frac{\overline{\upsilon \sin D}}{\overline{V_0 \sin^2 D}} \cdot$$

Plaskett and Pearce have pointed out that the use of the τ components through the formula $\bar{\pi} = 4.74\ \bar{\tau}/\bar{\rho}$, where ρ = residual radial velocity, is unsatisfactory for distant B stars: the mean parallaxes derived from them for the two nearer groups have here been given half-weight. The columns headed "reduced" in Table V were obtained by reducing the υ and τ values for each star to the value for the mean K intensity of the group, on the assumption that intensity is proportional to distance. These values were given equal weight with the unreduced figures.

43 Struve, *Ap. J.*, **79**, 273, 1934.

44 *M.N.*, **94**, 663, 1934.

45 *Pub. Dom. Ap. Obs.*, **5**, 203, 1933.

In deriving the mean distance $\bar{r}$ from the mean parallax, we need to know the factor by which $\bar{r}\bar{\pi}$ differs from unity. This factor depends on the amount of scatter introduced by (*a*) dispersion in distance in each group, which can be ascertained with sufficient accuracy by finding the value of $\bar{K}\cdot\overline{(1/K)}$ (K = K-line intensity), which in our groups is about 1.05; (*b*) errors of intensity measurement; and (*c*) irregularity in distribution in the calcium cloud. This last was found by Plaskett and Pearce[46] to be the principal contributor to a factor with mean value 1.15, which represents the combined effect

TABLE V

RELATION BETWEEN K-LINE INTENSITY AND DISTANCE DERIVED FROM υ AND τ COMPONENTS

Group	No. of Stars	Mean K* Intensity	Distance in Parsecs					K Intensity per Kpsc
			υ	υ Reduced	τ	τ Reduced	Weighted Mean	
I	21	5.2	234	....	343	....	270	19.3
II	16	14.7	....	....	543	....	708	20.6
	17	14.6	700	695	....	933		
III	18	28.2	(Distances range from 300 to 2200)				....	....

* For convenience the unit of Paper I, equivalent-width of 0.1 wave number, has been retained. Allowance has been made for stellar blends in those stars of type B2 and later which have sharp lines.

of *b* and *c*. We have adopted the round figure 1.2 as being sufficiently accurate for our limited material.

Group I includes all stars with measured interstellar lines of intensity less than 10 units. As might be anticipated, the proper motions are not very helpful in group III, K intensity >20; the derived distances depend greatly on whether or not the components are reduced to a common K intensity, and also on whether the two stars in *h* and χ Persei are treated as one object or two.

The term introduced into radial-velocity measures by the galactic rotation is given by

$$\rho = r\,A \sin 2(G-G_0) \cos^2 g\ .$$

[46] *Ibid.*, p. 206.

Adopting the Victoria[47] values for the constant A and the direction to the center, based on the study of 849 stars, we have found the mean distances of the three groups[48] of Table VI from the expression

$$\bar{r}=\frac{1}{0.0155}\,\frac{\bar{\rho}}{\sin 2(G-324.4)\cos^2 g}\,.$$

The use of this expression is equivalent to weighting each value of r by $\sin 2(G-G_0)\cos^2 g$. Five stars very close to the nodes had to be omitted, also several with uncertain orbits or abnormally high velocities. The two Perseus-cluster stars were treated as one object.

TABLE VI

DISTANCES DERIVED FROM THE GALACTIC ROTATIONAL TERM

Group	No. of Stars	K-Line Intensity	Distance in Parsecs		K Intensity per Kpsc
			Stars	Calcium	
a.	22	4.3	194	. . . .	22.1
b.	17	19.6	. . . .	595	33.0
	17	17.8	730	. . . .	24.4
c.	12	38.3	. . . .	1650	23.2
	10	38.1	1500	. . . .	25.4

In the more distant groups, b and c, K-line velocities were also generally available. Since the rotational term $\bar{r}A$ for the interstellar lines is just half what it is for the stars, the inclusion of the independent mean distances from calcium velocities adds weight to the result. Incidentally, this two-to-one relation between $\bar{r}A$ for the stellar and calcium velocities found by Plaskett and Pearce[49] holds well for the present limited selection. Considering only stars with both velocities measured, we have: strong K-line group, 10 stars, ratio 1.86; medium group, 11 stars, ratio 2.50; all 24 stars together, ratio 2.02.

As may be seen from Figure 8, in which K-line intensity is plotted against distance, the material of Tables V and VI is satisfactorily

[47] *M.N.*, **94**, 679, 1934.

[48] The grouping is not the same as in Table V.

[49] *Op. cit.*, p. 167.

consistent in view of the limited numbers of stars employed. This figure and the last columns of these tables offer good confirmation, based on measured intensities, of Plaskett and Pearce's contention that interstellar line intensity is directly proportional to the distance. Too much weight must not, however, be placed on our most distant group, since 7 of the 12 objects in it are included within an interval of 4° of longitude.

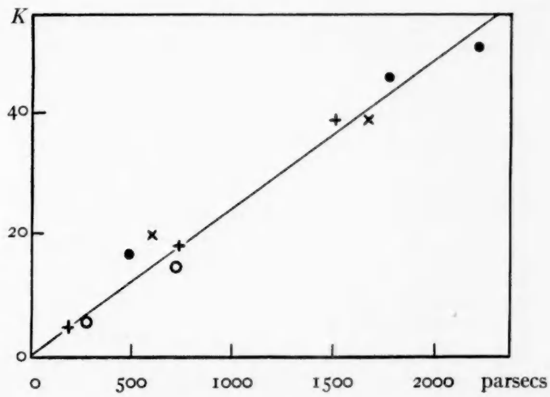

FIG. 8.—Mean relation between K-line intensity and distance. Circles represent proper-motion data; plus signs, radial velocities of stars; crosses, radial velocities of calcium lines; dots, galactic clusters.

The three dots in the figure represent galactic clusters in which I have measured K-line intensities. The adopted distances are based on the following published determinations:

h and χ Persei: Trumpler,[50] 1330; Anger,[51] 2200; mean, 1765 parsecs.
NGC 2264 (S Monocerotis): Trumpler,[52] 500; Anger, 480; mean, 490 parsecs.
NGC 6910. Trumpler,[50] 2200 parsecs.

These distances allow for space absorption. I have adjusted Miss Anger's distances to correspond to Trumpler's general absorption coefficient.

In Figure 8 the straight line represents the relation: K intensity =

[50] See R. S. Zug, *Lick Obs. Bull.*, **15**, 138 (No. 454), Table 4, 1933.

[51] *Harvard Circ.*, No. 397, 1935.

[52] *Pub. Lick Obs.*, **14**, 154, 1930.

24 units per kiloparsec. This rate of change leads to the following expression for determining absolute magnitudes:[53]

$$M = m - 3.1 - 5 \log K\ .$$

The material may now be divided into type- and luminosity-groups and the K-line intensity used, as well as the proper motions and radial velocities, for determining mean absolute magnitudes. The luminosity groups in Table VII are the so-called giants, intermediate stars, and dwarfs of the preceding sections to which the stars were assigned on the basis of spectral characteristics.

TABLE VII

MEAN ABSOLUTE MAGNITUDES FOR TYPE AND LUMINOSITY GROUPS

Luminosity Group	No. of Stars	Mean Type	υ	υ Red.	τ	τ Red.	Rotational Term	K-Line Int.	Weighted Mean
				Early Subtypes					
Giants	10*	B1.0	$-4.5_{1/2}$	$-4.5_{1/2}$	......	......	-5.7_{3}	-5.35_{5}	-5.4
Intermediates	20	O9.5	(Mean parallax negative)		......	......	-5.4_{3}	-3.9_{5}	-4.5
Dwarfs	7	B0.5	-3.0_{1}	-4.2_{1}	$-2.9_{1/2}$	$-1.4_{1/2}$	-1.7_{1}	-2.1_{4}	-2.4
				Late Subtypes					
Giants	9	B6	$-5.9_{1/2}$	$-4.5_{1/2}$	......	......	-5.8_{2}	-5.5_{3}†	-5.6
Intermediates	15	B4.0	-2.7_{1}	-2.7_{1}	$-2.5_{1/2}$	$-2.4_{1/2}$	-2.2_{1}	-2.4_{1}	-2.5
Dwarfs	6	B4.5	-0.6_{1}	-1.3_{1}	-2.5_{1}	-1.4_{1}	......	$+0.2_{1}$‡	-1.1
(Intermediates)§	11	B4.5	-1.4_{1}	-1.5_{1}	$-2.6_{1/2}$	$-2.6_{1/2}$	......	....	-1.8

* Two stars in h and χ Persei treated as one object.

† Mean type B3.5.

‡ Value from trigonometrical parallaxes, K-line intensities, and other data.

§ Stars observed elsewhere.

The numbers do not permit division into more than the two type-groups with the limits O7.5–B1.5, B2.5–B5.5 (the giant group ex-

[53] When K is measured in equivalent angstroms, this expression becomes

$$M = m - 12.2 - 5 \log K\ .$$

tends to type A). The last line of the table comprises stars rated as "intermediates" on the basis of hydrogen-line intensity as measured by other observers. Small appended figures indicate the combining weights used for the final column.

The values in this column show unmistakably that our spectral criteria have successfully divided the stars on a luminosity basis. The large difference between the giant and dwarf groups of 3 mag. in early subtypes, and of more than 4 mag. in late ones, is noteworthy. Figure 9 shows the relation of the present groups to deter-

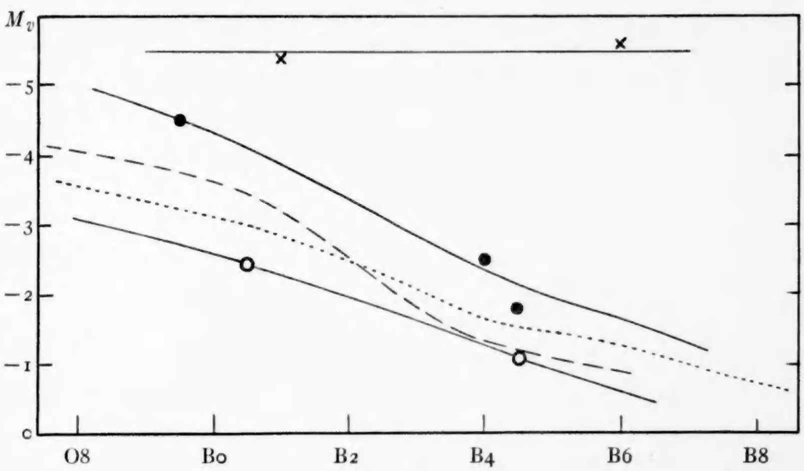

FIG. 9.—Mean absolute magnitude and spectral type. Crosses represent giants; dots, intermediate stars; circles, dwarfs. The dashed line represents Plaskett and Pearce's values; the dotted line, Öpik and Olmsted's.

minations of mean absolute magnitude for different subtypes based on much larger numbers of stars. The broken line represents the latest values of Plaskett and Pearce,[47] and the dotted line those of Öpik and Olmsted,[54] which are in close agreement with Strömberg's[55] curve for the main sequence. The fact that our intermediate groups are sensibly brighter than their means is not surprising, since many of our stars were chosen either on account of strong K lines or undue redness, both criteria favoring bright stars.

[54] *Harvard Circ.*, No. 380, 1932.

[55] *Mt. W. Contr.*, No. 442; *Ap. J.*, **75**, 115, 1932.

IV. COLLECTED RESULTS

For general purposes a B-type spectrum is sufficiently specified by (1) the mean spectral type, (2) the luminosity group, (3) the line grade.

The foregoing discussion has shown how measures of absorption lines enable a temperature classification to be established from ratios and, following this, how a luminosity grouping can be made from absolute intensities.

The spectral types and absolute magnitudes of the individual stars, assigning positions in this two-dimensional scheme, are collected with other general information in Table VIII. The arrangement of the table is as follows: The first two columns give the HD number and designation. In column 3, "c" signifies that the radial velocity is constant; "var," that it is variable; and "2 sp" that both spectra of a binary system have been recognized. Column 4 gives the apparent visual magnitude; columns 5 and 6, respectively, the Draper type, and the revised Victoria type with the emission symbol "e" added where needed. Types in parentheses are from sources referred to in the notes. Column 7 gives the spectral type and line grade as measured here. In column 8 the letters "g," "i," and "d" indicate giant, intermediate, and dwarf stars, as judged from the spectral measures alone.

The continuous curves as drawn in Figure 9 have been used to derive from the type and luminosity group the absolute magnitude, M_L, for each star. Column 9 in Table VIII gives this value; and column 10, the magnitude M_K derived from interstellar-line intensity. The mean, M_W, of these two columns, when the two values are reasonably accordant, should give a close approximation to the true luminosity.

For comparison column 11 lists M_{sp} the absolute magnitude corresponding to the spectroscopic parallax given by Schlesinger,[56] an adjusted value from several sources. Figure 10 compares M_W and M_{sp} and shows a serious difference in scale between the two systems. The straight line corresponds to $M_W = 1.67\ M_{sp}$.

[56] *General Catalogue of Stellar Parallaxes, Yale U. Obs.*, 1935.

TABLE VIII

CATALOGUE OF RESULTS

HD No.	Star	Vel.	Mag.	Spectral Type			Lum. Group	Absolute Magnitude			Notes
				HD	Vict.	Meas.		M_L	M_K	M_{sp}	
(1)	(2)	(3)	(4)	(5)	(6)	(7)	(8)	(9)	(10)	(11)	(12)
886	γ Peg	c ?	2.9	B2	B2ss	B2.5ss	i	−3.1		−2.3	
3360	ζ Cas	c ?	3.7	B3	B2sk	B2.5s	i	−3.1		−2.0	
4180	ο Cas	c	4.7	B2	B5ne	B5.0nn	i	−1.9		−1.7	
5394	γ Cas	c	2.3	B0p	B0nne	B0.5nn	d	−2.4	−2.5		
11415	ε Cas	c	3.4	B3	B5s	B4.5ns	i	−2.1		−1.4	
13854	—	c	6.4	B1p	B0sek	B1.0s	g	−5.5	−5.2	−3.4	1
14134	—	c	6.7	B0	B2sek	B1.5s	g	−5.5	−4.9	−2.9	2
21291	2H Cam	c	4.4	B9p		B6.5s	g	−5.5		−2.6	3
21389	—	var	4.8	A0p		B9s	g	−5.5		−5.2	4
22928	δ Per	c	3.1	B5	B8n	B7.5nn	i	−1.1		−1.0	5
23480	23 Tau	c	4.3	B5	B7ne	B6.0nn	i	−1.6		−0.5	6
24398	ζ Per	c	2.9	B1	B1s	B1.0s	g	−5.5	−5.5	−2.8	7
24534	X Per	c	6 v	B0p	B0nne	nn	d	−2.6	−2.1		8
24760f	ε Per f		8.1		(B8)		d				9
24912	ξ Per	var	4.1	Oe5	O7nek	O8.0n	i	−5.0	−4.4		10
26125	NGC 1514		9	K0	(O8)	s					11
28446b	1 Cam b	2 sp	5.8	B1	B2nk	B0.0n	d	−2.6	−3.3	−2.3	12
28446f	1 Cam f	c	6.9	B1	B0sk	B0.5ss	d	−2.4	−2.2		13
30614	9 Cam	c	4.4	B0	O9sek	O9.0ns	g	−5.5	−5.8	−3.2	14
32343	11 Cam	c	5.3	B3p	B3e	B5.0n	i	−1.9		−1.1	
32630	η Aur	c	3.3	B3	B3	B4.5ns	d	−1.1		−1.1	15
34085	β Ori	var	0.3	B8p		B8s	g	−5.5		−5.1	16
35497	β Tau	c	1.8	B8		B7.5ns	i	−1.1		−0.4	
36371	χ Aur	var	4.9	B1	B3ss	B3.5s	g	−5.5	−6.0	−2.0	17
36861	λ Ori b	c	3.7	Oe5	O8sk	O7.5n	i	−5.0	−5.1	−3.2	18
36862	λ Ori f	var	5.6	Oe5	B1sk	B0.5ns	d	−2.4	−3.2		19
37128	ε Ori	c	1.8	B0	B0k	B0.0s	g	−5.5	−6.2	−3.6	20
37202	ζ Tau	var	3.0	B3p	B3e					−1.3	20a
38771	κ Ori	c	2.2	B0	B0k	B0.5ns	g	−5.5	−5.1	−3.8	21
39698	57 Ori	var	5.9	B2	B3	B3.0ns	i	−2.7	−3.4		
40111	139 Tau	2 sp ?	4.9	B2	B0	B0.5ns	i	−4.1	−4.5	−2.0	22
41117	χ^2 Ori	var	4.7	B2p	B2ssek	B1.5s	g	−5.5	−6.3	−3.8	23
41534	—	c ?	5.6	B3	B3	B3.5ns	d	−1.4			24
44743	β C Ma	c ?	2.0	B1	B1ss	B1.0s	.i	−3.8	−4.3	−3.2	
47839	15 S Mon	c	4.7	Oe5	O7sk	O7.5ns	i	−5.0	−4.5		25
58050	—	c	6.4	B3	B3e	B3.0ns	d	−1.6	−1.6	−2.1	
59088	NGC 2392	c	11	Pe	(O8w)	O7ns	d		+0.6		26
74280	η Hya	var	4.3	B3	B5n	B5.0n	i	−1.9		−1.1	
87737	η Leo	c	3.6	A0p	(A2)	B8.0s				−2.9	27
87901	α Leo	c	1.3	B8	B6n	B8.0nn	i	−1.0		−0.2	28

TABLE VIII—*Continued*

HD No. (1)	Star (2)	Vel. (3)	Mag. (4)	Spectral Type: HD (5)	Spectral Type: Vict. (6)	Spectral Type: Meas. (7)	Lum. Group (8)	Absolute Magnitude: M_L (9)	Absolute Magnitude: M_K (10)	Absolute Magnitude: M_{sp} (11)	Notes (12)
89688	23 Sex	var	6.5	B3	B3	B3.5nn	i	−2.5	....	−1.1	29
91316	ρ Leo	c ?	3.9	B0p	B0sk	B1.0s	g	−5.5	....	−3.0	
93521	—	2 sp ?	6.9	B3	B3nn	nn	.....	.....	−2.0	.....	30
100600b	90 Leo b	c	6.0	B3	B3	B4.5n	i	−2.1	−1.1	−1.0	31
100600f	90 Leo f	var	7.3	B3	B5	B6.5n	i	−1.4	+0.2	.....	32
109387	κ Dra	var	3.9	B5p	B5e	B7.5n	i	−1.2	....	−1.1	
120315	η U Ma	c	1.9	B3	B3n	B5.0nn	d	−0.9	....	−1.1	
147394	τ Her	c	3.9	B5	B7s	B5.0ns	i	−1.9	....	−0.7	33
148184	χ Oph	c ?	4.9	B3p	B3e	nn	i	−2.8	−2.7	−1.6	
148479	α Sco f	.....	6.5	A3	(B4.n)	B4.0n	d	−1.2	....	.....	34
149438	τ Sco	c	2.9	B0	B1s	B0.0ss	d	−2.6	(−1.1)	−2.3	35
149757	ζ Oph	c	2.7	B0	B0nn	nn	i	−4.3	−3.9	−2.7	36
149881	—	var	6.6	B2	B2k	B0.5ns	i	−4.1	−3.2	−1.9	37
160762	ι Her	c	3.8	B3	B3s	B3.5ss	i	−2.5	....	−2.2	
162732	88 Her	c	6.4	B8	*note*	B8.5s	i	−1.0	....	−0.2	38
164353	67 Oph	c	3.9	B5p	B3s	B3.5s	g	−5.5	−5.8	−2.1	39
167971	—	.....	7.3	B0	....	O8.0ns	i	−5.0	−4.3	.....	
169454	—	.....	6.8	B0	(B0se)	B1.0s	g	−5.5	−4.5	.....	40
187811	12 Vul	c	4.9	B3	B5ne	B5.5nn	d	−0.8	....	−0.8	
190603	—	c	5.7	B0	B0ssek	B1.5s	g	−5.5	−4.7	−2.8	
191201	—	2 sp	7.1	B0	B0k	O9.5ns	i	−4.5	−3.6	.....	
192422	—	c	7.1	B2	B0sk	B0.0ns	i	−4.3	−3.8	.....	41
193322	—	var	6.0	B2p	O8k	O8.0ns	i	−5.0	−4.9	−1.6	42
194279	—	c	7.0	B0	B0sk	B1.5ss	g	−5.5	−5.2	.....	43
194839	—	c	7.5	B	B2sek	B0.5s	i	−4.1	−4.3	.....	44
195592	—	var	7.2	B	B0sek	O9.0ns	i	−4.6	−3.6	.....	45
197345	α Cyg	var	1.3	A2p	....	ss	g	.....	....	−4.1	
198478	55 Cyg	c ?	4.9	B2	B2sk	B3.0s	g	−5.5	−5.9	−2.1	46
200120	f¹ Cyg	var	4.9	B0p	B3nne	B4.5nn	i	−2.1	....	−2.1	47
204172	69 Cyg	c	5.8	B0	B0k	B0.5ns	i	−4.1	−3.6	−4.2	48
205021	β Cep	var	3.3	B1	B1	B1.5ns	i	−3.6	(−3.0)	−2.7	49
206165	9 Cep	c	4.9	B2p	B2sk	B2.5s	g	−5.5	−5.6	−2.1	50
208185	—	.....	8.2	B3	(B3s)	B3.5ss	i	−2.5	−1.8	−1.8	51
208392	—	c	7.1	B3	B3nnek	B1.5ns	d	−2.1	−3.4	−1.7	52
208947	—	2 sp	6.3	B3	B3k	B3.5ns	i	−2.5	−3.2	−2.2	53
210809	—	.....	7.7	B2	(O8k)	O8.5ns	i	−4.8	−3.4	.....	
210839	λ Cep	c	5.2	Od	O6wnek	O6ns	.....	−5.2	−4.9	−2.9	
212455	—	.....	8.4	B2	(B3k)	B4.0s	g	−5.5	−4.4	.....	54
212571	π Aqr	c	4.6	B1p	B1nnek	B1.5nn	i	−3.6	−3.1	−1.4	
213420	6 Lac	c	4.5	B3	B3k	B3.5ns	i	−2.5	−4.1	−2.0	
214680	10 Lac	c	4.9	Oe5	O9sk	O8.5ss	i	−4.8	−3.1	−2.2	55
+60°2522	NGC 7635	.....	8.7	....	(O7)	ns	.....	.....	....	.....	56
224151	—	var	6.1	B0	B0k	B1.0ns	i	−3.8	−3.7	−2.4	57

NOTES TO TABLE VIII

No.	HD	
1	13854	Adams and Joy, B2. In *h* and χ Persei.
2	14134	Adams and Joy, B4; Merrill, B3se*a*. In *h* and χ Persei. *He* singlets abnormally strong relative to triplets.
3	21291	Large color excess (Elvey). Comp. 9 mag., 2″.4.
4	21389	Large color excess (Elvey).
5	22928	Adams and Joy, B5. In Perseus moving cluster.
6	23480	Adams and Joy, B5ne. (*b*, B8.5; *c*, B4.5.) *H* and Si^+ have normal B4 intensity, but *He* and Mg^+ are much too weak for this type. In Pleiades.
7	24398	C^+ 2.5, C^{++} 1.5.
8	24534	Irregular variable, mag. 6.2–6.9.
9	247605f	Type by Mt. Wilson. 9″, c.p.m. with ϵ Persei, B2, in Perseus moving cluster. The spectroscopic parallax of the primary gives $M=+2.1$ for the companion.
10	24912	No N^{++} visible! Victoria notes emission wing to λ 4649. *H* lines relatively sharper than *He*.
11	26125	Type by Payne. Central star in an irregular ring, 2′×1′.5, of faint nebulous matter (Curtis). Payne gives nebular magnitude as 10, photographic. Van Maanen gives $\mu=0''.004$. Radial velocity $=+35.4$ km/sec (Hubble).
12	28446b	Adams and Joy, B1s. 10″ from, and c.p.m. with 28446f. *H* lines relatively sharper than *He*.
13	28446f	Adams and Joy, B2s.
14	30614	Struve, B0. Mg^+ very strong for type.
15	32630	In Perseus moving cluster.
16	34085	Comp. 7 mag., 9″, fixed, is itself a close binary.
17	36371	Si^+ 3, Mg^+ 2.
18	36861	Payne, O9. Mg^+ very strong for type. 4″ from HD 36862, fixed.
19	36862	(*d*, B2.0; *e*, B0.5; *g*, B0.0). O^+, N^+, N^{++}, Si^{++}, Si^{+++} are all about one-third normal intensity, while C^+, C^{++}, Si^+, Mg^+ are normal.
20	37128	He^+ weak; C^{++} 1.8; C^+ 0.
20*a*	37202	The spectrum of this star is very peculiar.
21	38771	Mg^+ 2.0
22	40111	C^+ 0; C^{++} 0.8. *H* lines relatively sharper than *He*.
23	41117	C^+ 0.3.
24	41534	Adams and Joy, B4n. (*b*, B2.5; *c*, B4.5; *d*, B3.5.) Voûte's star. $\mu=0''.123$. $\pi=0''.048$ (Voûte, trigonometric), whence $M_v=+4.1$. Radial velocity $+94.2\pm1.7$. Very close to solar antapex.
25	47839	Comp. mag. 8.0, 3″. In the open cluster NGC 2264.
26	59088	Type by Payne. Nucleus of planetory NGC 2392, irregular elliptical, 19″×15″. Interstellar K-line intensity = 29.0 (in 0.1 wave-number units). The magnitude is photographic.
27	87737	Type by Mt. Wilson. (*b*, B7.0; *c*, B9.0.) Si^+ 0.5; Mg^+ rather weak and much sharper than λ 4471 *He*. Included in Miss Payne's list of c stars.
28	87901	Adams and Joy, B8n.
29	89688	Adams and Joy, B4. C^+ 1.6. Strongest C^+ lines found.

NOTES TO TABLE VIII—*Continued*

30	93521	(*b*, B5.0; *c*, B3.5; *d*, B2.0; *e*, B0.5.) Almost certainly composite. Victoria notes "on a number of plates lines appeared double, but evidence not consistent nor definite enough to publish measures." *H* lines relatively much sharper than *He*.
31	100600b	3″ from HD 100600f, fixed.
32	100600f	Si^+ exceptionally strong, though the star is not a giant.
33	147394	The lines have exceptionally sharp cores.
34	148479	Type by Mt. Wilson. (*a*, B4.5; *b*, B5.0; *c*, B3.5; *d*, B2.5.) 3″ from and c.p.m. with Antares. The spectroscopic parallax of the primary gives $M_v = +1.3$ for the B4 star. The Harvard A3 spectrum is a mistake. Interstellar K-line intensity = 13.8 (in 0.1 wave-number units).
35	149438	In Scorpio-Centaurus cluster.
36	149757	*H* lines not exponential; relatively sharper than *He*.
37	149881	C^+ 2.5; C^{++} normal.
38	162732	Adams, A1sp; Joy, B9s. Edwards (*M.N.*, **92**, 389, 1932) gives B8, but notes that strong class A2 lines are present. This, coupled with the strength of the *He* lines, suggests a c star, but the hydrogen lines are normal for a dwarf. Their cores are very sharp.
39	164353	Si^+ 3. Comp. 8 mag., 55″, fixed.
40	169454	Type by Merrill. O^+ 1.3. Strongest oxygen lines found. O^{++} lines underexposed. This star, with many very sharp lines, is suggested as a suitable object for further study with higher dispersion. The K-line intensity given in Paper I is in error. The correct value is 34.8.
41	192422	Si^{++} 2; Si^{+++} normal. Interstellar K intensity = 32.9. (Incorrectly given in Paper I.)
42	193322	Comp. mag. 8.2, 2″.7, binary.
43	194279	Brightest star in NGC 6910.
44	194839	Mg^+ 2.
45	195592	Merrill, B1se. Si^{++} 3; Si^{+++} 1.3.
46	198478	Struve, B3. N^+ 2.5; Mg^+ 1.7; Si^+ 1.7.
47	200120	(*a*, B4.5; *b*, B5.5; *c*, B3.5.)
48	204172	C^{++} 2; Si^{+++} 2.
49	205021	C^+ weak; N^+ 0.4; O^+ 1.3. Short-period Cepheid. Comp. mag. 8, 14″, fixed.
50	206165	O^+ 2.0; Mg^+ 1.8; Si^+ 2; Si^{++} 1.7.
51	208185	Type by Mt. Wilson. Comp. mag. 8.3, 1″.8. Brighter star only on slit with good seeing. See note to Table VI, *Mt. W. Contr.*, No. 540.
52	208392	Comp. mag. 8.8, B8, 62″, c.p.m. The nitrogen lines suggest B0.5 and silicon lines B2.0. Victoria notes weak diffuse lines, $H\beta$ not distinct, $H\alpha$ emission suspected. This is not confirmed here. $H\beta$ is very distinct, and the lines are moderately sharp. Thus change is suggested. The probable error in the radial velocity (Moore) is only ± 1.8 km/sec (6 plates).
53	208947	Victoria notes similar spectra of nearly equal intensity.

NOTES TO TABLE VIII—*Continued*

54	212455	(*b*, B3.0; *c*, B5.0; *d*, B4.0.) Mg^+ 2.2; Si^+ 2.5. The lines have very sharp cores.
55	214680	N^{++} 0.5.
56	BD 60°2522	Nuclear star in the giant planetory NGC 7635. Type by Miss Payne. Magnitude is photovisual. The HD type is evidently a mistake. The spectrum is described by Hubble (*Ap. J.*, **56**, 186, 1922). Only the *H* lines have been measured here.
57	224151	(*b*, B1.5; *c*, B0.0; *d*, B1.0.) N^+ 0.1. All the lines are asymmetrical on our plate.

The mean difference between the individual values of M_{sp}, after conversion to the present scale, and M_W is ± 0.88 mag. This value is

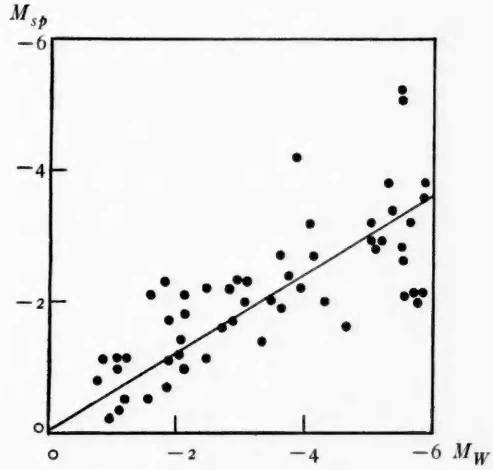

FIG. 10.—Comparison of published spectroscopic absolute magnitudes (ordinates) with those of the present paper (abscissae).

half as large again as the average difference between columns 9 and 10.

Notes following the table give spectral type and authority for determinations differing from the Victoria classification. Types in parentheses are discordant measured values preceded by letters "a" to "g," which refer to the classification ratios given in Table I. The figures following the atomic symbols indicate observed intensities, in terms of the normal for the spectral type.

As is evident from these notes, a large proportion of the stars listed show individual peculiarities the full interpretation of which will need

detailed study with higher dispersion. Meanwhile attention may be drawn to some cases presenting such abnormality that they cannot be fitted into the scheme designed for the remainder.

In most of the bright-line B stars the *H* absorption lines, though they may be diffuse, are roughly equal in total intensity to those in normal stars. The spectra of γ Cassiopeiae and X Persei are exceptional in this respect. The total absorption of the very diffuse *H* lines on which the comparatively narrow emission components are centered is unusually low; in addition, the intensity decreases from $H\delta$ to $H\beta$, and in γ Cassiopeiae the latter line is too shallow to be seen on our plates. The *He* lines also are much weaker than in normal stars of the same type. In χ Ophiuchi, B3e, the *H* lines are again weak, but *He* is strong, and normal for a dwarf of this class. Some explanation other than rotation is necessary to account for the dish-shaped lines in these stars.

The spectrum of HD 93521 suggests the admixture of a B3 dwarf and an O-type star. Such a combination would imply an unusually low absolute magnitude for the O component. On the assumption of equality of brightness, the interstellar line intensity gives -1.3 for the absolute magnitude of each star, but the high galactic latitude and considerable distance render this estimate of low weight.

The spectra of the nuclear stars in the giant planetaries NGC 1514, 7635 have been examined by Hubble.[57] He remarks that the Pickering series of He^+ is prominent, λ 4542 being the strongest line other than the lines of *H*, while λ 4686 is faint and hazy. A casual inspection of the first of these objects would, however, suggest a late-B type, for the *H* lines are very strong with wings, typical, in fact, of a B8 dwarf and nearly three times as intense as those in any other O-type star. In addition, as Hubble notes, the Mg^+ line is nearly as strong as λ 4542. The second object has very weak *H* lines. Hubble mentions that the intensity in the ultra-violet is characteristically strong for both stars. For NGC 1514 he finds a photovisual magnitude of 9.4 against a mean photographic value of 8.5 (three observers). The HD visual magnitude is, however, only 8.6. In view of the possible white-dwarf nature of this star, further observations in the region of the Balmer limit would be of great interest.

[57] *Mt. W. Contr.*, No. 241; *Ap. J.*, **56**, 186, 1922.

It may be useful to add a few words on the extension and adaptation of the scheme of classification discussed in this paper to fresh material. In the case of calibrated plates the foregoing procedure could be considerably shortened. Thus, for classification ratios a limited number of suitably chosen and rapidly measurable line depths would suffice. The addition of total absorptions for one or two *H* and *He* lines would provide all the data necessary for settling the luminosity group with some certainty, though an estimate of absolute magnitude based on K-line intensity would be a useful addition. It is obvious, however, that future classifications of large numbers of stars for statistical purposes will continue to be based on visual inspection of uncalibrated spectra. The line ratios customarily used for this purpose are not really consistent with the methods of the present paper; for instance, the use of the ratio of *He* 4471 to Mg^{+} 4481 is clearly inadvisable, at least in types earlier than B6, as the lines are subject to opposite luminosity effects. I prefer to suggest that intensity estimates should be made for two or three of the more prominent lines of each atom, and that ratios based on these estimates should be used to determine the mean type through a simplified form of Table I. The estimation on an arbitrary scale of, say, a dozen of the fainter lines in each spectrum should be a simple matter, for the scale need be consistent only for the one plate.

Precise luminosity grading presents more difficulties. For the later subtypes it must depend on hydrogen-line sharpness; in the earliest types the relative intensities of the metallic and the fainter helium lines will doubtless prove most useful. It is hoped to attempt to establish some such rapid visual method in the near future.

In conclusion, my hearty thanks are due to Professor H. H. Plaskett for helpful discussions and for his interest and advice during the course of this work, and to Dr. J. S. Plaskett and Dr. Pearce for their unpublished proper-motion data.

CARNEGIE INSTITUTION OF WASHINGTON
MOUNT WILSON OBSERVATORY;
TRINITY COLLEGE, CAMBRIDGE
November 1935

INVESTIGATIONS ON PROPER MOTION

NINETEENTH PAPER: PROPER MOTIONS OF 651 STARS IN 97 SELECTED AREAS*

P. TH. OOSTERHOFF

ABSTRACT

Proper motions of faint stars.—Examination of plates taken at intervals of about twenty-one years on 97 Selected Areas, including the -15° declination zone, revealed 651 stars having proper motions between $0\overset{''}{.}050$ and $0\overset{''}{.}726$. By comparison with the *Radcliffe Catalogue* the probable error of a motion was found to be $\pm 0\overset{''}{.}011$. The percentage of stars having proper motions larger than $0\overset{''}{.}049$ increases from 0.29 for galactic regions to 2.60 for high galactic latitudes. The amount of the mean motion decreases with magnitude, though for stars fainter than the thirteenth magnitude it remains constant. The antapex determined by Airy's method from the proper motions given in this paper and in *Mt. Wilson Contr.* No. 412 is $A = 7^h9^m$, $D = -41\overset{\circ}{.}4$. Mean parallaxes were computed for different groups of magnitude and proper motion by formulae given by van Maanen and Willis and by Seares. The discussion of the material is provisional, since the effects of selection have not been fully taken into account. A list of 16 variable stars found during this investigation is added.

In *Mount Wilson Contribution* No. 412, A. van Maanen and H. C. Willis derived proper motions for 122 stars in 42 Selected Areas. At the request of Dr. van Maanen the writer has completed this investigation for the northern Selected Areas and the zone at -15° declination.

The early plates were taken nearly twenty-five years ago by Messrs. Fath and Babcock at the Newtonian focus ($f = 25$ ft.) of the 60-inch reflector, the exposure-time being 1 hour on Lumière Σ plates, 6.5×8.5 inches. The recent exposures of 1 hour were made on Eastman 40 or Imperial Eclipse Soft 850 plates, 4×5 inches, by Messrs. Thorndike, Willis, and Oosterhoff.

Owing to differences in the observing conditions, there are considerable variations in the limiting magnitude from plate to plate; but, on the average, stars of the eighteenth to the nineteenth magnitude can be seen near the center of the field. The 97 Selected Areas not discussed by van Maanen and Willis have been examined with the blink arrangement of the Zeiss stereocomparator. Stars showing

* *Contributions from the Mount Wilson Observatory, Carnegie Institution of Washington,* No. 542.

TABLE I

Selected Area	Central Star	α 1900	δ 1900	β	No. Stars Examined	No. P.M. Stars	Interval between Plates
							years
1	+89° 13	$7^h58^m2^s$	+88° 56′.0	+28°	340	5	19.48
2	75 2	0 4 50	75 16.3	+13	920	6	19.93
3	74 196	4 7 39	74 58.2	+17	990	5	19.48
4	74 350	8 4 20	74 47.6	+32	340	4	19.18
5	75 474	12 28 8	75 2.6	+42	220	7	19.18
6	75 585	16 13 43	74 54.3	+36	310	7	21.58
7	74 859	20 24 20	75 7.4	+20	530	9	13.95
8	60 162	0 59 38	60 14.2	− 3	2150	10	18.98
9	60 636	3 3 32	60 15.3	+ 2	1550	6	22.12
10	60 867	5 7 44	60 9.3	+13	1550	6	19.48
11	60 1038	7 6 46	59 56.8	+26	480	5	15.28
12	59 1223	9 2 44	59 39.6	+41	200	6	15.90
13	59 1351	11 2 58	59 45.4	+53	180	5	20.95
14	59 1511	13 22 21	59 25.1	+57	190	4	19.18
15	60 1603	15 16 34	59 53.0	+48	230	4	21.71
16	59 1823	17 28 41	59 45.8	+33	450	2	21.12
17	60 1943	19 22 41	60 9.0	+19	1300	6	20.02
18	59 2380	21 24 27	60 6.6	+ 6	3950	8	19.06
19	59 2728	23 23 1	60 1.4	− 1	2250	5	19.06
20	45 192	0 40 19	45 20.9	−18	1900	5	19.93
21	44 352	1 35 51	45 4.3	−17	1900	10	22.07
22	44 569	2 38 12	45 10.6	−13	2100	6	21.41
24	44 1016	4 38 38	44 54.5	0	1850	7	24.24
26	44 1519	6 36 19	44 49.2	+18	1300	14	23.96
27	44 1667	7 38 12	44 48.9	+28	630	3	19.20
28	45 1635	8 39 50	44 56.6	+39	400	9	19.19
29	45 1757	9 38 31	44 52.7	+49	200	3	20.95
30	45 1855	10 37 21	45 9.1	+60	160	5	21.28
31	44 2117	11 36 54	44 41.8	+68	200	6	19.02
32	45 2070	12 50 33	44 50.1	+72	170	9	23.81
33	45 2137	13 50 7	45 12.9	+68	170	4	20.95
34	45 2228	14 47 47	45 1.2	+59	200	10	19.58
35	44 2518	15 49 29	44 49.2	+49	320	11	21.11
36	45 2453	16 45 58	45 22.5	+39	390	10	20.03
37	45 2610	17 48 31	45 0.4	+28	810	9	21.92
38	45 2779	18 46 12	45 12.4	+18	1500	9	20.02
39	44 3265	19 46 51	44 53.8	+ 9	4250	11	26.02
40	44 3596	20 46 33	44 58.4	0	3100	8	26.02
41	44 3974	21 49 36	44 58.9	− 8	4400	2	19.07
42	44 4263	22 48 45	45 9.7	−13	2600	5	19.07
43	44 4520	23 49 55	44 50.2	−16	1750	6	20.03
46	30 414	2 29 27	30 14.6	−27	630	6	19.56
48	30 665	4 22 33	30 8.4	−12	1800	11	22.16
49	29 910	5 23 40	29 44.9	− 2	3400	8	20.03
50	29 1248	6 24 22	29 53.8	+10	3050	2	20.04
51	30 1518	7 24 21	30 2.2	+22	860	6	21.68
52	30 1719	8 25 43	30 2.9	+34	460	6	22.99
53	30 1873	9 24 34	30 0.7	+47	260	7	20.03
55	30 2175	11 29 48	29 58.7	+74	120	4	21.73
56	29 2251	11 58 12	29 40.7	+80	180	5	20.03
58	+29 2486	13 59 59	+29 37.4	+73	260	7	21.93

TABLE I—*Continued*

Selected Area	Central Star	α 1900	δ 1900	β	No. Stars Examined	No. P.M. Stars	Interval between Plates
							years
67........	+29°4855	23h 0m 57s	+30°11′.0	−28°	710	8	18.90
71........	+14 545	3 11 37	+15 2.4	−34	300	11	21.84
72........	+15 603	4 10 5	+15 9.0	−24	360	8	18.98
73........	+14 881	5 14 53	+14 57.5	−12	1200	3	19.45
74........	+15 1160	6 15 15	+15 5.8	+ 1	2450	7	23.03
76........	+15 1800	8 15 34	+15 1.4	+27	480	9	18.98
78........	+15 2188	10 13 54	+15 10.2	+54	170	7	21.83
79........	+15 2326	11 17 42	+14 52.3	+67	140	5	18.66
80........	+15 2441	12 12 32	+15 0.0	+76	150	7	20.03
81........	+14 2590	13 12 2	+14 42.0	+76	160	12	24.10
93........	+ 0 307	1 49 42	+ 0 17.6	−58	230	5	23.91
94........	− 0 454	2 50 48	+ 0 6.6	−49	290	3	24.07
95........	− 0 617	3 49 8	− 0 0.4	−38	250	8	22.81
96........	− 0 793	4 47 43	− 0 3.0	−25	620	5	18.03
97........	+ 0 1227	5 52 18	+ 0 0.9	−11	1000	4	22.16
98........	− 0 1468	6 47 4	− 0 10.6	+ 1	3600	7	21.20
99........	− 0 1854	7 49 40	− 0 13.9	+15	1850	6	21.72
100........	− 0 2087	8 48 52	− 0 14.0	+28	550	3	21.72
101........	+ 0 2588	9 51 32	+ 0 0.8	+41	400	7	22.16
105........	+ 0 3084	13 32 40	− 0 7.0	+60	380	12	24.70
106........	+ 0 3224	14 36 31	− 0 0.3	+51	400	3	22.38
112........	− 0 4072	20 37 17	+ 0 5.3	−25	1750	5	18.98
116........	−15 49	0 13 0	−14 52.0	−76	200	12	20.04
117........	−14 248	1 12 6	−14 42.8	−76	200	8	19.97
118........	−15 401	2 15 20	−14 52.6	−65	210	6	22.06
119........	−14 627	3 10 8	−14 48.9	−54	220	7	22.15
120........	−15 757	4 12 10	−15 6.4	−40	360	5	21.76
121........	−14 1094	5 14 53	−14 52.3	−26	580	12	21.77
122........	−15 1328	6 12 19	−15 5.4	−13	1500	9	21.84
123........	−14 1834	7 15 13	−15 4.5	0	4300	5	21.92
124........	−15 2370	8 13 42	−15 10.5	+12	2150	5	24.01
125........	−14 2802	9 12 20	−15 5.4	+24	750	8	21.97
126........	−14 3093	10 16 0	−14 59.1	+35	500	11	23.18
127........	−15 3236	11 13 0	−15 16.5	+42	370	3	17.83
128........	−14 3489	12 13 49	−15 13.9	+47	350	5	22.07
129........	−14 3690	13 13 58	−15 2.4	+47	300	7	22.15
130........	−14 3900	14 7 46	−15 9.4	+43	530	5	20.19
131........	−15 4071	15 11 26	−15 12.5	+34	520	5	19.88
132........	−14 4389	16 11 41	−15 4.8	+24	920	6	18.98
133........	−15 4512	17 12 41	−15 5.4	+12	2500	10	20.13
134........	−14 4955	18 10 19	−14 57.3	0	2800	6	19.88
135........	−15 5308	19 12 59	−14 59.0	−13	5300	8	20.07
136........	−15 5597	20 9 46	−15 5.3	−26	1450	8	19.96
137........	−15 5934	21 9 59	−14 49.0	−39	600	7	19.95
138........	−15 6174	22 10 38	−14 56.0	−53	320	10	19.96
139........	−15 6394	23 13 55	−14 47.8	−66	200	4	19.95
Totals and mean	....	....	....	......	104,020	651	20.78

a decided displacement were measured with an ocular micrometer in both x and y directions, identical with the directions of α and δ at the center of the field. The images of faint neighboring stars, or of stars approximately of the same brightness as the proper-motion stars, were, however, first superposed as accurately as possible. The motions found range from $0\overset{''}{.}023$ to $0\overset{''}{.}726$ per year. The discovery of small proper motions depends considerably on the galactic latitude, since their detection is very difficult if only a few comparison stars are visible in the field. Other handicaps in the detection of small motions are poor quality, overexposure, and any considerable coma of the photographic image. For this reason the number of proper motions smaller than $0\overset{''}{.}050$ per year will be very incomplete. Such

TABLE II

Galactic Latitude	Stars Investigated	Number of P.M. Stars	Percentage	Number of Fields
0°–19°	78210	226	0.29	33
20 –39	16970	195	1.15	28
≧40	8840	230	2.60	36

stars, numbering 117, have not been included in the catalogue. No doubt many stars of proper motion between $0\overset{''}{.}050$ and $0\overset{''}{.}100$ have also been missed; but, as may be seen from the frequency distribution of the proper motions in Table IV, the number in the interval $0\overset{''}{.}050$–$0\overset{''}{.}059$ is larger than that in the next interval; and it is believed that practically no stars with motions larger than $0\overset{''}{.}100$ have been missed.

The data for the Selected Areas investigated are collected in Table I. The numbers of stars given in the sixth column have been computed in the same way as for *Mount Wilson Contribution* 412. The areas examined are approximately five times as large as those measured for the *Mount Wilson Catalogue*.[1] But, since the number of stars falls off rapidly with increasing distance from the center, it was assumed that the number examined in each region was about two

[1] Seares and others, *Publications of the Carnegie Institution of Washington*, No. 402, 1930.

TABLE III

PROPER MOTIONS OF 651 STARS

Current No.	Sel. Area	No. in Cat.	Mag.	α 1900	δ 1900	x	y	μ_x	μ_y	μ
1	1	H 196	12.68	$6^h 35^m 9$	+89° 1′8	−20′4	+ 9′5	−0″008	−0″101	0″101
2		H 130	15.29	6 49.5	88 50.0	−20.6	− 2.9	+ .012	+ .152	.152
3		21s	14.66	7 29.7	88 57.5	− 7.7	+ 1.7	− .028	− .052	.059
4		Anon.	16.6	7 53.5	89 9.0	− 1.0	+13.0	+ .097	+ .065	.117
5*		Anon.	16.2	8 57.2	88 41.0	+20.2	−12.4	− .002	− .120	.120
6	2	Anon.	17.0	23 59.1	75 13.8	−22.0	− 2.3	+ .176	+ .047	.182
7		H 281	14.01	0 2.4	75 30.0	− 9.3	+13.7	+ .070	− .046	.084
8		Anon.	14.2	2.8	74 59.9	− 7.9	−16.4	+ .053	.000	.053
9		201	10.51	5.1	75 17.9	+ 1.0	+ 1.6	− .070	+ .024	.074
10		Anon.	15.9	8.1	74 57.4	+12.7	−18.8	+ .076	+ .026	.081
11		Anon.	16.8	0 11.4	75 20.6	+25.0	+ 4.6	+ .117	+ .008	.117
12	3	Anon.	15.7	4 3.3	74 58.1	−16.9	+ 0.1	+ .056	− .062	.084
13		35s	16.65	5.6	56.0	− 8.2	− 2.2	+ .048	− .154	.161
14		53s	16.23	6.5	48.7	− 4.6	− 9.5	+ .044	− .077	.089
15		235	13.76	9.2	54.3	+ 6.0	− 3.9	+ .547	− .478	.726
16		Anon.	16.1	4 13.2	46.2	+22.0	−11.8	− .050	+ .070	.086
17	4	H 26	11.77	8 0.4	27.6	−15.9	−19.9	− .041	− .213	.217
18		Anon.	15.8	0.6	45.4	−14.9	− 2.1	+ .012	− .063	.064
19		34	16.13	4.1	43.9	− 1.0	− 3.7	− .078	− .042	.089
20		H 288	14.79	8 10.8	74 50.4	+25.4	+ 3.1	− .030	− .075	.081
21	5	Anon.	16.6	12 22.8	75 5.5	−20.5	+ 3.1	− .110	+ .034	.115
22		55	9.27	28.1	75 2.6	0.0	0.0	− .188	− .044	.193
23		58	17.15	28.4	74 50.3	+ 0.9	−12.3	− .088	+ .009	.088
24		61	16.60	28.6	75 0.9	+ 2.0	− 1.7	− .012	+ .056	.057
25		Anon.	16.7	29.0	74 45.4	+ 3.2	−17.2	+ .078	− .012	.079
26		H 315	13.70	32.6	75 0.5	+17.4	− 1.9	− .065	+ .036	.074
27		Anon.	15.2	12 34.2	74 51.3	+23.9	−11.0	− .091	+ .030	.096
28	6	H 85	14.97	16 10.3	34.8	−13.5	−19.4	− .055	− .159	.168
29†		Anon.	16.5	16 11.4	+74 43.3	− 9.0	−10.9	−0.073	−0.130	0.149

30		3	16.93	16h 12m.0	+74° 52′.6	− 6′.7	− 1′.7	−0″.085	+0″.099	0″.130
31		H 181	12.29	16.9	42.0	+12.7	−12.2	− .176	+ .066	.188
32		H 233	14.27	17.1	74 52.3	+13.3	− 1.9	− .067	− .015	.069
33		H 369	12.95	19.0	75 10.9	+20.1	+16.8	− .178	+ .074	.193
34		H 249	14.86	16 20.2	74 50.7	+25.5	− 3.2	+ .005	+ .091	.091
35	7	H 554	15.94	20 18.8	75 13.9	−21.2	+ 6.8	+ .015	+ .058	.060
36		H 598	14.08	22.2	18.4	− 7.9	+11.1	+ .052	+ .100	.113
37		45	17.06	23.3	2.8	− 4.1	− 4.5	+ .034	+ .043	.055
38		75	12.94	23.7	6.4	− 2.3	− 0.9	+ .101	+ .190	.215
39		108	10.23	24.3	7.4	0.0	0.0	+ .002	+ .051	.051
40		61*s*	14.09	26.6	7.9	+ 8.7	+ 0.6	+ .073	+ .066	.098
41		H 483	12.58	27.8	8.6	+13.4	+ 1.4	.000	+ .072	.072
42		Anon.	15.6	27.8	75 8.7	+13.4	+ 1.5	+ .015	+ .079	.080
43		Anon.	17.0	20 27.9	74 58.3	+14.0	− 8.9	+ .011	+ .051	.052
44	8	Anon.	10.2	0 56 40s	60 9.9	−22.1	− 4.3	+ .073	− .070	.101
45		Anon.	13.8	56 53	60 33.8	−20.2	+19.6	+ .080	− .066	.104
46		H 7	14.40	57 2	59 59.4	−19.5	−14.8	− .061	+ .007	.061
47		H 671	13.84	37	60 21.1	−14.9	+ 6.9	+ .050	− .023	.055
48		Anon.	14.5	57 58	33.0	−12.3	+18.8	+ .083	+ .002	.083
49		Anon.	15.9	0 58 5	27.1	−11.4	+12.9	+ .116	− .008	.116
50		664	18.15	1 0 37	17.0	+ 7.3	+ 2.8	− .473	− .113	.486
51		Anon.	10.9	1 19	31.0	+12.5	+16.8	+ .070	− .018	.072
52		Anon.	13.8	2 17	13.5	+19.8	− 0.7	− .077	− .014	.078
53		Anon.	11.4	1 2 43	28.3	+22.8	+14.1	+ .083	− .073	.111
54	9	Anon.	17.0	3 0 21	12.5	−23.8	− 2.8	− .002	− .072	.072
55		H 235	16.52	3 47	27.0	+ 1.8	+11.7	+ .051	− .079	.094
56‡		H 347	10.7	4 11	33.1	+ 4.8	+17.8	+ .108	− .215	.241
57‡			12.4	4 12	33.1	+ 4.9	+17.8	+ .090	− .214	.232
58		Anon.	15.7	6 29	24.8	+21.8	+ 9.5	+ .032	− .047	.057
59		Anon.	17.5	3 6 42	6.8	+23.6	− 8.5	+ .007	− .112	.112
60	10	67	16.21	5 7 18	6.5	− 3.3	− 2.8	+ .083	− .101	.131
61		155	17.14	8 5	5.6	+ 2.5	− 3.7	+ .044	− .089	.099
62		171	16.67	10	14.4	+ 3.2	+ 5.1	− .020	− .094	.096
63		211	7.03	8 33	4.2	+ 6.0	− 5.1	− .019	− .156	.157
64		H 342	15.41	5 9 44	+60 23.8	+14.8	+14.5	+0.227	−0.434	0.490

TABLE III—*Continued*

Current No.	Sel. Area	No. in Cat.	Mag.	α 1900	δ 1900	x	y	μ_x	μ_y	μ
65		Anon.	15.4	5ʰ 10ᵐ 47ˢ	+60° 1′.6	+22′.8	− 7′.7	+0″.011	−0″.055	0″.056
66	11	H 328	11.67	7 5 0	59 54.9	−13.2	− 1.9	− .049	− .057	.075
67		53	17.10	6 26	60 4.8	− 2.5	+ 8.0	− .017	− .057	.059
68		H 240	6.73	7 10	59 48.9	+ 3.1	− 7.9	− .093	− .248	.265
69		H 496	13.52	7 56	60 9.3	+ 8.7	+12.5	− .007	− .116	.116
70		H 619	15.00	7 8 32	60 13.5	+13.2	+16.7	− .032	− .072	.079
71	12	H 247	13.52	8 59 47	59 44.6	−22.3	+ 5.1	− .044	− .071	.084
72		Anon.	16.2	9 0 31	35.8	−16.8	− 3.8	− .059	− .107	.122
73		19	7.74	2 9	33.4	− 4.4	− 6.1	− .181	− .016	.182
74		83	14.46	3 51	38.2	+ 8.5	− 1.4	+ .020	− .068	.071
75		H 216	10.89	4 16	31.8	+11.7	− 7.8	− .091	− .207	.226
76		Anon.	15.4	9 5 16	59 46.4	+19.2	+ 6.8	− .158	− .068	.172
77	13	Anon.	16.7	11 1 12	60 6.3	−13.1	+20.9	+ .120	− .004	.120
78		H 208	13.50	1 12	59 50.7	−13.2	+ 5.3	− .085	− .065	.107
79		7	11.49	2 0	47.9	− 7.2	+ 2.5	+ .056	− .011	.057
80		H 127	13.22	9	31.5	− 6.1	−13.9	− .087	+ .009	.087
81		24	17.78	11 2 26	43.6	− 4.0	− 1.8	+ .025	− .103	.106
82	14	Anon.	16.8	13 19 55	18.7	−18.7	− 6.3	+ .056	− .086	.103
83		13	13.32	21 26	24.9	− 7.0	− 0.2	− .081	+ .026	.085
84		H 165	14.93	24 11	22.3	+14.0	− 2.7	+ .042	− .049	.065
85		H 175	14.80	13 25 55	22.6	+27.2	− 2.3	+ .061	− .085	.105
86	15	72	16.56	15 16 40	59 57.1	+ 0.8	+ 4.1	− .062	− .020	.065
87		H 555	11.58	17 30	60 13.2	+ 6.9	+20.2	− .137	− .085	.161
88		H 472	16.24	18 2	60 6.9	+11.0	+13.9	− .043	+ .103	.112
89		H 385	15.09	15 18 55	59 50.0	+17.7	− 3.0	− .018	− .096	.098
90	16	89	16.93	17 29 16	40.5	+ 4.5	− 5.3	+ .042	+ .062	.075
91		Anon.	15.9	17 31 42	59 29.9	+23.0	−15.9	− .013	+ .083	.084
92	17	H 314	15.37	19 20 33	60 21.8	−15.8	+12.8	− .042	− .062	.075
93		H 340	15.03	21 17	27.8	−10.4	+18.8	+ .038	+ .071	.081
94		H 350	13.48	22 6	20.3	− 4.4	+11.3	+ .060	+ .022	.064
95		97s	16.84	19 22 26	+60 17.4	− 1.9	+ 8.4	+0.029	+0.089	0.094

96		H 272	12.97	$19^h 23^m 37^s$	+60° 18′.9	+ 6′.9	+ 9′.9	+0″.005	+0″.059	0″.059
97		H 374	15.61	19 23 44	20.5	+ 7.8	+11.5	+ .058	+ .074	.094
98	18	217	12.95	21 24 2	6.4	− 3.1	− 0.2	+ .043	+ .055	.070
99		271	11.93	9	60 12.3	− 2.2	+ 5.7	+ .019	+ .055	.058
100		H 171	11.77	24 27	59 54.1	0.0	−12.5	+ .066	+ .056	.087
101		H 234	16.72	25 11	59 51.2	+ 5.5	−15.4	+ .048	+ .099	.110
102		732	17.43	15	60 5.8	+ 6.0	− 0.8	+ .037	+ .047	.060
103		Anon.	16.8	23	59 46.1	+ 7.1	−20.5	+ .061	+ .033	.069
104		790	16.60	25	60 2.9	+ 7.2	− 3.7	+ .070	+ .081	.107
105		H 975	15.49	21 25 43	60 14.8	+ 9.4	+ 8.2	− .115	− .004	.115
106	19	Anon.	16.7	23 20 39	59 49.4	−17.9	−11.9	+ .088	+ .065	.109
107		725	10.58	21 58	60 4.6	− 7.9	+ 3.3	+ .457	+ .048	.460
108		Anon.	10.4	22 21	21.4	− 5.0	+20.1	+ .146	+ .118	.188
109		145	11.55	22 44	60 0.2	− 2.2	− 1.1	+ .062	+ .037	.072
110		Anon.	16.5	23 25 14	59 46.7	+16.7	−14.6	+ .097	+ .119	.154
111	20	H 265	15.53	0 39 19	45 29.5	−10.6	+ 8.6	+ .087	.000	.087
112		Anon.	16.3	39 47	1.9	− 5.7	−19.0	+ .110	− .045	.119
113		170	11.40	40 27	15.3	+ 1.3	− 5.6	+ .084	+ .008	.084
114		H 203	13.35	41 30	12.6	+12.4	− 8.3	+ .081	− .014	.082
115		Anon.	13.0	0 42 18	38.9	+20.7	+18.0	+ .088	+ .006	.088
116	21	Anon.	15.1	1 33 38	20.8	−23.4	+16.5	+ .084	− .036	.091
117		H 398	14.32	34 3	5.4	−19.0	+ 1.1	− .042	− .062	.075
118		H 585	15.58	34 12	18.0	−17.4	+13.7	+ .061	− .006	.061
119		106	12.66	35 34	2.9	− 2.9	− 1.4	+ .007	− .060	.060
120		107	17.26	35	2.8	− 2.7	− 1.5	− .006	− .067	.067
121		H 665	15.34	35 55	45 16.8	+ 0.7	+12.5	+ .049	− .031	.058
122		H 162	9.67	37 5	44 48.1	+13.1	−16.2	+ .131	− .010	.131
123		H 170	7.08	37 11	44 49.1	+14.3	−15.2	+ .126	+ .033	.130
124		Anon.	15.8	38 2	45 10.5	+23.1	+ 6.2	+ .135	− .100	.168
125		Anon.	14.6	1 38 7	3.6	+24.0	− 0.7	+ .103	− .063	.121
126	22	Anon.	15.2	2 35 47	2.5	−25.6	− 8.1	− .032	− .105	.110
127		405	17.69	38 46	16.7	+ 6.0	+ 6.1	+ .074	− .017	.076
128		H 958	16.90	39 9	27.3	+10.1	+16.7	+ .039	− .043	.058
129		H 752	9.84	39 57	45 11.0	+18.5	+ 0.4	+ .093	− .095	.133
130		Anon.	13.8	2 40 6	+44 59.6	+20.2	−11.0	−0.102	−0.095	0.139

TABLE III—*Continued*

Current No.	Sel. Area	No. in Cat.	Mag.	α 1900	δ 1900	x	y	μ_x	μ_y	μ
131		Anon.	16.2	$2^h40^m13^s$	+45°30′.8	+21′.2	+20′.2	+0″.054	−0″.055	0″.077
132	24	Anon.	16.7	4 36 37	44 55.1	−21.5	+ 0.6	− .014	− .092	.093
133		H 177	15.26	37 20	41.6	−13.9	−12.9	− .006	− .052	.052
134		H 178	14.54	37 21	44 42.0	−13.7	−12.5	− .017	− .057	.059
135		H 538	15.66	38 12	45 6.3	− 4.7	+11.8	+ .017	+ .066	.068
136		197	10.28	38 38	44 54.5	0.0	0.0	+ .049	− .051	.071
137		Anon.	16.4	39 50	45 8.8	+12.6	+14.3	+ .013	− .059	.060
138		H 631	9.99	4 40 26	45 7.1	+18.9	+12.6	+ .051	− .081	.096
139	26	Anon.	17.5	6 34 10	44 50.7	−22.9	+ 1.5	+ .004	− .064	.064
140		Anon.	16.2	28	31.4	−19.9	−17.8	+ .039	− .055	.067
141		Anon.	16.2	44	44 38.2	−17.0	−11.0	− .123	− .020	.125
142		Anon.	16.5	34 58	45 8.8	−14.4	+19.6	− .079	− .148	.168
143		H 19	15.83	35 6	44 32.8	−13.0	−16.4	+ .025	− .046	.052
144		H 342	11.13	35 44	45 7.0	− 6.3	+17.8	+ .008	− .065	.065
145		Anon.	17.5	36 8	44 35.3	− 2.0	−13.9	+ .029	− .074	.079
146		Anon.	17.7	15	44 34.9	− 0.7	−14.3	+ .055	− .024	.060
147		Anon.	16.5	22	45 1.2	+ 0.5	+12.0	+ .018	− .055	.058
148		H 58	9.40	22	44 31.0	+ 0.4	−18.2	+ .058	− .055	.080
149		H 370	13.05	29	45 2.6	+ 1.8	+13.4	− .040	− .049	.063
150		110*s*	17.57	31	44 39.2	+ 2.1	−10.0	− .003	− .051	.051
151		Anon.	15.4	36 53	45 10.7	+ 5.9	+21.5	− .050	− .060	.078
152		Anon.	14.0	6 38 16	44 54.3	+20.6	+ 5.1	− .020	− .112	.114
153	27	H 112	15.04	7 35 54	32.2	−24.6	−16.7	+ .075	− .103	.127
154		71	17.15	38 12	54.7	− 0.1	+ 5.8	+ .011	− .053	.054
155		Anon.	15.7	7 39 43	47.2	+16.0	− 1.7	− .020	− .063	.066
156	28	H 74	12.86	8 38 45	48.5	−11.6	− 8.1	− .137	− .181	.227
157		Anon.	15.9	38 56	36.2	− 9.7	−20.4	− .020	− .094	.096
158		29	16.91	39 36	56.4	− 2.6	− 0.2	− .038	− .040	.055
159		69	11.59	40 25	56.6	+ 6.2	0.0	− .054	− .063	.083
160		68*s*	15.51	40 50	44 59.1	+10.6	+ 2.5	+ .020	− .162	.163
161		Anon.	16.4	8 41 2	+45 0.7	+12.6	+ 4.1	−0.029	+0.125	0.128

162		H 45	15.91	8h 41m 41s	+44° 38′.8	+19′.7	−17′.8	+0″.053	+0″.068	0″.086
163		H 103	15.55	41 46	44 40.3	+20.6	−16.3	+ .060	− .057	.083
164		Anon.	16.7	8 42 16	45 1.9	+25.7	+ 5.3	− .208	− .138	.250
165	29	20	11.16	9 38 2	44 56.9	− 5.1	+ 4.2	+ .080	− .157	.176
166		61	17.83	38 54	53.2	+ 4.1	+ 0.5	+ .036	− .051	.062
167		Anon.	16.5	9 39 28	44 59.5	+10.1	+ 6.8	− .026	− .072	.077
168	30	H 267	14.43	10 35 51	45 14.1	−15.8	+ 5.0	+ .064	− .028	.070
169		Anon.	16.8	36 20	44 59.6	−10.8	− 9.5	− .112	+ .020	.114
170		54	11.26	38 2	45 10.0	+ 7.3	+ 0.9	+ .043	− .073	.085
171		Anon.	16.6	38 46	6.6	+15.1	− 2.5	− .039	− .086	.094
172		H 371	15.67	10 39 48	45 21.1	+25.9	+12.0	− .101	+ .007	.101
173	31	H 197	15.50	11 34 55	44 57.6	−21.2	+15.8	− .043	− .034	.055
174		H 75	15.40	35 37	24.1	−13.9	−17.7	− .081	− .002	.081
175		Anon.	17.0	35 52	54.6	−11.0	+12.8	− .095	− .040	.103
176		Anon.	17.2	36 8	31.0	− 8.3	−10.8	− .051	.000	.051
177		66	17.24	37 28	47.4	+ 6.0	+ 5.6	− .120	+ .034	.125
178		Anon.	16.1	11 37 36	25.1	+ 7.5	−16.7	− .086	− .041	.095
179	32	H 149	14.76	12 49 24	39.8	−12.3	−10.3	− .178	− .055	.186
180		1s	16.57	34	46.8	−10.4	− 3.3	− .045	+ .058	.073
181		2	16.41	49 43	44 47.2	− 8.8	− 2.9	− .001	− .104	.104
182		3s	14.85	50 26	45 1.5	− 1.2	+11.4	− .078	+ .002	.078
183		27	11.96	32	44 55.8	− 0.1	+ 5.7	− .092	+ .004	.092
184		H 329	14.86	42	45 4.1	+ 1.7	+14.0	− .146	− .084	.168
185		33	17.00	50 45	44 46.2	+ 2.1	− 3.9	− .050	.000	.050
186		H 216	15.19	51 45	42.7	+12.9	− 7.4	− .020	− .124	.126
187		H 174	13.41	12 52 19	44 37.5	+19.0	−12.6	− .050	− .039	.063
188	33	47	9.40	13 50 7	45 12.9	0.0	0.0	− .130	+ .093	.160
189		Anon.	16.8	51 45	13.8	+17.3	+ 0.9	− .072	+ .205	.217
190		Anon.	16.6	52 2	7.1	+20.3	− 5.8	+ .049	− .035	.060
191		H 287	16.40	13 52 38	45 13.1	+26.7	+ 0.2	− .092	− .116	.148
192	34	18	11.31	14 47 14	44 51.0	− 5.9	−10.2	− .010	− .215	.215
193		H 390	16.30	39	45 14.8	− 1.4	+13.6	− .061	− .045	.076
194		H 183	15.47	47 55	44 40.2	+ 1.3	−21.0	− .123	− .166	.207
195		Anon.	17.6	48 5	44 54.2	+ 3.2	− 7.0	− .056	− .080	.098
196		78	11.25	14 48 39	+45 1.3	+ 9.2	+ 0.1	−0.067	+0.041	0.079

TABLE III—*Continued*

Current No.	Sel. Area	No. in Cat.	Mag.	α 1900	δ 1900	x	y	μ_x	μ_y	μ
197		H 189	15.02	$14^h48^m45^s$	$+44°43'.6$	$+10'.3$	$-17'.6$	$+0''.005$	$-0''.066$	$0''.066$
198		Anon.	17.5	48 53	55.1	+11.6	− 6.1	− .332	− .366	.494
199		H 257	11.48	49 24	55.2	+17.2	− 6.0	− .092	+ .020	.094
200		H 199	14.42	49 34	44 48.8	+19.0	−12.4	− .061	+ .035	.070
201		H 344	14.42	14 50 4	45 7.9	+24.1	+ 6.7	− .072	+ .045	.085
202	35	Anon.	16.8	15 47 12	44 51.6	−24.3	+ 2.5	− .024	+ .056	.061
203		H 252	16.10	17	45.2	−23.3	− 3.9	− .040	+ .047	.062
204		H 253	15.35	31	42.6	−21.0	− 6.5	− .013	+ .074	.075
205		Anon.	16.1	52	44 32.6	−17.3	−16.6	+ .020	− .095	.097
206		H 413	15.95	47 58	45 6.2	−16.1	+17.1	− .020	+ .055	.059
207		H 420	14.70	48 17	7.6	−12.6	+18.5	.000	− .062	.062
208		H 434	16.11	48 54	6.0	− 6.1	+16.9	− .007	+ .099	.099
209		Anon.	16.7	49 3	45 2.6	− 4.6	+13.5	− .134	+ .133	.189
210		8*s*	16.92	49 46	44 39.6	+ 3.1	− 9.6	+ .046	− .083	.095
211		Anon.	17.0	50 49	43.4	+14.3	− 5.8	− .090	+ .122	.152
212		Anon.	17.0	15 50 49	44 43.2	+14.2	− 6.1	− .102	+ .118	.156
213	36	H 223	16.02	16 43 39	45 25.5	−24.4	+ 3.0	+ .011	+ .119	.120
214		Anon.	15.8	44 15	16.0	−18.2	− 6.5	− .122	+ .027	.125
215		H 238	13.05	34	29.7	−14.7	+ 7.2	+ .026	+ .052	.058
216		Anon.	16.5	44 39	31.8	−13.9	+ 9.3	− .074	+ .034	.081
217		Anon.	16.1	45 45	38.1	− 2.3	+15.6	− .001	− .067	.067
218		33*s*	16.19	46 3	31.0	+ 0.9	+ 8.5	+ .008	+ .112	.112
219		38*s*	15.04	19	12.1	+ 3.7	−10.4	− .025	− .064	.069
220		89	16.45	31	28.2	+ 5.8	+ 5.7	− .042	− .042	.059
221		H 342	13.75	46 54	36.5	+ 9.7	+.4.0	− .069	+ .031	.076
222		Anon.	16.5	16 47 52	33.4	+19.9	+10.9	− .241	+ .063	.249
223	37	H 270	15.16	17 46 10	45 5.2	−24.9	+ 4.7	− .011	+ .055	.056
224		Anon.	16.4	47 0	44 43.4	−16.2	−17.0	− .058	+ .145	.156
225		Anon.	16.7	47 3	45 14.0	−15.4	+13.5	− .013	− .084	.085
226		Anon.	16.4	48 0	44 44.8	− 5.4	−15.6	+ .087	+ .050	.100
227		56	16.84	17 48 4	+45 8.4	− 4.8	+ 8.0	−0.015	+0.066	0.068

228		H 124	15.27	17h 48m 33s	+44° 41′.8	+ 0′.4	−18′.7	−0″.088	+0″.002	0″.088
229		156	15.50	36	55.2	+ 0.9	− 5.3	− .063	− .058	.086
230		183	17.15	48 44	44 56.8	+ 2.3	− 3.6	+ .071	+ .024	.075
231		Anon.	16.8	17 49 33	45 16.6	+10.9	+16.1	+ .032	+ .068	.075
232	38	Anon.	16.7	18 44 35	16.7	−17.1	+ 4.3	− .017	− .100	.101
233		44*s*	16.28	45 25	9.2	− 8.2	− 3.2	− .039	− .094	.102
234		52	7.31	41	45 8.7	− 5.5	− 3.7	+ .016	+ .091	.092
235		H 64	14.21	41	44 58.5	− 5.4	−13.9	− .029	− .077	.082
236		Anon.	16.5	45 48	44 53.2	− 4.2	−19.2	− .017	− .171	.172
237		244	18.01	46 24	45 9.2	+ 2.1	− 3.2	− .009	− .067	.068
238		Anon.	16.7	47 0	1.1	+ 8.6	−11.3	− .030	− .058	.065
239		Anon.	16.8	8	18.7	+ 9.8	+ 6.3	+ .001	+ .132	.132
240		Anon.	17.1	18 47 10	45 18.9	+10.3	+ 6.5	− .012	+ .141	.142
241	39	Anon.	14.7	19 44 26	44 47.8	−25.7	− 6.0	+ .033	+ .054	.063
242		Anon.	15.1	46	45 12.0	−22.1	+18.2	+ .031	+ .050	.059
243		H 367	15.64	44 59	44 46.0	−19.9	− 7.8	+ .059	+ .050	.077
244		H 26	15.26	45 11	32.8	−17.8	−21.1	− .069	− .083	.108
245		H 811.	16.23	45 46	44 59.6	−11.6	+ 5.7	+ .028	+ .068	.074
246		Anon.	17.0	46 10	45 8.0	− 7.2	+14.1	+ .053	+ .021	.057
247		H 155	13.26	46 31	44 33.6	− 3.7	−20.2	+ .078	− .042	.089
248		1070	16.24	47 34	54.4	+ 7.5	+ 0.5	+ .025	+ .053	.059
249		642*s*	12.68	47 48	44 55.4	+10.1	+ 1.6	− .064	− .053	.083
250		H 1420	12.71	48 11	45 8.2	+14.1	+14.3	+ .050	+ .083	.097
251		Anon.	15.7	19 49 2	45 4.0	+23.0	+10.1	+ .054	+ .034	.064
252	40	H 15	15.52	20 44 56	44 49.0	−17.3	− 9.4	− .036	+ .076	.084
253		H 548	9.53	45 2	45 17.0	−16.0	+18.7	.000	+ .128	.128
254		Anon.	16.7	24	44 40.4	−12.4	−17.9	+ .189	+ .115	.221
255		Anon.	14.9	45 34	38.2	−10.5	−20.1	− .028	+ .045	.053
256		238	16.28	46 12	55.4	− 3.8	− 2.9	+ .033	+ .093	.099
257		H 90	15.77	47 21	46.4	+ 8.5	−11.9	+ .044	+ .027	.052
258		H 94	15.77	47 26	44 41.2	+ 9.4	−17.2	− .002	− .094	.094
259		Anon.	16.1	20 49 0	45 6.2	+25.9	+ 7.9	− .101	− .054	.115
260	41	542	10.06	21 49 36	44 58.9	0.0	0.0	+ .065	− .095	.115
261		668*s*	15.30	21 50 31	45 0.9	+ 9.7	+ 2.0	+ .048	− .029	.056
262	42	Anon.	14.2	22 46 29	+45 21.4	−23.9	+11.7	+0.085	+0.014	0.086

TABLE III—*Continued*

Current No.	Sel. Area	No. in Cat.	Mag.	α 1900	δ 1900	x	y	μ_x	μ_y	μ
263		Anon.	16.6	22h 46m 42s	+45° 8′.4	−21′.7	− 1′.3	+0″.082	+0″.033	0″.088
264		H 152	15.27	49 29	44 54.7	+ 7.8	−15.0	+ .062	− .007	.062
265		342s	15.91	49 31	45 17.6	+ 8.1	+ 7.9	+ .045	+ .033	.056
266		H 403	15.89	22 50 17	45 3.4	+16.2	− 6.3	+ .074	− .001	.074
267	43	H 63	12.47	23 50 9	44 33.1	+ 2.5	−17.1	+ .055	− .018	.058
268		209	12.95	13	48.1	+ 3.2	− 2.1	− .055	− .060	.081
269		Anon.	16.5	19	33.3	+ 4.4	−16.9	+ .138	− .038	.143
270		249s	17.01	50 52	48.7	+10.2	− 1.5	+ .096	− .017	.097
271		Anon.	16.2	51 19	44.9	+15.0	− 5.3	+ .083	− .027	.087
272		H 230	14.21	23 51 33	44 44.6	+17.5	− 5.6	+ .057	+ .006	.057
273	46	H 200	15.97	2 28 20	30 6.6	−14.3	− 8.0	+ .087	− .024	.090
274		Anon.	16.8	28 41	29.3	− 9.8	+14.7	+ .008	− .101	.101
275		H 452	15.97	29 2	32.6	− 5.3	+18.0	+ .071	+ .016	.073
276		Anon.	17.0	35	27.1	+ 1.9	+12.5	+ .102	+ .003	.102
277		H 384	15.54	38	29.9	+ 2.5	+15.3	+ .037	− .179	.183
278		Anon.	17.1	2 29 56	30 1.9	+ 6.4	−12.7	+ .034	− .047	.058
279	48	H 9	16.13	4 21 35	29 50.4	−12.6	−18.0	+ .021	− .045	.050
280		H 345	12.58	56	30 29.0	− 8.0	+20.6	+ .012	− .103	.104
281		10	16.45	21 59	6.7	− 7.3	− 1.7	+ .056	− .046	.072
282		177	16.12	22 23	30 4.2	− 2.2	− 4.2	+ .021	− .053	.057
283		Anon.	16.7	26	29 49.9	− 1.4	−18.5	+ .059	− .040	.071
284		Anon.	17.2	50	29 56.6	+ 3.6	−11.8	+ .044	− .044	.062
285§		H 393	16.00	51	30 22.6	+ 3.8	+14.2	+ .044	− .041	.060
286		H 397	15.64	22 53	26.5	+ 4.2	+18.1	+ .021	− .113	.115
287		225s	17.43	23 11	5.7	+ 8.1	− 2.7	+ .033	− .051	.061
288		H 310	9.94	49	19.0	+16.3	+10.6	− .092	− .088	.127
289		H 443	16.30	4 23 55	30 20.6	+17.6	+12.2	+ .059	− .073	.094
290	49	Anon.	12.8	5 21 42	29 49.9	−25.6	+ 5.0	− .033	− .041	.053
291		Anon.	16.2	21 49	45.4	−24.0	+ 0.5	− .008	− .073	.073
292		Anon.	16.4	22 21	44.0	−17.2	− 0.9	+ .022	− .055	.059
293		233	16.47	5 23 21	+29 41.5	− 4.1	− 3.4	+0.012	−0.055	0.056

294.		293s	17.97	$5^h 23^m 54^s$	+29° 52'.2	+ 3'.0	+ 7'.3	+0".054	−0".062	0".082
295.		304s	18.04	23 55	51.9	+ 3.2	+ 7.0	− .016	− .165	.166
296.		Anon.	16.0	24 41	49.4	+13.3	+ 4.5	− .021	− .054	.058
297.		Anon.	15.2	5 25 17	27.1	+21.1	−17.8	+ .005	− .093	.093
298.	50	Anon.	16.5	6 23 9	33.9	−15.9	−19.9	+ .018	− .087	.089
299.		257	17.13	6 24 11	29 54.7	− 2.5	+ 0.9	− .062	− .225	.233
300.	51	Anon.	16.6	7 23 11	30 10.4	−15.3	+ 8.1	+ .097	+ .001	.097
301.		11	14.55	23 50	30 1.8	− 6.8	− 0.5	− .008	− .070	.070
302‖		69s	17.55	24 23	29 53.2	+ 0.4	− 9.1	+ .005	− .069	.069
303.		H 196	14.78	32	29 44.8	+ 2.4	−17.4	+ .021	− .101	.103
304.		157	15.05	40	30 1.6	+ 4.0	− 0.7	− .033	− .079	.086
305.		162	15.29	7 24 42	30 7.8	+ 4.4	+ 5.6	+ .060	− .073	.094
306.	52	Anon.	16.9	8 24 58	29 54.7	− 9.9	− 8.2	− .004	− .074	.074
307.		8	16.51	25 21	59.4	− 4.9	− 3.5	+ .023	− .054	.059
308.		H 212	14.46	25 55	29 48.4	+ 2.5	−14.5	− .189	− .140	.235
309.		H 619	12.69	26 14	30 21.0	+ 6.7	+18.1	− .070	− .150	.166
310.		Anon.	17.1	26	9.8	+ 9.3	+ 6.9	+ .010	− .078	.079
311.		Anon.	17.2	8 26 56	30 8.0	+15.7	+ 5.1	− .077	− .014	.078
312.	53	H 257	14.11	9 22 55	29 50.9	−21.4	− 9.8	− .050	− .076	.091
313.		H 180	14.16	23 57	29 41.5	− 8.1	−19.2	− .141	+ .050	.150
314.		35	16.44	24 17	30 6.1	− 3.7	+ 5.4	− .049	− .043	.065
315.		63	17.59	31	29 55.0	− 0.5	− 5.7	+ .035	− .046	.058
316.		72	18.04	24 39	29 54.4	+ 1.2	− 6.3	+ .034	+ .068	.076
317.		126	17.55	25 11	30 4.8	+ 8.0	+ 4.1	+ .042	− .056	.070
318.		Anon.	17.0	9 25 32	30 3.5	+12.6	+ 2.8	+ .047	− .162	.169
319.	55	H 101	14.02	11 28 3	29 45.5	−22.7	−13.2	− .092	− .024	.095
320.		H 108	13.47	28 31	44.5	−16.7	−14.2	− .075	− .008	.075
321.		32	10.08	29 48	29 58.7	0.0	0.0	+ .099	− .053	.112
322.		H 261	14.27	30 47	30 13.0	+12.9	+14.3	− .071	+ .024	.075
323.	56	13	12.19	57 42	29 40.6	− 6.5	− 0.1	− .120	− .113	.165
324.		31	14.87	58 4	34.6	− 1.7	− 6.1	− .180	+ .044	.185
325.		34	11.38	58 6	34.3	− 1.1	− 6.4	− .182	+ .031	.185
326.		H 133	16.30	59 42	21.6	+19.7	−19.1	− .002	− .281	.281
327.		H 276	15.50	11 59 53	53.7	+22.1	+13.0	+ .009	− .105	.105
328.	58	2	15.61	13 59 14	+29 38.7	− 9.6	+ 1.3	−0.067	+0.002	0.067

TABLE III—*Continued*

Current No.	Sel. Area	No. in Cat.	Mag.	α 1900	δ 1900	x	y	μ_x	μ_y	μ
329		11	17.91	13^h 59^m 21^s	+29° 31′.2	− 8′.1	− 6′.2	−0″.061	−0″.168	0″.179
330		Anon.	16.6	47	50.2	− 2.5	+12.8	+ .090	− .047	.102
331		55	9.72	13 59 59	37.4	0.0	0.0	+ .009	− .050	.051
332		H 156	14.87	14 0 0	24.0	+ 0.4	−13.4	.000	− .053	.053
333		H 291	12.57	18	55.4	+ 4.2	+18.0	− .058	+ .007	.058
334		Anon.	16.2	14 0 36	29 47.7	+ 8.1	+10.3	− .113	− .075	.136
335	67	Anon.	16.2	22 59 15	30 7.6	−22.0	− 3.4	+ .043	+ .027	.051
336		Anon.	16.3	17	19.9	−21.6	+ 8.9	+ .035	− .036	.050
337		H 387	15.46	19	30 21.2	−21.1	+10.2	+ .059	+ .007	.059
338		H 125	13.23	43	29 53.9	−16.1	−17.1	+ .053	− .010	.054
339		Anon.	17.2	22 59 45	30 10.3	−15.6	− 0.7	+ .042	− .032	.053
340		22*s*	17.17	23 0 16	30 13.0	− 8.9	+ 2.0	+ .055	− .026	.061
341		Anon.	16.8	1 49	29 55.9	+11.2	−15.1	+ .104	+ .007	.104
342		Anon.	16.2	23 2 23	30 8.7	+18.5	− 2.3	+ .114	+ .057	.127
343	71	Anon.	17.3	3 10 11	14 50.8	−20.7	−11.5	+ .121	− .065	.137
344		Anon.	17.0	35	15 2.2	−15.1	− 0.1	− .005	− .083	.083
345		Anon.	16.9	10 59	14 51.0	− 9.3	−11.4	+ .059	− .017	.061
346		H 257	9.25	11 7	15 17.6	− 7.2	+15.3	+ .079	− .155	.174
347		43	11.40	39	8.2	+ 0.4	+ 5.8	− .019	− .091	.093
348		H 273	14.97	11 57	18.6	+ 4.9	+16.2	+ .121	− .018	.122
349		H 346	15.29	12 42	15 22.6	+15.6	+20.3	+ .075	+ .050	.090
350		H 99	8.73	53	14 49.0	+18.3	−13.3	+ .019	− .293	.294
351		Anon.	16.0	12 54	14 51.4	+18.5	−11.0	+ .019	− .274	.275
352¶		H 224	12.42	13 3	15 4.6	+20.8	+ 2.2	+ .144	− .125	.191
353¶		H 225	13.17	3 13 4	4.7	+20.9	+ 2.3	+ .141	− .116	.183
354	72	6*s*	17.35	4 9 26	15 4.8	− 9.4	− 4.2	+ .105	− .077	.130
355		Anon.	16.0	32	14 49.5	− 8.1	−19.5	+ .123	− .001	.123
356		17	15.22	46	15 8.2	− 4.8	− 0.8	+ .182	− .301	.352
357		H 229	11.82	9 53	27.2	− 3.1	+18.2	+ .106	+ .001	.106
358		63	6.89	10 5	9.0	0.0	0.0	+ .130	− .039	.136
359		68	17.50	4 10 9	+15 8.6	+ 0.8	− 0.4	+0.067	−0.055	0.087

360		Anon.	16.1	$4^h 10^m 50^s$	+14° 55′.5	+10′.7	−13′.5	+0″.039	−0″.054	0″.067
361		H 95	11.28	4 11 24	51.1	+19.1	−17.9	+ .062	− .091	.110
362	73	H 24	14.89	5 14 16	48.6	− 9.0	− 8.9	− .020	− .052	.056
363		279	17.71	15 11	53.2	+ 4.2	− 4.3	− .008	− .063	.064
364		166*s*	17.98	5 15 29	54.7	+ 8.7	− 2.8	+ .025	− .089	.092
365	74	Anon.	13.3	6 14 5	14 46.0	−16.8	−19.8	+ .010	− .070	.071
366		Anon.	16.5	14 20	15 21.6	−13.1	+15.8	+ .005	− .061	.061
367**		Anon.	17.8	15 3	14 58.1	− 2.8	− 7.7	+ .006	+ .052	.052
368		H 102	16.16	16 4	14 54.9	+12.0	−10.9	− .033	− .061	.069
369		H 279	12.80	25	15 8.5	+16.7	+ 2.7	− .071	+ .003	.071
370		H 150	8.76	37	14 54.7	+19.8	−11.1	+ .001	− .097	.097
371		BD+15°1170	10.8	6 16 47	15 4.0	+22.4	− 1.8	+ .081	− .152	.172
372	76	Anon.	15.9	8 14 58	14 48.0	− 8.7	−13.4	− .059	− .011	.060
373		24	13.87	15 14	15 9.0	− 4.8	+ 7.6	− .017	− .052	.055
374		23	13.09	14	14 56.8	− 4.8	− 4.7	− .029	− .047	.055
375		117	13.30	39	14 57.8	+ 1.3	− 3.7	+ .019	− .058	.061
376		161	18.24	49	15 4.4	+ 3.7	+ 3.0	+ .095	− .031	.100
377		186	16.84	15 58	15 7.8	+ 5.9	+ 6.3	+ .015	− .135	.136
378		195	17.46	16 1	14 55.2	+ 6.6	− 6.3	+ .060	+ .097	.114
379		Anon.	17.9	24	15 5.4	+12.3	+ 4.0	− .105	− .048	.115
380		H 149	15.09	8 16 48	14 46.4	+17.6	−15.0	− .023	− .058	.062
381	78	H 173	14.25	10 12 11	15 4.5	−24.8	− 5.7	− .116	+ .055	.128
382		H 364	14.72	12 39	15 32.0	−18.0	+21.8	− .066	+ .072	.098
383		H 131	14.72	13 44	14 57.1	− 2.5	−13.1	− .025	− .046	.052
384		Anon.	17.0	47	15 24.0	− 1.6	+13.8	+ .023	− .060	.064
385		Anon.	16.0	13 59	14 54.4	+ 1.3	−15.8	− .139	− .181	.228
386		66	16.56	14 17	15 9.0	+ 5.5	− 1.2	− .047	+ .018	.050
387		H 327	14.25	10 14 48	15 24.2	+12.9	+14.0	+ .069	− .033	.076
388	79	8	11.15	11 17 8	14 59.6	− 8.1	+ 7.3	− .512	+ .008	.512
389		H 109	12.51	17 52	38.6	+ 2.6	−13.7	− .083	− .118	.144
390		H 233	13.61	18 31	52.0	+12.0	− 0.3	− .101	+ .042	.109
391		H 175	9.10	19 6	43.0	+20.4	− 9.3	− .100	+ .042	.108
392		H 176	13.13	11 19 7	43.4	+20.7	− 8.9	− .056	− .008	.057
393	80	Anon.	16.7	12 11 30	44.0	−15.0	−16.0	− .022	− .045	.050
394		Anon.	17.2	12 12 28	+14 42.8	− 1.0	−17.2	−0.029	−0.042	0.051

TABLE III—*Continued*

Current No.	Sel. Area	No. in Cat.	Mag.	α 1900	δ 1900	x	y	μ_x	μ_y	μ
395		55	16.42	$12^h 12^m 36^s$	+15° 3′.8	+ 1′.1	+ 3′.8	+0″.033	−0″.077	0″.084
396		81	17.56	55	14 50.6	+ 5.7	− 9.4	− .041	− .072	.083
397		Anon.	17.1	12 57	38.0	+ 6.1	−22.0	− .145	− .021	.147
398		Anon.	16.5	13 9	14 44.5	+ 8.9	−15.5	− .054	+ .063	.083
399		Anon.	17.3	12 13 27	15 13.9	+13.2	+13.9	+ .001	− .105	.105
400	81	Anon.	16.3	13 10 15	14 35.4	−26.1	− 6.6	− .104	− .012	.105
401		H 103	14.45	39	27.4	−20.2	−14.6	− .052	− .019	.055
402		Anon.	16.5	10 57	29.7	−15.8	−12.3	− .049	+ .060	.077
403		H 208	13.60	11 5	47.9	−13.9	+ 5.9	− .031	− .285	.287
404		70	17.29	12 2	36.7	− 0.1	− 5.3	+ .022	− .061	.065
405		H 255	15.90	6	57.5	+ 0.9	+15.5	− .155	− .115	.193
406		106	19.44	25	35.8	+ 5.4	− 6.2	− .084	− .021	.087
407		Anon.	16.1	12 36	54.9	+ 8.0	+12.9	+ .029	− .063	.069
408		H 224	15.90	13 7	44.5	+15.6	+ 2.5	− .045	− .101	.111
409		Anon.	16.5	26	40.2	+20.2	− 1.8	− .035	− .114	.119
410		Anon.	16.6	37	34.2	+23.0	− 7.8	− .005	− .067	.067
411		Anon.	16.8	13 13 39	14 27.1	+23.5	−14.9	− .079	+ .038	.088
412	93	H 395	12.10	1 48 36	0 28.2	−16.6	+10.6	+ .026	+ .073	.077
413		21	14.61	49 26	8.9	− 4.1	− 8.7	− .038	− .042	.057
414		23	12.68	29	24.4	− 3.4	+ 6.8	+ .057	− .037	.068
415		30	12.48	49 32	5.9	− 2.7	−11.7	+ .056	+ .016	.058
416		H 420	16.07	1 50 7	+ 30.0	+ 6.2	+12.4	+ .051	− .013	.053
417	94	H 188	12.74	2 49 8	− 5.2	−25.0	−11.8	− .085	− .100	.131
418		H 241	16.86	52 12	− 9.9	+20.9	−16.5	+ .073	− .069	.100
419		H 328	10.86	2 52 31	+ 0 9.8	+25.7	+ 3.2	+ .104	+ .090	.138
420	95	Anon.	16.4	3 47 41	1.6	−21.7	+ 2.0	− .039	− .099	.106
421		Anon.	16.6	48 18	19.4	−12.5	+19.8	+ .223	− .244	.331
422		2S	17.31	28	+ 1.5	−10.0	+ 1.9	+ .084	− .061	.103
423††		Anon.	16.9	48 28	− 12.4	− 9.9	−12.0	+ .348	− .210	.406
424		H 137	15.93	49 57	14.1	+12.2	−13.7	− .026	− .102	.105
425		H 139	13.17	3 49 58	− 0 14.5	+12.5	−14.1	−0.025	−0.076	0.080

426		H 227	16.24	3h 50m 1s	− 0° 3′.1	+13′.3	− 2′.7	+0″.076	−0″.026	0″.080
427		H 282	16.51	3 50 19	+ 1.7	+17.8	+ 2.1	+ .044	− .036	.057
428	96	31	17.48	4 47 23	− 3.9	− 5.1	− 0.9	+ .016	− .159	.160
429‡‡		32	17.25	47 23	− 3.9	− 5.1	− 0.9	− .010	− .161	.161
430		H 777	15.23	48 26	+ 9.9	+10.7	+12.9	− .050	− .051	.071
431		H 263	15.08	48 45	− 11.4	+15.5	− 8.4	+ .070	− .074	.101
432		H 642	14.09	4 49 10	+ 8.0	+21.6	+11.0	+ .036	− .042	.055
433	97	Anon.	16.9	5 50 58	5.1	−20.1	+ 4.2	+ .006	− .121	.121
434		Anon.	11.6	50 58	+ 4.3	−20.0	+ 3.4	− .143	− .001	.143
435		Anon.	16.5	52 43	− 12.5	+ 6.2	−13.4	+ .074	+ .021	.077
436		Anon.	17.1	5 53 56	+ 9.9	+24.5	+ 9.0	− .054	− .084	.100
437	98	Anon.	16.8	6 45 31	+ 3.4	−23.2	+13.9	+ .012	− .096	.097
438§§		BD−0°1462	6.17	45 43	− 25.4	−20.2	−14.8	− .012	− .094	.095
439		208	17.24	46 47	6.2	− 4.6	+ 4.4	+ .089	− .088	.125
440		331s	17.44	47 28	4.0	+ 6.2	+ 6.6	− .012	+ .058	.059
441		Anon.	16.4	50	17.0	+11.6	− 6.5	+ .091	− .050	.104
442		H 775	16.35	50	16.6	+11.7	− 6.1	+ .102	− .056	.116
443		H 358	15.26	6 47 52	24.8	+12.1	−14.2	+ .176	− .044	.181
444	99	H 258	11.80	7 48 47	− 17.6	−13.4	− 3.7	− .097	− .055	.112
445		Anon.	16.0	48 52	+ 6.0	−12.1	+19.9	− .034	− .074	.081
446		Anon.	12.9	49 39	0.8	− 0.4	+14.7	− .009	− .051	.052
447		Anon.	11.6	50 26	+ 0.2	+11.3	+14.1	− .065	+ .034	.073
448		Anon.	16.1	32	− 2.0	+12.8	+11.9	− .024	− .079	.083
449		H 328	13.27	7 50 36	17.4	+13.9	− 3.5	− .016	− .070	.072
450	100	H 164	12.87	8 48 9	27.0	−10.8	−13.0	+ .072	− .058	.092
451		39	9.47	48 42	− 10.1	− 2.5	+ 3.9	− .037	− .121	.127
452		H 546	14.62	8 50 14	+ 1.2	+20.5	+15.2	− .104	− .022	.106
453	101	Anon.	16.2	9 49 50	+ 11.4	−25.5	+10.6	− .047	− .021	.051
454		Anon.	17.0	51 9	− 19.3	− 5.7	−20.1	− .080	+ .032	.086
455		64	15.64	11	− 3.5	− 5.2	− 4.3	− .231	+ .019	.232
456		Anon.	17.4	45	+ 14.7	+ 3.3	+13.9	+ .032	− .091	.096
457		Anon.	16.9	51 55	− 10.1	+ 5.7	−10.9	− .063	− .050	.080
458		H 418	12.39	52 0	+ 18.5	+ 7.0	+17.7	− .110	+ .034	.115
459		Anon.	17.4	9 52 20	+ 15.1	+11.9	+14.3	+ .024	− .047	.053
460	105	H 314	15.38	13 31 5	− 0 14.2	−23.6	− 7.2	−0.113	−0.031	0.117

TABLE III—*Continued*

Current No.	Sel. Area	No. in Cat.	Mag.	α 1900	δ 1900	x	y	μ_x	μ_y	μ
461		H 214	7.43	$13^h 31^m 8^s$	− 0° 25′.0	−23′.0	−18′.1	−0″.181	−0″.031	0″.184
462		H 218	16.27	14	22.4	−21.3	−15.5	− .050	− .012	.051
463		Anon.	17.5	14	4.2	−21.5	+ 2.8	+ .050	− .126	.136
464		Anon.	17.0	27	25.0	−18.2	−18.1	− .002	− .056	.056
465		1s	17.81	56	8.6	−11.0	− 1.6	− .034	+ .057	.066
466		3s	17.04	31 59	− 8.8	−10.2	− 1.8	− .069	− .030	.075
467		Anon.	17.1	32 25	+ 7.2	− 3.7	+14.2	+ .070	− .015	.072
468		H 569	16.82	33 19	+ 7.2	+ 9.9	+14.1	− .050	+ .005	.050
469		Anon.	17.6	35	− 14.6	+13.9	− 7.7	− .234	− .037	.237
470		H 267	16.45	33 46	24.6	+16.5	−17.7	− .027	− .049	.056
471		H 272	16.82	13 34 11	− 23.8	+22.8	−16.9	− .037	− .045	.058
472	106	H 684	16.24	14 34 56	+ 5.2	−23.9	+ 5.5	− .062	− .036	.072
473		H 432	13.78	37 37	− 17.2	+16.5	−16.9	− .118	+ .021	.120
474		H 760	16.32	14 37 48	+ 8.5	+19.3	+ 8.8	− .086	− .006	.086
475	112	H 1602	16.16	20 36 23	+ 19.0	−13.5	+13.7	.000	− .089	.089
476		H 636	10.09	36 28	− 4.7	−12.2	−10.0	+ .082	+ .030	.087
477		H 1805	11.51	38 0	+ 11.5	+10.8	+ 6.2	+ .098	− .047	.109
478		Anon.	17.0	23	− 10.4	+16.7	−15.7	+ .080	+ .068	.105
479		H 400	14.47	20 38 31	0 13.8	+18.7	−19.1	+ .103	+ .008	.103
480	116	H 310	16.58	0 11 18	14 54.4	−24.6	− 2.4	+ .093	+ .020	.095
481		Anon.	16.8	42	46.5	−18.8	+ 5.5	+ .120	− .071	.139
482‖‖		BD−15°40	11.0	43	15 0.6	−18.5	− 8.6	− .045	− .067	.081
483‖‖		BD−15°40	13.0	11 43	15 0.5	−18.6	− 8.5	− .039	− .078	.087
484		H 323	14.59	12 5	14 58.8	−13.4	− 6.8	+ .085	− .035	.092
485		5	17.25	23	14 56.8	− 9.0	− 4.8	+ .096	− .011	.097
486		H 401	11.48	12 43	15 9.8	− 4.2	−17.8	+ .213	+ .053	.219
487		H 410	14.67	13 22	15 9.4	+ 5.3	−17.4	− .038	− .055	.067
488		H 255	16.08	24	14 41.6	+ 5.7	+10.4	+ .074	− .008	.074
489		10s	16.87	13 44	53.7	+10.7	− 1.7	+ .068	− .022	.071
490		H 204	15.25	14 40	37.7	+24.1	+14.3	+ .118	+ .082	.144
491		H 283	15.13	0 14 45	−14 43.6	+25.5	+ 8.4	+0.060	+0.020	0.063

492	117	Anon.	16.9	$1^h 11^m 20^s$	−14° 27′.2	−11′.2	+15′.6	+0″.103	−0″.034	0″.108
493		10	16.28	29	47.8	− 8.9	− 5.0	+ .063	+ .015	.065
494		H 164	14.98	11 34	24.2	− 7.7	+18.7	+ .055	− .021	.059
495		Anon.	17.1	12 20	57.6	+ 3.3	−14.8	+ .101	− .006	.101
496		95	17.07	12 48	14 44.6	+10.1	− 1.7	− .022	− .050	.055
497		H 444	15.72	13 7	15 2.6	+14.7	−19.8	+ .060	+ .028	.066
498		H 250	16.00	10	14 36.0	+15.5	+ 6.8	+ .085	− .012	.086
499		Anon.	16.8	1 13 44	47.4	+23.7	− 4.6	+ .116	+ .004	.116
500	118	H 246	14.13	2 14 24	14 55.9	−13.5	− 3.3	+ .065	− .001	.065
501		Anon.	16.8	14 34	15 0.4	−11.3	− 7.8	+ .062	+ .044	.076
502		33	15.96	15 4	14 50.5	− 3.9	+ 2.1	+ .326	+ .160	.363
503		55	8.96	15 20	52.6	0.0	0.0	− .074	− .025	.078
504¶¶		BD−15°410	9.90	16 56	14 55.1	+23.1	− 2.5	− .052	− .018	.055
505		Anon.	16.7	2 16 56	15 5.4	+23.0	−12.8	+ .062	+ .064	.089
506	119	Anon.	16.2	3 9 10	10.2	−14.0	−21.3	− .218	− .255	.335
507		H 360	14.82	14	15 8.0	−13.0	−19.1	+ .047	− .050	.069
508		13	14.58	9 41	14 52.7	− 6.6	− 3.8	− .064	− .042	.077
509		H 116	16.17	10 20	28.0	+ 2.9	+20.9	+ .068	− .044	.081
510		H 260	16.26	10 51	41.3	+10.3	+ 7.6	+ .051	− .045	.068
511		H 265	14.82	11 7	45.2	+14.1	+ 3.7	+ .039	+ .050	.063
512		H 328	16.46	3 11 11	14 54.5	+15.2	− 5.6	+ .057	− .072	.092
513	120	Anon.	15.7	4 10 26	15 12.2	−25.1	− 5.8	+ .022	− .086	.089
514		Anon.	16.9	11 4	14 54.7	−16.1	+11.7	+ .006	− .088	.088
515		162	14.95	12 46	15 7.5	+ 8.7	− 1.1	+ .036	− .040	.054
516		Anon.	16.6	13 30	4.5	+19.2	+ 1.9	− .131	− .132	.186
517		H 206	13.94	4 13 31	15 4.5	+19.4	+ 1.9	− .115	− .137	.179
518	121	H 269	13.70	5 13 19	14 47.8	−22.8	+ 4.5	− .071	+ .027	.076
519		Anon.	16.0	13 57	38.4	−13.7	+13.9	− .032	− .092	.097
520		15	13.14	14 28	51.1	− 6.1	+ 1.2	− .040	− .041	.057
521		48	17.92	42	14 58.6	− 2.7	− 6.3	− .001	+ .072	.072
522		H 605	16.39	14 45	15 7.0	− 1.9	−14.7	+ .042	− .035	.055
523		Anon.	17.0	15 10	15 3.0	+ 4.0	−10.7	+ .016	− .048	.051
524		118	13.48	10	14 46.6	+ 4.1	+ 5.7	+ .077	− .003	.077
525		H 196	12.84	23	37.9	+ 7.2	+14.4	+ .052	− .044	.068
526		H 342	15.34	5 15 33	−14 44.6	+ 9.7	+ 7.7	+0.030	+0.040	0.050

TABLE III—*Continued*

Current No.	Sel. Area	No. in Cat.	Mag.	α 1900	δ 1900	x	y	μ_x	μ_y	μ
527		H 649	14.62	5h 15m 58s	−15° 6′.7	+15′.6	−14′.4	+0″.019	−0″.066	0″.069
528		Anon.	16.0	16 27	14 59.7	+22.6	− 7.4	− .053	− .059	.079
529		Anon.	16.2	5 16 36	43.4	+24.8	+ 8.9	+ .076	− .216	.229
530	122	Anon.	13.8	6 10 38	14 59.4	−24.4	+ 6.0	− .020	− .066	.069
531		Anon.	16.5	10 40	15 15.3	−23.8	− 9.9	+ .019	− .066	.069
532		Anon.	13.5	11 36	15 25.4	−10.3	−20.0	+ .034	− .056	.066
533		H 80	12.43	11 59	14 45.9	− 4.9	+19.5	+ .017	− .104	.105
534		160	11.38	12 13	15 12.2	− 1.5	− 6.8	+ .082	− .013	.083
535		195	16.90	18	11.9	− 0.3	− 6.5	− .014	+ .076	.077
536		H 762	16.50	12 20	15 19.5	+ 0.2	−14.1	− .031	− .067	.074
537		H 402	11.82	13 22	14 50.7	+15.2	+14.7	+ .060	+ .009	.061
538		H 656	14.62	6 13 38	15 1.1	+19.2	+ 4.3	+ .004	− .057	.057
539	123	Anon.	10.4	7 13 27	14 54.3	−25.5	+10.2	+ .048	− .057	.075
540		H 1051	15.56	14 12	15 14.1	−14.7	− 9.6	+ .038	− .077	.086
541		H 599	11.85	14.26	0.4	−11.2	+ 4.1	− .048	− .081	.094
542		406*s*	17.00	15 44	6.9	+ 7.5	− 2.4	+ .004	− .081	.081
543		Anon.	9.7	7 16 38	9.8	+20.6	− 5.3	+ .340	− .402	.526
544	124	Anon.	16.5	8 12 49	6.3	−13.0	+ 4.2	− .043	+ .062	.075
545		H 901	12.46	13 35	15 27.9	− 1.7	−17.4	+ .159	− .062	.171
546		Anon.	16.1	13 54	14 56.6	+ 2.7	+13.9	− .059	+ .014	.061
547		H 186	10.86	14 7	14 53.3	+ 5.9	+17.2	+ .058	− .038	.069
548		269*s*	14.33	8 14 20	15 5.5	+ 9.0	+ 5.0	+ .034	− .052	.062
549	125	Anon.	16.0	9 10 41	14 55.8	−23.8	+ 9.5	− .105	+ .007	.105
550		Anon.	15.3	10 55	14 54.6	−20.3	+10.7	− .079	+ .025	.083
551		57	12.98	12 6	15 4.8	− 3.2	+ 0.5	+ .046	− .051	.069
552		H 281	10.63	13 3	14 53.6	+10.4	+11.8	− .092	− .018	.094
553		H 132	14.96	19	49.4	+14.3	+16.0	− .002	− .061	.061
554		H 292	13.52	20	14 54.0	+14.7	+11.3	− .005	− .057	.057
555		Anon.	16.5	40	15 10.6	+19.4	− 5.3	+ .031	− .054	.062
556		Anon.	15.7	9 13 47	19.8	+21.1	−14.5	+ .038	− .059	.070
557	126	H 318	12.86	10 14 10	−15 8.7	−26.5	− 9.6	−0.162	+0.050	0.170

558		Anon.	16.9	10h 14m 58s	−14° 55′.7	−14′.8	+ 3′.4	−0″.132	+0″.039	0″.138
559		H 243	15.37	15 14	54.6	−11.0	+ 4.5	− .076	+ .005	.076
560		28s	15.75	28	14 58.9	− 7.6	+ 0.2	+ .044	− .053	.069
561		35	11.30	48	15 0.3	− 2.8	− 1.2	− .003	− .086	.086
562		37	15.46	48	15 1.6	− 2.7	− 2.5	− .061	+ .007	.061
563		Anon.	17.8	50	14 43.2	− 2.3	+15.9	+ .041	− .084	.093
564		61	7.49	15 59	14 59.1	0.0	0.0	− .214	+ .281	.353
565		59s	16.69	16 13	15 7.4	+ 3.3	− 8.3	− .064	− .003	.064
566***		H 282	15.4	47	14 57.7	+11.5	+ 1.4	− .050	+ .010	.051
567***			15.0	10 16 48	14 57.7	+11.6	+ 1.4	− .048	+ .020	.052
568	127	Anon.	16.8	11 11 46	15 30.7	−17.9	−14.2	+ .261	− .182	.318
569		11	14.49	12 27	17.8	− 8.1	− 1.3	+ .119	− .063	.135
570		80	17.99	11 13 1	13.0	+ 0.2	+ 3.5	− .035	+ .053	.063
571	128	H 699	14.20	12 12 13	20.9	−23.3	− 7.0	− .102	− .033	.107
572		Anon.	16.7	12 48	4.2	−14.9	+ 9.7	− .049	+ .032	.059
573†††		Anon.	18.1	13 57	7.3	+ 1.8	+ 6.6	− .062	+ .005	.062
574		H 738	14.94	14 8	27.0	+ 4.5	−13.1	− .093	+ .023	.096
575		H 480	15.87	12 14 31	4.0	+10.0	+ 9.9	+ .025	+ .075	.079
576	129	H 698	14.34	13 12 22	15 4.4	−23.3	− 2.0	− .087	+ .038	.095
577		H 545	15.77	12 51	14 58.0	−16.2	+ 4.4	− .080	− .064	.102
578		H 861	16.44	13 20	15 12.1	− 9.2	− 9.7	− .094	+ .012	.095
579		H 400	15.73	44	14 41.9	− 3.5	+20.5	+ .084	− .341	.351
580		H 884	15.52	13 59	15 15.2	+ 0.1	−12.8	− .096	− .033	.102
581		H 602	16.71	14 45	14 51.2	+11.3	+11.2	− .077	− .001	.077
582		H 912	12.33	13 15 1	15 12.1	+15.2	− 9.7	− .085	+ .013	.086
583	130	H 623	13.61	14 5 56	15.4	−26.4	− 6.0	− .091	− .047	.102
584		Anon.	17.3	6 56	5.8	−12.1	+ 3.6	− .019	− .088	.090
585		8	16.49	7 8	15 17.0	− 9.1	− 7.7	− .077	+ .019	.079
586		H 412	14.81	8 51	14 53.0	+15.7	+16.4	− .092	− .168	.192
587		H 413	10.99	14 8 55	14 53.0	+16.8	+16.3	− .082	− .168	.187
588	131	H 1046	14.21	15 11 28	15 25.9	+ 0.3	−13.4	− .063	− .026	.068
589		Anon.	17.6	11 54	15 1.8	+ 6.4	+10.7	− .107	+ .026	.110
590		H 411	16.51	12 44	14 52.0	+18.8	+20.5	− .104	− .105	.148
591		H 882	11.32	12 52	15 15.3	+20.7	− 2.8	− .150	− .010	.150
592		H 1155	15.88	15 13 9	−15 24.4	+24.7	−11.9	−0.256	−0.161	0.302

TABLE III—*Continued*

Current No.	Sel. Area	No. in Cat.	Mag.	α 1900	δ 1900	x	y	μ_x	μ_y	μ
593	132	Anon.	17.0	$16^h10^m54^s$	−14°45′.0	−11′.4	+19′.9	−0″.027	+0″.170	0″.172
594		26	15.31	11 15	14 55.8	− 6.2	+ 9.1	+ .024	− .117	.119
595		154	17.76	11 54	15 2.4	+ 3.3	+ 2.5	− .095	− .029	.099
596		H 1704	13.18	12 15	21.0	+ 8.3	−16.1	− .206	− .113	.235
597		Anon.	17.3	43	10.2	+14.9	− 5.3	− .156	− .026	.158
598		Anon.	16.8	16 12 46	13.4	+15.7	− 8.5	− .142	− .026	.144
599	133	Anon.	16.5	17 11 19	15 12.1	−19.9	− 6.7	− .090	− .017	.092
600		Anon.	17.0	46	14 59.5	−13.3	+ 5.9	+ .032	− .064	.072
601		H 494	16.40	11 48	15 15.0	−12.9	− 9.6	+ .004	− .050	.050
602		Anon.	17.1	12 1	11.7	− 9.6	− 6.3	− .053	+ .013	.055
603		Anon.	17.5	9	15 12.3	− 7.7	− 6.9	+ .006	− .058	.058
604		Anon.	15.2	12 57	14 47.7	+ 3.9	+17.7	− .052	− .087	.101
605		1200	14.99	13 7	15 4.6	+ 6.2	+ 0.8	− .138	− .004	.138
606		Anon.	16.9	20	14 52.8	+ 9.4	+12.6	− .040	− .071	.081
607		Anon.	17.1	28	15 20.7	+11.3	−15.3	− .091	− .013	.092
608		H 840	14.11	17 13 30	15 20.6	+11.7	−15.2	− .051	− .013	.053
609	134	Anon.	12.2	18 8 45	14 53.0	−22.8	+ 4.3	− .073	− .077	.106
610		H 238	16.35	10 20	40.2	+ 0.3	+17.1	− .034	− .107	.112
611		Anon.	14.8	23	39.0	+ 0.9	+18.3	− .029	− .064	.070
612		Anon.	16.2	10 52	37.7	+ 8.0	+19.6	− .013	− .049	.051
613		Anon.	12.7	11 55	40.4	+23.3	+16.9	− .006	− .089	.089
614		Anon.	12.0	18 12 6	40.7	+25.8	+16.6	− .009	− .089	.089
615	135	H 480	15.39	19 11 40	14 57.6	−19.1	+ 1.4	− .068	+ .082	.107
616		H 1055	16.30	12 7	15 7.3	−12.6	− 8.3	− .052	− .077	.093
617		H 572	11.11	14	14 50.6	−10.9	+ 8.4	− .115	− .134	.177
618		166*s*	15.15	30	15 5.6	− 6.9	− 6.6	− .029	− .057	.064
619		944	15.51	12 53	14 50.3	− 1.3	+ 8.7	− .021	− .072	.075
620		576*s*	15.64	13 33	14 54.3	+ 8.3	+ 4.7	+ .106	− .145	.180
621		H 1413	14.89	14 4	15 1.6	+15.8	− 2.6	− .057	− .057	.081
622		Anon.	12.0	19 14 27	18.0	+21.3	−19.0	− .011	− .099	.100
623	136	H 905	12.04	20 8 44	−15 11.0	−14.8	− 5.7	−0.050	−0.139	0.148

624........		Anon.	17.0	$20^h\ 9^m 32^s$	$-14°\ 59'.1$	$-\ 3'.3$	$+\ 6'.2$	$+0''.011$	$-0''.071$	$0''.072$
625........		H 971	16.17	44	15 18.0	− 0.3	−12.7	− .060	− .187	.196
626........		182	8.62	46	15 5.3	0.0	0.0	− .135	− .217	.256
627........		Anon.	17.2	9 47	14 53.9	+ 0.3	+11.4	+ .044	− .026	.051
628........		Anon.	16.7	10 34	15 3.6	+11.6	+ 1.7	+ .052	+ .013	.054
629........		H 1032	16.41	10 35	17.6	+11.9	−12.3	− .046	+ .020	.050
630........		H 1093	15.26	20 11 26	15 11.9	+24.2	− 6.6	+ .071	− .041	.082
631........	137	H 542	16.02	21 8 52	14 43.5	−16.1	+ 5.5	− .356	− .320	.479
632........		77	17.49	9 49	47.8	− 2.3	+ 1.2	+ .057	+ .015	.059
633........		H 381	16.83	10 16	30.8	+ 4.3	+18.2	+ .029	− .048	.056
634........		171	18.11	10 21	54.4	+ 5.5	− 5.4	+ .094	− .136	.165
635........		H 905	16.89	11 0	14 50.3	+14.8	− 1.3	+ .034	− .039	.052
636........		Anon.	17.3	7	15 5.8	+16.5	−16.8	− .075	− .035	.083
637........		H 931	14.95	21 11 23	14 59.9	+20.3	−10.9	− .092	− .115	.147
638........	138	Anon.	17.8	22 9 19	54.3	−18.9	+ 1.7	+ .109	− .083	.137
639........		Anon.	18.0	9 20	54.0	−18.7	+ 2.0	+ .118	+ .012	.119
640........		63	15.64	10 34	14 57.7	− 0.9	− 1.7	− .126	− .204	.240
641........		Anon.	17.0	11 34	15 14.7	+13.6	−18.7	+ .107	+ .011	.108
642........		Anon.	16.9	45	7.3	+16.4	−11.3	− .017	− .053	.056
643........		Anon.	17.1	45	2.4	+16.4	− 6.4	− .058	− .039	.070
644........		H 647	13.02	45	1.7	+16.4	− 5.7	− .038	− .038	.054
645........		H 648	15.20	11 47	1.2	+16.9	− 5.2	+ .077	+ .007	.077
646........		Anon.	17.4	12 4	15 11.3	+20.9	−15.3	+ .061	+ .088	.107
647........		H 500	13.27	22 12 10	14 53.8	+22.4	+ 2.2	− .016	− .066	.068
648........	139	Anon.	16.7	23 13 1	14 36.1	−13.1	+11.7	+ .020	− .098	.100
649........		H 473	15.76	13 57	15 0.2	+ 0.4	−12.4	+ .113	− .053	.125
650........		H 492	15.38	15 12	15 0.7	+18.4	−12.9	+ .112	+ .008	.112
651........		H 235	16.81	23 15 24	−14 31.2	+21.4	+16.6	+0.149	−0.043	0.155

* 0'.3 f and 0'.3 n of H 112.

† 0'.1 p H 163.

‡ Given as one star in *Harvard Ann.*, **101.** Images partly overlap.

§ Images on both plates elongated. Probably a close double.

‖ The MW magnitudes of 68 *s* and 69 *s* probably should be interchanged.

¶ Images of 352 and 353 overlap.

** 10″ f and 3″ s of MW 130 s.

†† 15″ f and 20″ s of H 111.

‡‡ 1'.2 f and 2'.3 n of 428.

§§ Photographic magnitude from the *Henry Draper Catalogue.*

‖‖ Images of 482 and 483 overlap.

¶¶ Photographic magnitude from the *Henry Draper Catalogue.*

*** Images of 566 and 567 overlap. Given as one star in *Harvard Ann.*, **102.**

††† 12″ s of MW 84.

and one-half times that given in the *Catalogue*.[2] Among the 104,000 stars examined, 651 (1 in every 160) were found to have a considerable proper motion. As may be seen from Table II, the percentage of proper-motion stars increases rapidly with galactic latitude. Comparing Table II with the corresponding table given by van Maanen and Willis, we notice that the percentage of proper-motion stars is considerably larger in the present paper. This discrepancy becomes much smaller, however, if we consider only those stars having motions larger than 0."099. The average number of these stars per area is 1.9 for van Maanen and Willis and 2.5 in the present case. The difference probably is due mainly to the fact that the stereocomparator used by van Maanen and Willis has a relatively small field (16 as against 130 square minutes), which renders the discovery of small displacements very difficult through the lack of a sufficient number of comparison stars. In addition, the mean time-interval between the plate pairs of their material was 18 years, as against 21 years for the present discussion.

The detailed results for the 651 proper-motion stars are given in Table III. The number in the identification column is that of the *Mount Wilson Catalogue* for stars occurring in this catalogue. Otherwise, it is that of the Harvard-Groningen DM[3] preceded by an "H," or, in a few cases, the BD number. Stars appearing in none of these catalogues are indicated by "Anon." The magnitudes in Table III are from the *Mount Wilson Catalogue*, or from the Harvard-Groningen DM reduced to the international scale.[4] In some cases the corrections had to be extrapolated from the published values. The magnitudes for anonymous stars are estimates which may be considerably in error and are given to one decimal only. The right ascensions and declinations are for 1900. The rectangular co-ordinates in the seventh and eighth columns are relative to the central star. The last three columns give the proper motions in the x and y directions and the total motions.

[2] *Mt. W. Contr.*, No. 301, Table I*a*; *Ap. J.*, **62**, 320, 1925.

[3] *Harvard Ann.*, **101**, 1918; **102**, 1923.

[4] Seares, Joyner, and Richmond, *Mt. W. Contr.*, No. 289, Table III; *Ap. J.*, **61**, 303, 1925.

The stars of Table III which also appear in the *Radcliffe Catalogue*[5] enable us to calculate the probable error of the proper motions. For this computation the stars with motions smaller than 0".050, which have not been included in Table III, were also used. As the accuracy was substantially the same in both co-ordinates, the residuals in x and y were used together in a single solution. From 208 stars the

TABLE IV

FREQUENCY DISTRIBUTION OF PROPER MOTIONS OF 651 STARS

Interval	n	Interval	n
0".050–0".059	105	0".180–0".189	15
.060– .069	84	.190– .199	6
.070– .079	82	.200– .249	20
.080– .089	77	.250– .299	7
.090– .099	58	.300– .349	4
.100– .109	55	.350– .399	4
.110– .119	35	.400– .449	1
.120– .129	22	.450– .499	5
.130– .139	20	.500– .549	2
.140– .149	12	.550– .599	0
.150– .159	10	.600– .649	0
.160– .169	15	.650– .699	0
0.170–0.179	11	0.700–0.749	1

mean probable error of an annual proper motion was thus found to be ±0".011. For three intervals of magnitude the results are as follows:

Radcliffe Magnitude	Probable Error	Number of Stars
<10.0	±0".016	20
10.0–12.9	±0.012	64
>12.9	±0.011	124

The distribution of the proper motions according to magnitude is shown in Table V. In the mean the brighter stars have larger proper motions than the fainter stars, as might be expected. For stars faint-

[5] *Radcliffe Catalogue of Proper Motions in the Selected Areas 1 to 115*, Oxford University Press, 1934.

er than the thirteenth magnitude, the mean proper motion seems to be nearly constant. This result is probably due to the fact that for very faint stars small motions are more easily overlooked than for brighter stars.

The proper motions derived in this paper, combined with those by van Maanen and Willis, are excellent material for a derivation of the solar antapex, since the fields are well distributed over a considerable part of the sky. For this purpose the stars were divided into three

TABLE V

DISTRIBUTION OF PROPER MOTION ACCORDING TO MAGNITUDE

Mag.	n	$\bar{\mu}$	Mag.	n	$\bar{\mu}$
<8.00	9	0″.177	<10.00	27	0″.163
8.00– 9.99	18	.156			
10.00–10.99	18	.141			
11.00–11.99	34	.124	10.00–12.99	92	.122
12.00–12.99	40	.112			
13.00–13.99	44	.106			
14.00–14.99	73	.090	13.00–15.99	228	.101
15.00–15.99	111	.106			
16.00–16.99	194	.104			
17.00–17.99	101	.096	>15.99	304	0.103
>17.99	9	0.148			

magnitude groups, 11.00–13.99, 14.00–16.99, and >16.99, including 139, 420, and 147 stars, distributed over 79, 118, and 84 Selected Areas, respectively. Airy's method was applied; but since in this method large proper motions receive undue weight, certain stars have been rejected, namely, the few with proper motions larger than 0″.499, a number for which the residual appeared to be at least five times the probable error, and some with proper motions larger than 0″.099 which evidently are physically related to a neighboring star having the same motion. Although without influence on the final results, two stars from the list of van Maanen and Willis with motions smaller than 0″.050 were also discarded.

The mean μ_α and μ_δ were computed for each of the three magnitude groups in each Selected Area. Indicating the right ascension and the declination of the antapex by A and D, the parallactic mo-

tion by p, and the components of the vector toward the antapex by X, Y, and Z, we have

$$p \cos A \cos D = X;\ p \sin A \cos D = Y;\ p \sin D = Z$$

$$-X \sin \alpha + Y \cos \alpha = \mu_\alpha$$

$$-X \cos \alpha \sin \delta - Y \sin \alpha \sin \delta + Z \cos \delta = \mu_\delta$$

$$\tan A = \frac{Y}{X}\ ;\ \tan D = \frac{Z}{\sqrt{X^2 + Y^2}}\ .$$

These equations were solved by least squares for each magnitude group, with equal weights assigned to each Selected Area. The results, together with their weighted mean, are shown in Table VI.

TABLE VI

CO-ORDINATES OF THE ANTAPEX

Mag.	A	P.E.	D	P.E.	p	P.E.
11.00–13.99.......	6^h55^m	$\pm 25^m$	$-42^\circ.7$	$\pm 4^\circ.4$	$0''.092$	$\pm 0''.007$
14.00–16.99.......	7 9	16	41.6	2.6	.081	.004
>16.99.........	7 21	24	39.6	4.4	.067	.005
Weighted mean.	7 9	11	−41.4	2.0	.079	.003
>16.99, weighted	7 46	±25	−37.0	±4.7	0.062	±0.005

The agreement between the three solutions is satisfactory and even better than might be expected from the computed probable errors. The systematic change with the mean apparent magnitude shown by A and D probably is purely accidental. That in p, however, is in the direction to be expected a priori and, in view of the accuracy obtained, may be real. It should be remembered that the effect of selection in the material discussed will yield too large a value for p. A second solution for the third group, with weights assigned to each Selected Area according to the number of proper-motion stars used, gave the results in the last line of Table VI. The differences between

the two solutions for the third group are all within their probable errors.

The position of the antapex differs considerably from that determined from the proper motions of bright stars. A comparison with other determinations based on relatively faint stars (Table VII) shows a fair agreement. The large values of A and D from Wolf stars with proper motions larger than $0''.50$ may be due to a probably large percentage of stars with very high linear tangential velocities. The solution by van Maanen and Willis based on Herschel's and

TABLE VII

CO-ORDINATES OF ANTAPEX

Authority		Mag.	A	D
Oosterhoff		11–13	$6^h.9$	$-43°$
		14–16	7.2	42
		≧17	7.4	40
van Maanen and Willis*	Ross	14–15	7.9	36
	Wolf $\mu < 0''.50$	14–16	7.1	36
	Wolf $\mu \geqq 0.50$	14–16	8.6	52
Van de Kamp and Vyssotsky†		....	7.0	−36

* Only the results derived by Airy's method are given here. The values from Table VI in van Maanen and Willis' paper, 7^h3^m and $-38°.5$, were derived from part of the material used here.

† *Proc. Nat. Acad.*, **21**, 422, 1935. The mean limiting magnitude of the plates is 12.5 pv.

Bessel's methods yields systematically smaller values for both quantities.

Finally, mean parallaxes were computed for stars within certain limits of apparent magnitude and proper motion (Table VIII). The results for the last two proper-motion groups are practically of no significance, the number of stars included being too small. The mean values in the fourth column of Table VIII were obtained from Kapteyn's equation,

$$\log \bar{\pi} = -1.207 - 0.011\, m + 0.862 \log \mu \,,$$

with constants determined by van Maanen and Willis from the τ-components of the proper motions and an assumed mean peculiar

tangential velocity of 50 km/sec. In a discussion of these results Seares obtained[6] the formula

$$\log \bar{\pi} - \log \mu = -0.973 - 0.0175H \qquad (H > 7.5) \qquad H = m + 5 \log \mu \,,$$

which involves no assumption as to tangential velocity, the scale of distance being fixed by stars of known parallax. Results from this

TABLE VIII

MEAN PARALLAXES

Mag.	$\bar{m}$	μ	$\bar{\pi}_1$ Comp.	$\bar{\pi}_2$ Comp.	n
	Stars with $\mu = 0''.050$–$0''.099$				
8.00–10.99	10.04	0''.075	0''.0052	(0''.0067)	14
11.00–13.99	12.68	.073	.0047	(.0059)	72
14.00–16.99	15.76	.072	.0043	.0051	247
>16.99	17.39	0.070	0.0040	0.0047	71
	Stars with $\mu = 0''.100$–$0''.299$				
8.00–10.99	9.89	0.166	0.0102	(0.0139)	20
11.00–13.99	12.45	.156	.0091	.0118	44
14.00–16.99	15.92	.140	.0076	.0093	121
>16.99	17.38	0.137	0.0072	0.0086	37
	Stars with $\mu = 0''.300$–$0''.499$				
8.00–10.99	10.58	0.460	0.0242	0.0342	1
11.00–13.99	....	....	....	....	0
14.00–16.99	16.07	.373	.0176	.0226	10
>16.99	17.82	0.490	0.0213	0.0271	2
	Stars with $\mu > 0''.499$				
8.00–10.99	9.70	0.526	0.0278	0.0401	1
11.00–13.99	12.46	0.619	0.0298	0.0416	2
14.00–16.99	....	....	....	....	0
>16.99	....	....	....	....	0

formula are given in the fifth column of Table VIII. For the three values in parentheses the condition for H is not satisfied. The paral-

[6] *Mt. W. Contr.*, No. 438; *Ap. J.*, **74**, 320, 1931.

laxes derived from Seares's formula are about 20 per cent larger than those obtained by van Maanen and Willis. Part of this difference at least is to be ascribed to the value of the linear velocity used by van Maanen and Willis.

From the mean parallactic motion (Table VI) and the mean parallaxes we can derive the linear solar motion relative to these faint stars of large proper motion. Using the parallaxes of Seares and of van Maanen and Willis, we obtain 55 and 66 km/sec, respectively.

TABLE IX

VARIABLE STARS FOUND DURING SEARCH FOR PROPER MOTIONS

Current No.	Sel. Area	No. in Cat.	α 1900	δ 1900	x	y	Mag. Bright	Mag. Faint
1*..	39		$19^h47^m47^s$	+45° 5′.8	+ 9′.8	+11′.9	16.0	17.9
2...	41	....	21 50 28	+44 53.4	+ 9.3	− 5.5	15.9	18.0
3...	51	....	7 25 9	+29 45.2	+10.4	−17.1	15.6	16.4
4...	73	....	5 16 4	+15 7.8	+17.0	+10.3	16.7	17.7
5...	74	....	6 14 4	+15 21.6	−17.0	+15.8	15.3	15.9
6...	96	....	4 47 36	+ 0 4.4	− 1.9	+ 7.4	18.3	19.0
7...	105	....	13 32 41	− 0 26.2	+ 0.3	−19.3	17.1	17.7
8...	112	H 835	20 37 54	− 0 1.5	+ 9.4	− 6.8	15.9	16.9
9...	129	....	13 12 47	−14 55.9	−17.2	+ 6.6	16.0	17.8
10...	133	835	17 12 18	−14 58.2	− 5.7	+ 7.2	16.2	17.3
11...	133	....	17 13 9	−14 54.4	+ 6.6	+11.0	14.8	>17.5
12...	133	H 816	17 13 13	−15 21.2	+ 7.5	−15.8	15.3	16.7
13...	135	....	19 12 6	−14 40.5	−12.9	+18.5	15.2	16.5
14...	135	....	19 12 12	−15 8.4	−11.2	− 9.4	13.7	16.7
15...	135	....	19 12 23	−15 16.7	− 8.4	−17.7	16.2	16.8
16...	138	....	22 10 17	−14 47.3	− 5.0	+ 8.7	18.0	>18.0

* Another star 4″ n and 4″ f.

These velocities seem rather high; but, as pointed out by Strömberg,[7] there exists a rather close relation between the group motion and the internal velocity dispersion of different groups of stars. It seems doubtful, however, whether Strömberg's formulae may be applied to these stars of large proper motion, as none of his groups was selected according to proper motion. The selection in the present material necessarily results in a high value for the linear mean tangential velocity, and consequently in a large solar motion. A quantita-

[7] *Mt. W. Contr.*, No. 293; *Ap. J.*, **61**, 363, 1925.

tive evaluation of the effects of selection on the velocities would be extremely difficult.

During the search for stars with large proper motion 16 variable stars were found. Since attention was concentrated on the detection of displacements, other variables which are faint or have small amplitudes may easily have escaped notice. Only one of the stars listed is given in the *Mount Wilson Catalogue*.

I wish to express my thanks to Dr. van Maanen, who kindly put his material at my disposal and who has shown his continued interest throughout the investigation.

CARNEGIE INSTITUTION OF WASHINGTON
MOUNT WILSON OBSERVATORY
January 1936

ERRATUM

In *Mt. Wilson Contr.*, No. 412, by van Maanen and Willis, Table III, the positions given for stars No. 66 and No. 67 should be interchanged.

THE INFRA-RED PHOTOMETRY OF LONG-PERIOD VARIABLE STARS

CHARLES HETZLER

ABSTRACT

A photographic method of relative exposure times has been found to give consistent results in obtaining, at an effective wave-length of about 8500 A, magnitude-curves of the brighter red variables of long period, using Eastman I P emulsions. From the curves, both infra-red and visual (due mostly to the A.A.V.S.O.), plotted homogeneously for about thirty variables, the relative shapes and magnitude ranges, and the infra-red indices at maximum and at minimum, are at once apparent. A conspicuous persistence of the infra-red maximum after the visual curve has declined is noted for some variables, especially R Lyncis, W Andromedae, *o* Ceti, R Camelopardalis, and U Cygni, the latter apparently reaching a higher intensity in the infra-red after the visual peak is passed. These phenomena may or may not always occur for any particular variable. For seventeen variables (several cycles have been included for a number of these) the mean infra-red magnitude range is $2^{M}4$ as compared with $5^{M}0$ visually; the mean infra-red index (infra-red mag *minus* visual mag) is $3^{M}9$ at maximum and $6^{M}4$ at minimum light.

Observations at 8500 A of Nova Herculis and of the K-type variable R Scuti are included.

Mean results for three stars at 9500 A show a range of $1^{M}4$ against $4^{M}6$ visually. Complete curves were not attempted at this wave-length.

o Ceti is used to illustrate the order of accuracy of temperatures or diameters computed from the infra-red data. The visual and infra-red magnitude ranges are compared, for some variables, with black-body radiation, assuming temperatures from other data. Wien's displacement law *plus* absorption by titanium or zirconium oxide accounts, in a general way, for most of the observed phenomena, but mottled surfaces, changes of diameter, veiling due to condensed particles, and other factors may complicate the problem.

The variable star work here reported was started and carried on for about two years at the Allegheny Observatory, using the Thaw 30-inch refractor. The wave-length region of 8500 A made the work especially suitable for twilight, moonlight, and poor seeing conditions. A similar program is now being carried on with the 24-inch reflector at the Yerkes Observatory. It should be of considerable interest to compare results obtained with the refractor and the reflector on the same variables, especially since the method is essentially the same. While this paper will deal mostly with the refractor results, some early data obtained with the reflector are included. Reflector points are shown in solid black at the ends of the curves for a number of the variables, and indicate that the agreement is satisfactory.

DERIVATION OF MAGNITUDES AT 8500 A

Improvement in photographic processes is continually opening new fields for the astronomer. The Thaw refractor, when used with a No. 87 Wratten filter and Eastman I P emulsion, was found to have a sharp infra-red focus about 100 mm beyond the photographic focus. The combination of filter, emulsion, and focus doubtless gives a compact spectral region effectively at about 8500 A. At this wave-length only the brighter stars of bluer type are comparable in energy with the very red stars, while the brighter red variables have great intensity even at minimum light. It is therefore possible to obtain energy-curves of these variables at 8500 A, a spectral region especially suitable for their investigation since, as pointed out by Merrill,[1] their atmospheres are here more, if not entirely, free of titanium oxide band absorption. The magnitude ranges in this clear region, the occurrences of maxima and minima, together with the shapes of the infra-red curves, as compared with the corresponding visual phenomena, should add a chapter to our understanding of these important stars. Simultaneous photographic and ultra-violet curves are also desirable. The ultra-violet is perhaps another clear region: at the Yerkes Observatory simultaneous curves are being attempted for a few of the variables in this region, especially near maximum light.

With few exceptions the field stars are too faint in the infra-red for simultaneous comparison with the brighter red variables. Therefore, nearby bright stars are used as standards, and comparison is effected by successive exposures under uniformly transparent conditions. Our atmosphere is relatively very transparent to infra-red radiations. The transmission varies as the secant power of the zenith-distance. For 95 per cent transparency the difference in transmission between, say, 45° and 60° zenith distance, is very small:

$$T_{45}-T_{60}=0.95^{\sec 45^\circ}T_z-0.95^{\sec 60^\circ}T_z=0.03T_z\,.$$

Differences in seeing, moisture, and dust, however, make all work at low or at different altitudes less desirable. Each variable is always compared with the same nearby star, which is deemed superior

[1] *Trans. Int. Astr. Union*, **4**, 160, 1932.

to comparisons with the polar sequence, since stars can be taken at any altitude without corrections for varying atmospheric transmission. The comparison stars are compared with Vega, which is considered to be of zero infra-red magnitude. Stars to be compared are given a series of exposures of different duration on the same part of the emulsion, the exposure times being such as to obtain images as nearly equal as possible. Accuracies within a few hundredths of a magnitude are possible by this method, especially if the nearly equal images are properly measured. In most of the present work careful eye estimates were deemed to be sufficiently accurate, and magnitudes were rounded off to the nearest tenth. In determining relative magnitudes, based upon exposure times necessary to give equal images, tests were made under actual working conditions. The 30-inch aperture was reduced to one-twenty-fifth by blocking out all except one or more round holes. This reduction of $3\overset{M}{.}5$ covers the extreme range of the variables at 8600 A. The images with the reduced aperture were quite comparable to those with the full aperture, and the relative exposure times for equal images were found to be in the ratio of about 30 to 1. A time ratio of 2.65 is thus equivalent to a brightness difference of 1 mag., which differs from reciprocity by $0\overset{M}{.}05$ for each magnitude. This ratio, which is certainly correct within a few hundredths of its value under average conditions, was used throughout the work; its error will affect both ranges and indices of the variables, but is probably negligibly small except for the average of many results.[2] Since each variable was usually compared with the same star, an error in the magnitude of the comparison star will merely shift the curve as a whole, affecting the indices, but not the ranges, of the variables.

MAGNITUDES OF THE COMPARISON STARS

The infra-red magnitudes of the comparison stars constitute, by themselves, an interesting set of data for bright stars of various spectral types. These magnitudes (Table I), which are incidental,

[2] While preliminary tests show that the time ratio per magnitude for the reflector (all images are taken near the axis) is practically the same as for the refractor, the value will be determined carefully when the complete reflector results are given. A wire screen will probably be used to reduce the aperture, since the Allegheny method does not give comparable images with the short-focus reflector.

TABLE I

MAGNITUDES OF COMPARISON STARS

No.	Star	Ptg.† Mag.	Vis.† Mag.	Mag. at 8500 A	Spectrum and Indices						
					B	A	F	G	K	Ma	Mb
1	α Cet	4.4	2.8	−0.2*	....	....	....	....	....	4.6 3.0	....
2	α Lyr	0.1	0.1	0.0	....	0.1 0.1	....	....	....	....	....
3	α UMa	3.1	2.0	+0.3	....	....	....	....	2.8 1.7	....	....
4	α Aql	1.1	0.9	0.4	....	0.7 0.5	....	....	....	....	....
5	γ And	3.4	2.3	0.4	....	....	....	....	3.0 1.9	....	....
6	δ Vir	5.3	3.7	0.5	....	....	....	....	....	4.8 3.2	....
7	α Cyg	1.4	1.3	1.0	....	0.4 0.3	....	....	....	....	....
8	α Leo	1.3	1.3	1.0	0.3 0.3	....	....	....	....	....	....
9	η Dra	3.8	2.9	1.2	....	....	....	2.6 1.7	....	....	....
10	β Cas	2.9	2.4	1.6	....	....	1.3 0.8	....	....	....	....
11	β Aur	2.0	2.1	1.6	....	0.4 0.5	....	....	....	....	....
12	η Oph	2.5	2.6	1.9*	....	0.6 0.7	....	....	....	....	....
13	α Cep	2.7	2.6	2.0	....	0.7 0.6	....	....	....	....	....
14	γ Cep	4.6	3.4	2.0	....	....	....	....	2.6 1.4	....	....
15	α And	2.1	2.2	2.0	....	0.1 0.2	....	....	....	....	....
16	γ Hya	4.2	3.3	2.1*	....	....	....	2.1 1.2	....	....	....
17	γ UMi	3.1	3.1	2.3	....	0.8 0.8	....	....	....	....	....
18	BD 60°856	4.8	4.2	2.7*	....	....	....	2.1 1.5	....	....	....
19	δ UMa	3.4	3.4	2.8	....	0.6 0.6	....	....	....	....	....
20	δ Gem	3.8	3.5	2.8*	....	....	1.0 0.7	....	....	....	....
21	υ And	4.7	4.2	2.9*	....	....	....	1.8 1.3	....	....	....
22	BD 23°4224	8.8	7.5	2.9*	....	....	....	....	....	....	5.9 4.6
23	ε Vir	5.8	5.2	4.1*	....	....	....	1.7 1.1	....	....	....
24	BD 59°1065	6.3	5.3	3.5*	....	....	....	....	2.8 1.8	....	....

* Based upon only one or two comparisons. † HD values.

TABLE I—*Continued*

No.	Star	Ptg.† Mag.	Vis.† Mag.	Mag. at 8500 A	Spectrum and Indices						
					B	A	F	G	K	Ma	Mb
25	θ Cyg	5.1	4.6	3.8	....	....	1.3 0.8	....	....	....	....
26	BD 38° 54	8.3	7.0	4.0*	....	....	....	....	....	4.3 3.0	....
27	BD 61°1312	7.5	6.5	4.7*	....	....	....	....	2.8 1.8	....	....

deduced by taking the means of intercomparisons from the best plates which have several variables and their comparison stars, are listed together with the photographic and visual magnitudes. The corresponding indices, i.e., photographic magnitude *minus* infra-red magnitude and visual magnitude *minus* infra-red magnitude, are listed according to spectral class, to which they are seen to be fairly true. Many of these magnitudes are doubtless very good; somewhat better values for a few will follow with further work.

INFRA-RED AND VISUAL CURVES OF THE VARIABLES

Results for about thirty variables are shown in the form of curves (Figs. 1 to 6). Each infra-red magnitude was derived by adding the adopted magnitude of the comparison star to the magnitude difference between comparison star and variable, all comparisons being based on relative exposure times. Magnitudes are weighted as "very good," "good," "fair," and "poor," shown respectively on the curves as circles, squares, triangles, and crosses. The points represent individual observations, each based on a single plate for any particular variable. As far as known factors are concerned, the circles usually represent superior observations, but occasional unknown factors may render these less accurate than those judged, from the appearances of the images, to be less reliable. The simultaneous visual curves have been drawn on the same scales as the visual curves, so that the corresponding magnitude ranges and the color (infra-red) indices are at once apparent. The visual curves were obtained by plotting all the observations of the A.A.V.S.O., but the

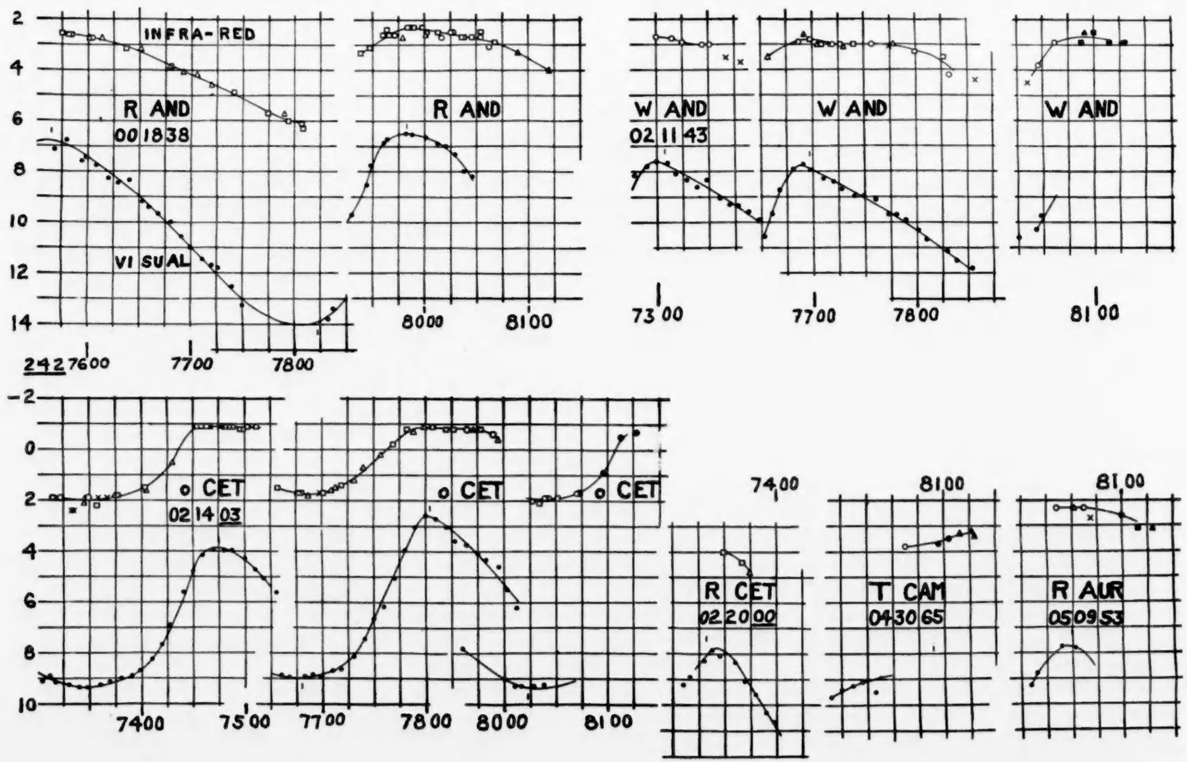

FIG. 1.—Infra-red curves (above) with individual observations—circles, squares, triangles, and crosses in order of weight. Visual curves (below) with ten-day-mean points. Ordinates are magnitudes, abscissas are JD 2420000. Scale of co-ordinates: 1 square = 1 mag. ×25 days.

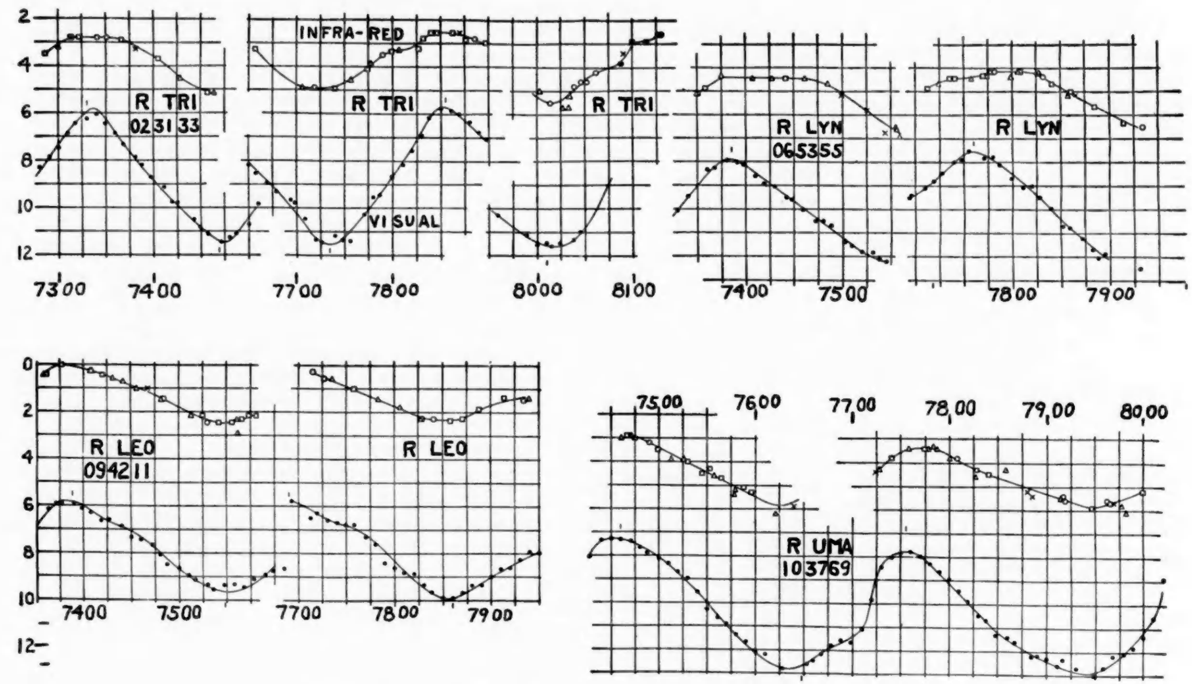

FIG. 2.—The co-ordinates are the same as in the previous figure

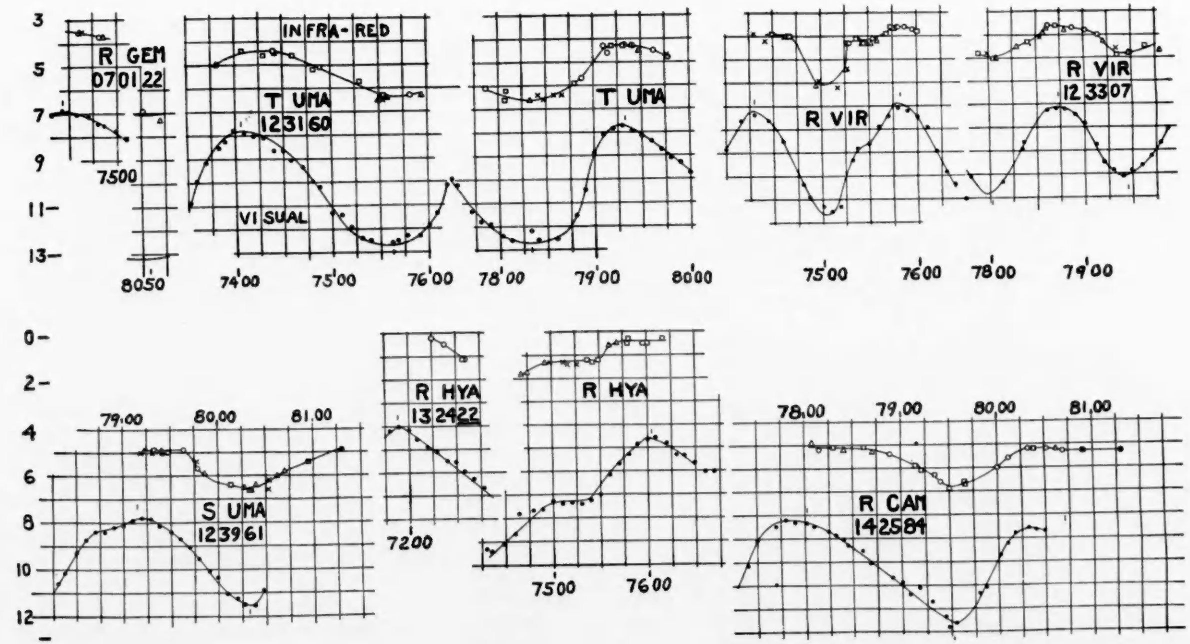

FIG. 3.—The co-ordinates are the same as in the previous figures

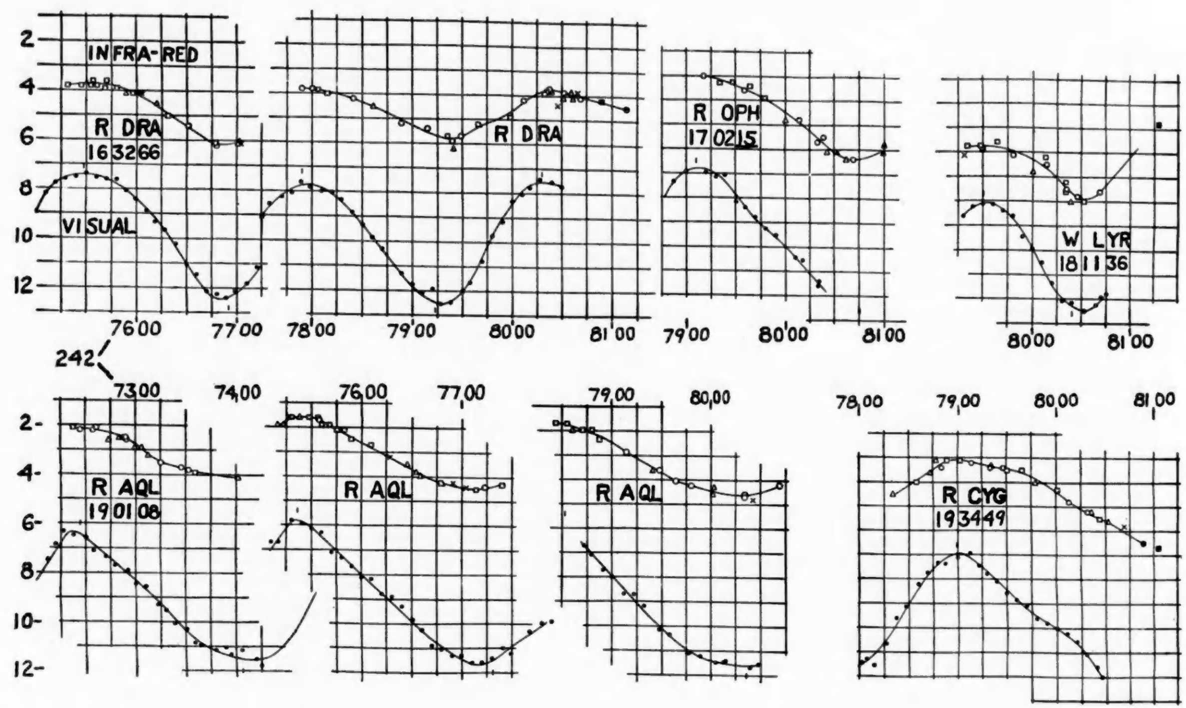

FIG. 4.—The co-ordinates are the same as in the previous figures

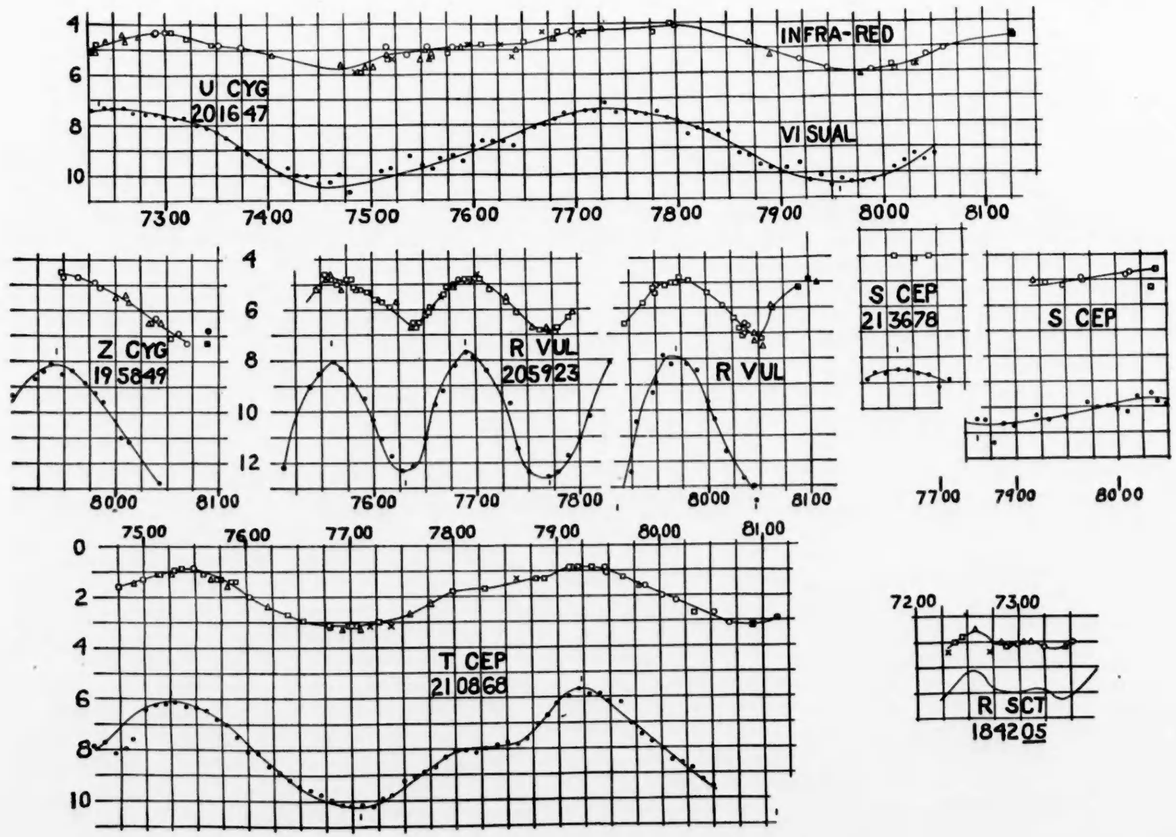

FIG. 5.—The co-ordinates are the same as in the previous figures

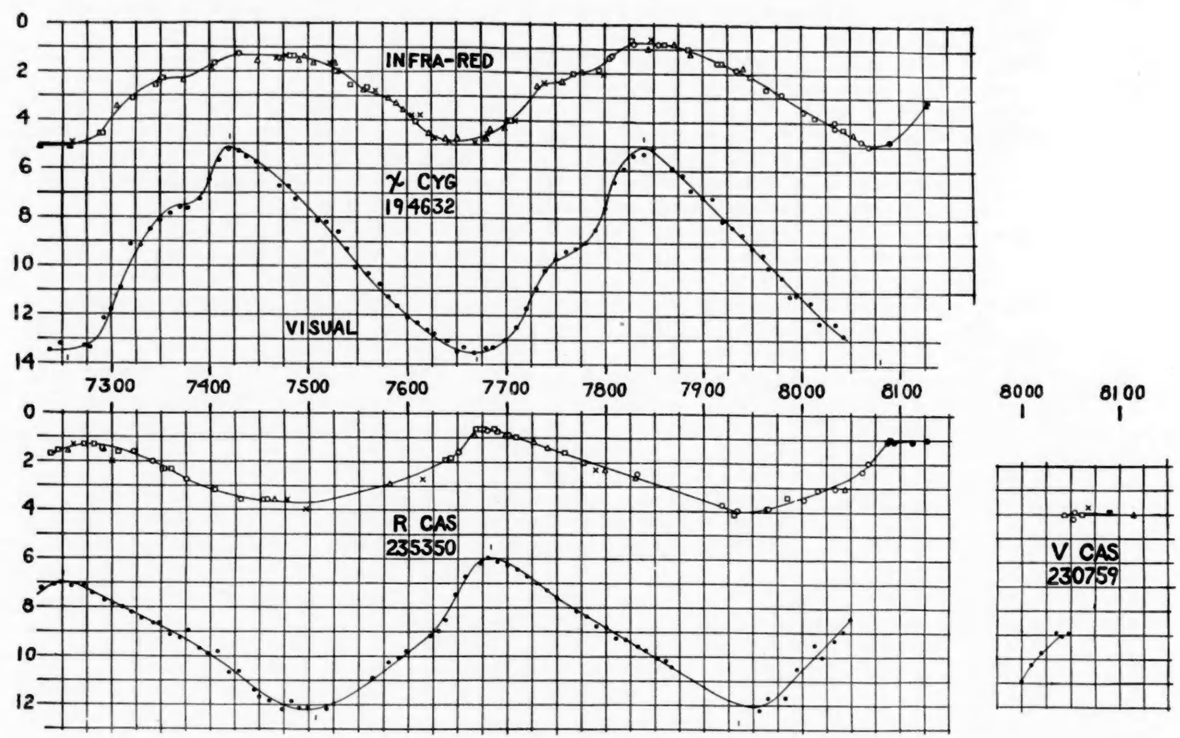

FIG. 6.—The co-ordinates are the same as in the previous figures

individual points have not been shown. In addition, Professor Campbell, of the Harvard College Observatory, has kindly supplied me with ten-day-mean points and their curves, which include foreign observations, for the last five years, for my entire list of variables. The solid circles representing the mean points have been superposed upon the curves plotted by me. Professor Campbell has also indicated probable positions of the maxima and minima (shown by short vertical lines) derived by a method based on long experience. Other visual observations will be available for a number of the variables—e.g., those by Nijland.[3] Photographic magnitudes may also be available in some instances, possibly on Harvard survey plates.

DISCUSSION OF THE CURVES

A summary of data from the curves is given in Table II, including visual averages for the last five years. The visual-magnitude range during the time of the infra-red observations is sometimes quite different from the mean range and is tabulated under "corresponding visual range." Also included, for five variables, are the visual and infra-red magnitude ranges for black bodies between the temperatures deduced for these variables from radiometric measures by Pettit and Nicholson.[4]

For seventeen variables the mean infra-red index at maximum of $3\overset{\mathrm{M}}{.}9$ is less than the mean index at minimum of $6\overset{\mathrm{M}}{.}4$ by $2\overset{\mathrm{M}}{.}5$. In other words, the infra-red curves average $2\overset{\mathrm{M}}{.}5$ flatter than the visual curves. The mean visual range of $5\overset{\mathrm{M}}{.}0$ is about twice the mean infra-red range of $2\overset{\mathrm{M}}{.}4$, while for black bodies ranging between the temperatures estimated for these variables the visual range should be only 1.5 times the infra-red range. It is thought that titanium oxide absorption bands help to make the visual minimum relatively low. Joy estimated that for **o** Ceti the absorption is $2\overset{\mathrm{M}}{.}0$ even at maximum, and about twice as great at minimum:

> The spectrum falls off toward the violet as the energy shifts toward the red with decreasing temperature, and there is a large amount of absorption arising from the greatly increased strength and extent of the titanium oxide bands. These two causes appear to work together near minimum to produce the relatively weak continuous spectrum in the region λλ 4200–6200.[5]

[3] *Proc. R. Acad. Amsterdam.*

[4] *Ap. J.*, **78**, 320, 1933.

[5] *Ibid.*, **63**, 281, 1926.

TABLE II

DATA FROM THE CURVES

No.	Variable	Comp. Star	Period Days	Spec.	Mean Visual Magnitude		Mean Visual Range	Range at 8500 A	Corres. Visual Range	Index: Visual *minus* 8500 A		Black-Body Mag. Range	
					At Max.	At Min.				At Max.	At Min.	Vis.	8500 A
001838	R And	15 and 26‡	407	Se	7.1(6)*	14.3(5)	7.2	3.6(1)	7.2(1)	4.2(2)	7.9(1)		
021143	W And	5 and 21	397	M7e	7.5(5)	13.9(3)	6.4			4.9(2)			
021403	o Cet	1	332	M5e	3.4(4)	9.3(7)†	5.9	2.8(2)	5.5(2)	4.6(2)	7.3(3)	1920° 3.9 2640°	2.5
022000	R Cet	1	165	M4e	8.0(9)	13.0(4)	5.0			3.8(1)			
023133	R Tri	5 and 21	268	M6e	6.4(8)	11.6(6)	5.2	2.5(2)	5.8(2)	3.0(2)	6.3(3)	2460° 3.2 3270°	2.3
043065	T Cam	18	266	Se	8.0(5)	13.9(4)	5.9			4.8(1)?			
050953	R Aur	11	468	M7e	7.5(5)	13.6(4)	6.1			5.4(1)			
065355	R Lyn	11 and 24	378	Se	7.9(5)	13.6(2)	5.7			3.4(2)			
070122	R Gem	20	370	Se	7.2(5)					3.4(1)			
094211	R Leo	8	315	M7e	5.8(5)	9.8(6)	4.0	2.4(1)	4.0(1)	5.8(1)	7.4(2)	1800° 2.7 2170°	1.8
103769	R U Ma	3	299	M4e	7.6(7)	12.8(7)	5.2	2.7(2)	5.3(2)	4.4(2)	7.0(2)		
123160	T U Ma	19	255	M4e	7.9(8)	12.8(8)	4.9	2.1(2)	5.0(2)	3.4(2)	6.2(2)		
123307	R Vir	6 and 23	147	M4e	7.1(12)	11.0(8)	3.9	1.6(3)	3.8(3)	3.4(3)	5.6(3)		
123961	S U Ma	19 and 27	229	Se	7.8(9)	11.7(10)	3.9	1.7(1)	3.7(1)	2.9(1)	4.9(1)		
132422	R Hya	16	417	M7e	4.6(5)	9.8(5)	5.2			4.1(1)			
142584	R Cam	17	266	Se	8.4(9)	13.2(6)	4.8	1.7(1)	4.0(1)	3.2(2)	5.8(1)		
163266	R Dra	9	246	M6e	7.6(9)	12.3(8)	4.7	2.3(2)	4.0(2)	3.8(3)	5.5(2)		

TABLE II—*Continued*

No.	Variable	Comp. Star	Period Days	Spec.	Mean Visual Magnitude		Mean Visual Range	Range at 8500 A	Corres. Visual Range	Index: Visual *minus* 8500 A		Black-Body Mag. Range	
					At Max.	At Min.				At Max.	At Min.	Vis.	8500 A
170215	R Oph	12	302	M5e	7.4(6)	13.4(3)	6.0	3.4(1)		3.8(1)			
180445	Nova Her	2			1.6(1)					0.7(1)			
181136	W Lyr	2	195	M4e	7.9(11)	12.3(8)	4.4	2.1(1)	4.4(1)	2.3(1)	4.6(1)		
184205	R Sct	4	144?	K5e						1.8(1)			
190108	R Aql	4	302	M6e	6.1(6)	11.5(7)	5.4	2.6(3)	5.6(2)	4.2(2)	7.2(3)	2.4	1920° 1.6 2320°
193449	R Cyg	25	428	Se	7.2(5)	13.7(5)	6.5			3.8(1)			
194632	χ Cyg	7 and 25	413	M7e	5.3(5)	13.4(4)	8.1	4.0(2)	8.4(2)	4.1(2)	8.5(2)	4.6	1630° 2.9 2260°
195849	Z Cyg	7 and 25	267	M5e	8.5(8)	14.1(2)	5.6			3.5(1)			
201647	U Cyg	7 and 25	453	R8e	7.3(4)	10.5(5)	3.2	1.7(2)	3.2(2)	3.1(2)	4.6(2)		
205923	R Vul	22	136	M4e	7.9(12)	12.6(7)	4.7	2.1(3)	4.9(3)	3.0(3)	5.8(3)		
210868	T Cep	13	396	M6e	6.1(5)	10.4(5)	4.3	2.2(1)	4.3(1)	5.0(2)	7.1(1)		
213678	S Cep	14	482	N8e	8.8(4)	11.6(5)	2.8			4.5(1)			
230759	V Cas	10	225	M6e	7.9(9)	11.9(9)	4.0			4.0(1)?			
235350	R Cas	10	426	M7e	6.3(5)	12.3(5)	6.0	2.9(2)	5.7(2)	5.5(2)	8.3(2)		
Mean								2.4	5.0	3.9(17)	6.4	3.4	2.2

* The figures in parentheses indicate the number of separate determinations.

† For *o* Ceti the visual minimum would be slightly lower to allow for the companion, the magnitude of which is about 11.

‡ Where two comparison stars are given, the first is fundamental in this paper.

The ordinary color index does not increase at minimum and is much less than for other low-temperature stars because of the extent of the absorption over the entire color-index range. The infra-red indices increase at minimum, however, because the absorption bands are less, if not negligible, near 8500 A. It is of interest to note that the infra-red indices of the Ma and Mb comparison stars (Table I) of $3^{M}_{.}0$ and $4^{M}_{.}6$, respectively, are much closer to the indices of the variables at maximum than at minimum. In general, the dwarf M stars are not comparable in infra-red intensity with the giant variables of the same visual magnitude at minimum.

Whether the 25 per cent or more of the visual magnitude range, which is not accounted for by temperature change, is due entirely to differential band absorption, or whether there are other effects such as veiling (selective or not) by condensed particles, or changes of diameter, is a difficult problem. Temperatures are low enough, and there is some evidence (e.g., magnitude changes without changes in color or spectrum) of non-selective absorption by clouds of liquid particles. The temperatures may also be complicated by spottedness, by the longer wave-lengths coming from deeper layers, or by other modifications of black-body conditions. A cycle of alternate absorbing, heating, clearing, and cooling of the overlying atmospheres, with the expansion and contraction perhaps not greatly affecting the diameter as a whole, is as good a general picture as present data warrant.

For a majority of the variables the infra-red curves, except for being shallower, correspond closely with the visual curves. On the rise to maximum the correspondence is especially close: shoulders or still-stands in the visual are duplicated in the infra-red. In only a few instances is there any indication that the infra-red radiation increases after the visual maximum, as Pettit and Nicholson have suggested for the total radiation of some of these stars. But for a number of the variables the infra-red peak seems to persist until long after the visual light has declined. It seems that in some cases, at least, the curves by Pettit and Nicholson might have been drawn to interpret the points in this way. It is of interest to investigate whether such phenomena are invariably true of certain stars, whether they sometimes occur for others, and whether there is any

definite correlation with other known factors. It may be of significance that at least some of the variables which show the persistence of the infra-red maximum also show a shoulder in the rise to maximum. Comparisons of infra-red curves of S-type variables, in which zirconium oxide predominates, with the M-type variables, which are strongest in titanium oxide, are particularly pertinent.

Assuming that at 8500 A the band absorption is negligible, and that no other veiling is present, the infra-red data should help in determining the temperature change alone, provided that black-body conditions prevail. Since the parallax and diameter of *o* Ceti are known, it may be used as an example (although the magnitude of its comparison star may be somewhat inferior because of its low altitude). Assuming that the diameters of Mira and Vega are 250 and 2.4 times that of the sun, that their parallaxes are $0\farcs02$ and $0\farcs124$, and that Vega has a temperature of 11,000°, the maximum and minimum magnitudes of Mira at 8500 A indicate temperatures of 2670° and 1920°, almost exactly in agreement with those deduced by Pettit and Nicholson (Table II). A calculation can be made using the sun instead of Vega. The infra-red index of a G-type star, from Table I, is about $1\overset{M}{.}5$. Subtracting this from the sun's visual magnitude of $-26\overset{M}{.}7$, we have $-28\overset{M}{.}2$ as its infra-red magnitude. The resulting temperatures for Mira are 2300° and 1700°, in good accordance with the estimates of 2300° and 1800° by Joy. The range in magnitude, without postulating changes of diameter, agrees well, therefore, with the best available calculations of temperatures.

R SCUTI AT 8500 A

This variable of type K5ev was observed for a time because its maximum brightness of $5\overset{M}{.}0$ and range of $4\overset{M}{.}0$ made it feasible and of interest to compare it with the giant variables. Its irregularity, however, made it seem less profitable for continued investigation. A brief curve is included (Fig. 5).

NOVA HERCULIS AT 8500 A

A number of infra-red observations of this spectacular star, made near its peak, are given in Table III. Comparison was made with Vega. There seems to have been no conspicuous change in color

near or directly following the maximum, the infra-red index being consistently that of about an F-type star (Table I).

TABLE III

INFRA-RED OBSERVATIONS OF NOVA HERCULIS

Date	JD	Mag at 8500 A	Quality	Rough Vis. Mag.
1934 Dec. 18, A.M.	790.0	1.6	f	2.6
22, P.M.	794.5	0.9	vg	1.6
27, A.M.	799.0	1.1	f	....
27, P.M.	799.5	1.6	p	2.7
28, A.M.	800.0	1.9	f	2.9
1935 Jan. 2, A.M.	805.0	1.5	f	2.6
2, P.M.	805.5	1.3	vg	2.9
3, A.M.	806.0	1.4	g	2.7
5, A.M.	808.0	1.5	vg	3.0
5, P.M.	808.5	1.5	g	2.7
12, A.M.	815.0	1.4	vg	2.8
Mar. 23, A.M.	884.9	3.6	p	4.4
29, A.M.	890.9	3.8	g	4.4

WORK AT 9500 A

Using the No. 87 Wratten filter with Eastman I Q plates at a distance of 130 mm beyond the photographic focus of the Thaw refractor, a few of the brighter variables were investigated at the spectral region near 9500 A, the methods being similar to those described for work at 8500 A. Complete curves were not attempted, but observations were made, particularly, near maximum and minimum. Table IV shows the magnitudes, indices, and ranges obtained for several variables. R Aquilae, X Cygni, and R Cassiopeiae were not observed at maximum or minumum but at the phases indicated. The magnitudes of the comparison stars at 9500 A were not derived from direct observations, but were extrapolated from the known magnitudes at 5500 A and 8500 A.

The mean magnitude range at 9500 A (for three stars) of $1^{M}_{.}4$ against $4^{M}_{.}6$ visually is reasonable enough from other data. The indices from 8500 A to 9500 A are only rough values, yet the agreement for three stars possibly indicates a correct order of magnitude.

TABLE IV

DATA AT 9500 A

Comp. Star	Computed Mag. at 9500 A	Variable	Magnitude at 9500 A (Dates)			Range at 9500 A	Corres. Vis. Range	8500–9500 A Index		
			At Max.	Inter.	At Min.			At Max.	Inter.	At Min.
α Cet	−1.2	o Cet	−2.3(Jan. 20 and 29, '34)	......	−0.5(Oct. 26 and 31, '33)					
			−2.2(Jan. 27, '35)	......	−0.6(Sept. 28, '34)	1.7	5.5	1.4	.....	2.4
α Leo	+0.9	R Leo	−1.4(Oct. 26 and 30, '33)	......	+0.2(Apr. 7, '34)	1.4	4.0	1.2	.....	2.2
			−1.0(Oct. 7 and 16, '34)							
			(Dec. 23, '33)	−1.1	Phase 0.16	After max.	......	.....	1.6	.....
α Cep	1.8	T Cep	−0.0(Apr. 30, '34)	......	+0.9(Oct. 6 and 7, '34)	0.9	4.3	0.9	.....	2.2
α Aql	0.2	R Aql	(May 2, '34)	+0.5	Phase 0.07	Near max.	......	.....	1.3	.....
α Cyg	0.9	χ Cyg	(Oct. 30, '33)	+1.2	Phase 0.9	Near max.	......	.....	1.1	.....
β Cas	+1.3	R Cas	(Nov. 3, '33)	+1.3	Phase 0.3	Toward min.	......	.....	1.5	.....

The approximate formula[6]

$$T=\frac{1900^\circ}{I_{85-95}+0.1}$$

can be derived for the temperature of a star, where I is the difference in magnitude at 8500 A and at 9500 A. This indicates temperatures of 1500° at maximum and 800° at minimum. Since a small wave-length interval is used, an error in the effective wave-length changes these values somewhat, but in any case they are rather low. On the other hand, the temperatures of 3200° and 2400°, computed for *o* Ceti from the magnitudes at 9500 A on assumptions the same as at 8500 A, are rather high. All these results depend on the calculated magnitudes of the comparison stars at 9500 A, and are therefore only provisional. The simplest explanation, both of the low temperatures derived from the 8500 A to 9500 A indices and of the high temperatures derived from the 9500 A magnitudes directly, is that the comparison star magnitudes at 9500 A are systematically too bright. Departures from black-body conditions are at least suggested. The magnitude ranges at 9500 A, which are independent of the comparison star magnitudes, were the main object of the investigation.

Acknowledgments are due to the Allegheny Observatory, where most of the work was done, and to the Yerkes Observatory, where the material has been discussed and where new observations have been obtained. At Allegheny, Dr. Burns was especially interested and helpful, while Dr. Jordan was most kind in granting the use of the observatory facilities for the work.

Yerkes Observatory
University of Chicago
February 1936

[6] Russell, Dugan, and Stewart, *Astronomy*, p. 733, 1927. I assume $3^{\mathrm{M}}3$ and $3^{\mathrm{M}}0$, respectively, as the absolute magnitude of the sun at 8500 A and at 9500 A.

FURTHER EVIDENCE ON THE ACCURACY OF POSITIONS FROM PHOTOGRAPHIC PLATES TREATED BY THE NORMALIZING PROCESS

P. VAN DE KAMP AND A. N. VYSSOTSKY

ABSTRACT

The *normalizing process*, previously discussed in this *Journal*, was tested on four additional emulsions. The positions of thirty-one stars in the open cluster I.C. 4665 were measured. It is concluded that the general use of the normalizing process is not warranted for 5 × 7 in. Cramer Iso Presto plates, except where improvement of positional accuracy near the edge is desired.

In an earlier article[1] a report was made on the accuracy of photographic positions from plates "normalized" before exposure by soaking them in water, followed by dehydration in alcohol. It was found that the normalizing process considerably increases the positional accuracy of the stars near the edges of the plate; for the remaining area of the plate the process was found to give an appreciable increase in positional accuracy for one emulsion, but had not produced any effect on the second emulsion. Four more emulsions were investigated in order to obtain further evidence on this question. The open cluster I.C. 4665 (R.A. $=17^{h}4^{m}.4$, Decl. $=+5^{\circ}45'$)was chosen as a suitable test object. Sixteen plates were taken on six nights, equally spread over four different emulsions of Cramer Iso Presto plates, hereafter designated as C, D, E, and F. Each plate contains two exposures of six minutes each, separated about 2.5 mm in the direction of right ascension. Half of the plates (two of each emulsion) had been "normalized." The positions of thirty-one stars ranging in brightness from $6^{M}.9$ to $10^{M}.5$ were measured. Twelve comparison stars were used for the derivation of plate constants. Using the same method of reduction employed in the preceding article, the results presented in Tables I and II were obtained.

For comparison, results previously obtained (emulsions A and B) are given. Table I shows that, within the errors, for three emulsions (A, D, and F) an appreciable increase in accuracy is found, for two

[1] *Ap. J.*, **80**, 301, 1934.

TABLE I

PROBABLE ERRORS OF MEASURED POSITIONS FOR ALL EXCEPT EDGE STARS

(x and y combined; unit = 1 mm)

Emulsion	Not Treated	No.	Normalized	No.
C....................	0.00212 ± .00010	112	0.00217 ± .00010	112
D....................	.00196 ± .00009	112	.00172 ± .00008	112
E....................	.00176 ± .00008	112	.00212 ± .00010	112
F....................	.00248 ±0.00011	112	.00191 ±0.00009	112
A....................	0.00182 ± .00004	480	0.00149 ± .00003	480
B....................	.00130 ±0.00003	480	.00131 ±0.00003	480

TABLE II

PROBABLE ERRORS OF MEASURED POSITIONS FOR EDGE STARS

(x and y combined; unit = 1 mm)

Emulsion	Not Treated	No.	Normalized	No.
C....................	0.0045 ± .0006	12	0.0041 ± .0006	12
D....................	.0046 ± .0006	12	.0027 ± .0004	12
E....................	.0017 ± .0002	12	.0040 ± .0006	12
F....................	.0055 ±0.0008	12	.0016 ±0.0002	12
A....................	0.00333 ± .00025	40	0.00178 ± .00013	40
B....................	.00284 ±0.00021	40	.00146 ±0.00011	40

emulsions (B and C) there is practically no change, while for only one emulsion (E) a decrease in accuracy is obtained. For stars within 1 cm of the edge, however, the process undoubtedly has a favorable effect (five out of six emulsions). On the other hand, it should be kept in mind that by simply drying plates in alcohol a similar effect has sometimes been obtained.

Table III gives the mean values derived from all emulsions investigated. For the two groups of stars, the first value is the weighted mean according to the number of star positions measured on each emulsion, the second is the straight mean.

TABLE III

PROBABLE ERRORS OF MEASURED POSITIONS

(x and y combined; unit = 1 mm)

	Not Treated	No.	Normalized	No.
All stars except edge stars (1)...	0.00172	1408	0.00158	1408
(2)...	.00191		.00179	
Edge stars (1)...	.00346	128	.00218	128
(2)...	0.00375		0.00261	

It is seen that with the exception of the edge stars the improvement caused by the normalizing process is, on the average, small.

We conclude that the evidence so far obtained does not warrant the general use of the normalizing process for the particular brand and size of plate studied, except where improvement of positional accuracy near the edge is desired. Undoubtedly the process may improve particular emulsions and may therefore rightly be considered as a useful safeguard, especially in cases when the results must depend on a small number of plates.

LEANDER MCCORMICK OBSERVATORY
UNIVERSITY OF VIRGINIA
January 8, 1936

ON REDDENING IN B-TYPE STARS

JESSIE RUDNICK

ABSTRACT

Spectrophotometric differential energy-curves of normal and reddened B-type stars are found to approach those predicted for Rayleigh scattering over the region of long wave-lengths. The observed energy-curves deviate more and more on passing toward the violet, corresponding to a change in the exponent in Rayleigh's law. The observations are interpreted in the light of Götz's theoretical work. Approximate limits to the sizes of the scattering particles are found to be 300 $m\mu$ and 60 $m\mu$.

In accordance with Wien's approximation to Planck's law, the difference in magnitude between a normal star and a star affected by Rayleigh scattering, at any wave-length, is

$$\Delta m = -2.5 \log \frac{E_1(\lambda)}{E_2(\lambda)} = c\left(\frac{c_2}{\lambda T_1} - \frac{c_2}{\lambda T_2} - \frac{\beta H}{\lambda^4}\right) . \qquad (1)$$

The notation is that of Struve, Keenan, and Hynek,[1] where H is the thickness of the absorbing medium. The departure of this formula from that given by Planck's law is negligible, over the range of wave-lengths used.

For other types of scattering, the exponent α of λ in the scattering term may take on a value different from 4. If we consider two stars of equal temperature, the shape of the curve produced by plotting Δm against frequency depends upon the exponent of λ, and the slope of the curve may be varied by changing the value of βH. For particles having radii larger than $\lambda/2\pi$ it has been shown in the laboratory that the scattering obeys the more general law developed by Mie[2] for spherical particles of all sizes and indices of refraction. This law has been adapted to water particles by Stratton and Houghton[3] and to dielectrics having other indices of refraction by Götz.[4]

If I is the intensity of the transmitted light and I_0 its initial intensity,

$$\frac{I}{I_0} = e^{-kH} . \qquad (2)$$

[1] *Ap. J.*, **79**, 1, 1934.

[2] *Ann. d. Physik*, **25**, 377, 1908.

[3] *Phys. Rev.*, **38**, 159, 1931.

[4] *A.N.*, **255**, 63, 1935.

k, the coefficient of absorption, is the product of the number of particles per unit volume N, by the energy loss per particle

$$k = 2\pi\rho^2 NK(x) \ , \tag{3}$$

where

$$x = \frac{2\pi\rho}{\lambda} \ .$$

ρ is the radius of the particles and K is a function of x alone for a given index of refraction n. Götz[4] has plotted log K against log ρ/λ for $n=1.33$ and $n=\infty$. It is well known that for particles which are large in comparison with λ the scattering is non-selective. If the radius of the particles is less than $\lambda/2\pi$, Rayleigh's law of scattering applies. Thus, for a given ρ, the curves plotted by Götz are independent of λ at very short wave-lengths and obey Rayleigh's law at long wave-lengths. Between these two straight-line portions the curve for each index of refraction has two maxima and a minimum, the wave-lengths of which are determined by the size of the particles. These indicate that α does not vary smoothly between 0 and 4 for intermediate portions of the curve, but actually becomes negative for some values of λ. For $n=\infty$ the maxima and minimum are very flat and the curve may be regarded roughly as two straight lines which intersect at $\rho/\lambda = 0.15$. For larger values of ρ/λ the scattering is non-selective and for smaller values it follows Rayleigh's law. The curve for $n=1.33$ has, however, very pronounced maxima and minimum.

In order to investigate the applicability of Götz's theory to the case of the reddened B stars, two pairs were selected consisting of one reddened star and one of normal color. The pairs were also chosen so that the apparent magnitudes and spectral types were similar. Table I gives the data concerning the stars. For these two pairs relative energy-curves were determined from objective-prism spectra obtained with a 6-inch reflector, of 60-inch focus, used in connection with a 15° objective prism. The scale of the plates is 200 A/mm at $H\gamma$ and Wratten and Wainwright Hypersensitive Panchromatic plates were used for the exposures. A few additional exposures were obtained on Eastman Special Emulsions IU and IR, hypersensitized with ammonia. The prism was crossed by a wire

grating for calibration; the exposure times, which ranged from one to five minutes on different plates, were equal for each individual plate. The exposures were made only at times when the two stars had equal zenith distances, and the spectrum of a bright calibration star was obtained at the beginning and end of each plate as a check on the constancy of the transparency of the sky.

The relative spectral intensities were measured at ten wave-lengths distributed between λ 6300 and λ 4000. These positions were selected to avoid the neighborhood of any of the strong Balmer series lines and also regions where the sensitivity of the plate changed rapidly. Measures farther to the violet than λ 4000 were not attempted because of the overlapping of successive members of the Balmer series. The measures were made on the Ross thermoelectric

TABLE I

Star	Spectrum (HD)	Color Index (Stebbins and Huffer)
ζ Per	B1	+0.17
ϵ Per	B1	.00
55 Cyg	B2	+ .25
22 Cyg	B3	−0.04

photometer, and individual reduction-curves were derived for each wave-length. The range in wave-length included in each measure varies from about 100 A at λ 6300 to about 30 A at λ 4000.

Figure 1 gives the relative energy-curves of the two pairs of stars; the differences in magnitude are plotted against $1/\lambda$. The probable error of an individual determination of Δm is 0.05 mag. The broken curve represents the best fit obtainable on the assumption of Rayleigh scattering over the whole range of wave-lengths.

The curves in Figure 1 confirm the conclusion of other investigators [1, 5, 6] that Rayleigh's law of scattering is not satisfied for the entire range of wave-lengths.

It should be mentioned that the reality of the upward curvature in the case of ζ Per $-$ ϵ Per is not definitely established, since the two points in the red are not as reliable as the others. The probability

[5] Gerasimovič, *Harvard Circ.*, No. 339, 1929. [6] Trumpler, *Pub. A.S.P.*, **42**, 267, 1930.

of such a curvature is increased, however, by the fact that Trumpler's[6] spectrophotometric determinations of magnitude differences for several distant cluster stars compared with nearby stars show a similar upward curvature if Δm is plotted against $1/\lambda$ instead of against λ, as he has done. The curvature for 55 Cyg−22 Cyg is not quite as well defined as that for ζ Per−ϵ Per, and it is possible that if a longer arc were included, it, too, would show an upward curvature.

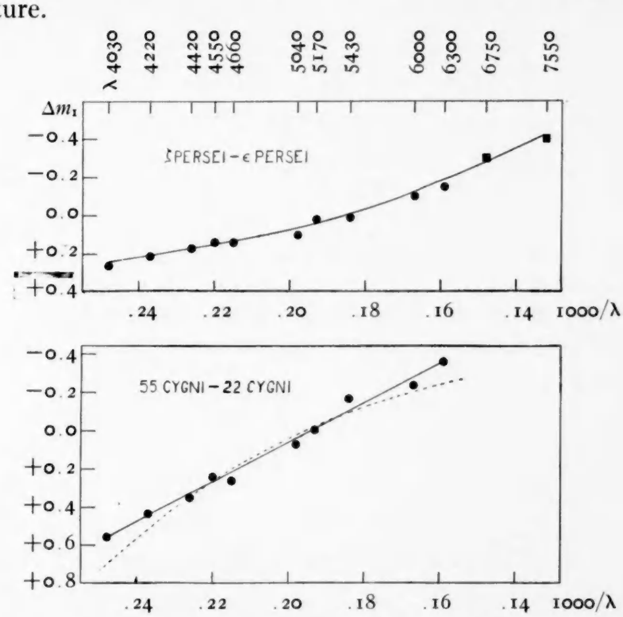

FIG. 1.—Relative energy-curves for two pairs of B stars. Ordinates are differences in magnitude between reddened and normal stars. Abscissae are $1000/\lambda$. Circles are values obtained from W. and W. Hypersensitive Panchromatic plates and squares are values obtained from Eastman IU and IR plates. The dotted curve is the best fit obtainable for Rayleigh scattering.

If this curvature should be confirmed by future investigations, it would definitely disprove the hypothesis that the reddening is caused by a temperature difference between stars of the same spectral class ($T_1 \neq T_2$ in eq. [1]). Meanwhile we have strong spectroscopic evidence in favor of equal temperatures for such stars.

In order to compare the observational results with the curves of Götz, let us consider ρ as constant. Then assume that

$$K = C_1 \lambda^{-a} . \tag{4}$$

When $\alpha=4$, this is of the form of the term for Rayleigh scattering in equation (1). From equations (2), (3), and (4) we have

$$\Delta m = -2.5 \log \frac{I}{I_0} = C_2 \lambda^{-\alpha} . \tag{5}$$

It is not possible to determine Δm directly, since we do not know the value of I_0 in (2), but the variation of Δm with wave-length may be obtained by using the equation

$$\Delta m = \Delta m_1 - D , \tag{6}$$

where Δm_1 is the measured difference in magnitude between the reddened star and a normal star and D is a constant which fixes the zero point. From equations (4), (5), and (6)

$$\log (\Delta m_1 - D) = -\alpha \log \lambda + \log C_2 = \log K + \log C_3 . \tag{7}$$

Therefore, if we plot $\log (\Delta m_1 - D)$ against $\log \lambda$, we should obtain a curve which will correspond to some part of Götz's curves and will also determine the value of α.

The value of D depends upon the luminosities and distances of the stars, as well as upon the coefficient of absorption. Accurate values of the parallaxes are not available for ζ Per and ϵ Per so that it is not possible to determine D directly. We should not, however, expect negative values of Δm because the phenomenon of reddening is probably due to absorption or scattering of some kind. Therefore the zero point cannot be lower than the highest point on the relative energy-curve of Figure 1 ($\Delta m_1 = -0.40$ mag.). Nevertheless, $\log (\Delta m_1 - D)$ has been plotted against $\log \lambda$ for values of D ranging from 0.00 to -3.00 mag. The resulting curves are shown in Figure 2.

In order to determine which of these curves are most probable, the accepted values for the coefficient of absorption, 0.67 mag. per kiloparsec at λ 4400 and 0.35 mag. per kiloparsec at λ 5500, have been used to compute the distance between ζ Per and ϵ Per for the various values of the zero point D. The results are given in Table II. The two values for the relative distance computed from the two coefficients of absorption are the same only for an inadmissible value of D—namely, $D = -0.22$ mag. Trumpler[6] found that the coefficients of absorption varied for the clusters he studied but that the

ratio of photographic to visual coefficient was constant. The ratio found for ζ Per does not agree with his constant value. It seems likely, though, that the coefficient of absorption for photographic light is not less than 0.5 nor more than 1.0 mag. per kiloparsec. Changing the coefficient of absorption for λ 4400 within this range does not seriously affect the distances obtained. In order to assume

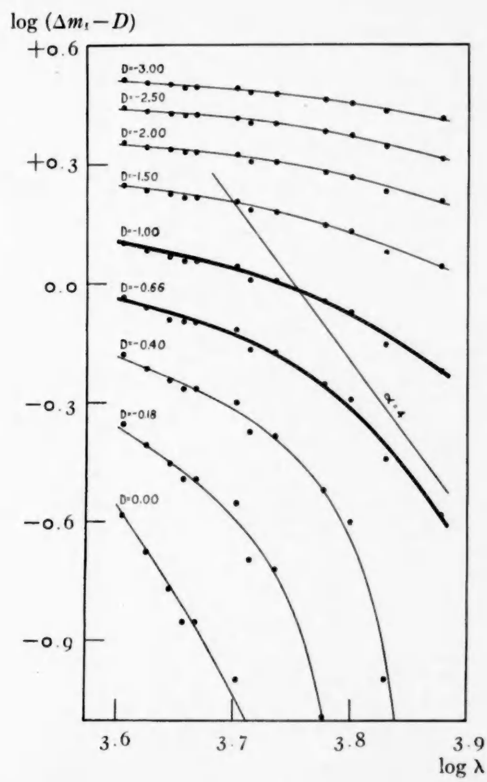

FIG. 2.—Curves for ζ Persei $-\epsilon$ Persei, plotting log $(\Delta m_1 - D)$ against log λ. The constant D depends upon the luminosities of the two stars and upon the coefficient of absorption. The two heavy curves are those for the most probable values of D. The straight line has the theoretical slope for Rayleigh scattering.

a reasonable distance for ζ Per, the lower limit for D has been set at -1.25 mag. If negative values of $(\Delta m_1 - D)$ are to be avoided, the upper limit for D must be -0.40 mag., which is the value of Δm_1 for the highest point of the relative energy-curve. Therefore the two most probable curves in Figure 2 are those for $D = -0.66$

mag. and $D = -1.00$ mag. For reference, the straight line which would be obtained for $\alpha = 4$ is shown in the diagram. It is evident from the experimental curves that, for ζ Per, α varies but is always positive. Comparison of these curves with those of Götz shows that the observed portion probably lies on the long wave-length side of the second maximum. We may, therefore, expect that at very long wave-lengths Rayleigh's law will be satisfied and at some point to the violet of the region investigated the curves will reach a maximum, beyond which α will be negative and scattering will make the star appear bluer.

TABLE II

Zero Point D	λ 4400		λ 5500	
	Absolute Absorp.	Distance $k = 0^m67/1000$ pc	Absolute Absorp.	Distance $k = 0^m35/1000$ pc
0^m00	$+0^m18$	270 pc	-0^m01	....
−0.22	0.40	600	+0.21	600 pc
0.40	0.58	860	0.39	1110
0.66	0.84	1250	0.65	1850
1.00	1.18	1490	0.99	2830
1.50	1.68	2500	1.49	4260
2.00	2.18	3250	1.99	5860
2.50	2.68	4000	2.49	7110
−3.00	+3.18	4750	+2.99	8550

If each of the two heavy experimental curves of Figure 2 is arbitrarily assumed to have a maximum at λ 3000, we may determine a value of the diameter of the particles for the two indices of refraction for which curves have been computed. For $n = 1.33$, $\rho = 300$ $m\mu$; for $n = \infty$, $\rho = 60$ $m\mu$. These values are the approximate limits of the sizes of particles involved; the latter size agrees quite well with the results obtained by other investigators.[7]

I wish to express my sincere thanks to Dr. Otto Struve and Dr. William W. Morgan for their many valuable criticisms and suggestions.

Yerkes Observatory
Williams Bay, Wisconsin
February 1936

[7] Schalén, *Upsala Meddelanden*, No. 64, 1936.